PREDICTION OF VIBRATIONAL SPECTRA OF 2-OXOPYRIMIDINE TAUTOMERS

BY

PEDRO J. ZAVALA

A DISSERTATION PRESENTED TO THE GRADUATE SCHOOL
OF THE UNIVERSITY OF FLORIDA IN
PARTIAL FULFILLMENT OF THE REQUIREMENTS
FOR THE DEGREE OF DOCTOR OF PHILOSOPHY

UNIVERSITY OF FLORIDA

1988

Copyright
by
Pedro J. Zavala

ACKNOWLEDGEMENTS

I am specially grateful to my research director Dr. Willis B. Person for his understanding, friendship, and guidance throughout this doctoral program.

Kind regards and thanks to Dr. Madelyn Lockhart for coordinating various activities involving my studies at the University of Florida.

I am grateful to each member of my doctoral committee for their friendship and help throughout my student years.

Special thanks to Dr. Krystyna Szczepaniak for providing experimental results and opportune advice, and to Dr. George Purvis for helping with computer facilities during many occasions. Thanks also to all the past and present members of my research group for their friendship throughout the years.

The support for this work from the National Institute of Health (Grant No GM 32988) is gratefully acknowledged

TABLE OF CONTENTS

	Page
ACKNOWLEDGEMENTS	iii
ABSTRACT	vi
CHAPTER	
1. INTRODUCTION	1
1.1 Tautomerism of Monooxopyrimidines	1
1.2 Theoretical Perspective	5
1.3 Aims of the Present Work	21
2. THEORY	24
2.1 Ab Initio Calculation	24
2.2 Vibrational Spectra	31
3 INTERPRETATION OF THE IR SPECTRUM OF 2-PYRIMIDINOL	39
3.1 Experimental Techniques	39
3.2 Theoretical Techniques	40
3.3 Assignment of Bands	47
3.4 Summary	70
4 EFFECT OF UPGRADING THE FORCE FIELD IN DIFFERENT COORDINATE SYSTEMS ON PREDICTED IR SPECTRUM OF 2-PYRIMIDINOL	76
4.1 Methods	76
4.2 Survey of Results	90
4.3 Conclusions	107

5. EFFECT OF CONVERGENCE, INTEGRAL THRESHOLD, AND CHOICE OF REFERENCE STATE IN AB INITIO CALCULATIONS ON THE PREDICTED IR SPECTRUM OF 2-PYRIMIDINOL 113

5.1 Convergence and Integral Threshold 113

5.2 Reference Geometry 127

5.3 Conclusions. 142

6. PREDICTION OF THE IR SPECTRUM OF 2-PYRIMIDINONE 148

6.1 Conclusions from Uracil Studies 149

6.2 IR Spectrum of 2-Pyrimidinone 159

7. SUMMARY AND COMMENTS 193

REFERENCES 197

BIOGRAPHICAL SRETCH 202

Abstract of Dissertation Presented to the Graduate School of the University of Florida in Partial Fulfillment of the Requirements for the Degree of Doctor of Philosophy

PREDICTION OF VIBRATIONAL SPECTRA OF 2-OXOPYRIMIDINE TAUTOMERS

BY

Pedro J Zavala

April 1988

Chairmen: Willis B. Person
Major Department: Chemistry

Ab initio calculations have been carried out at the Hartree-Fock self-consistent field level (HF SCF) for the structure, force constants, and atomic polar tensors (APTs) of the keto and enol tautomers of 2-oxopyrimidine. These results were used to determine the frequencies, potential energy distributions (PEDs), and intensities of the fundamental bands in the infrared (IR) spectra of these tautomers.

Since the enol tautomer is found to be predominant for 2-oxopyrimidine molecules in an isolated noble gas matrix, the calculated spectrum for this tautomer can be compared directly with the IR spectrum observed for this matrix. The agreement between calculated and observed spectra is excellent. This agreement confirms the conclusion that only the enol tautomer exists in the matrix environment. Although it has not yet been possible to determine the experimental

IR spectrum of the isolated keto tautomer of 2-oxopyrimidine, its predicted spectrum can be compared with experimental spectra of crystalline samples of 2-oxopyrimidine and matrix isolated diketo tautomer of uracil.

Simple statistical analysis are introduced to investigate the effect of scaling the calculated force fields in different coordinate systems, on the predicted IR band frequencies, PEDs, and intensities of these tautomers. The choice of reference state in force field and APT's determination and the degree of precision in ab initio calculations (convergence and integral threshold) are similarly studied. Various observations and recommendations are given. The statistical and mathematical approaches used in studying these effects need to be developed substantially.

CHAPTER 1
INTRODUCTION

The study of pyrimidine molecules is important in the ongoing research on nucleic acids. Nucleic acid bases, which are involved in various key roles in genetic and biochemical cellular processes, are either purines or pyrimidines. This work concentrates on the interpretation of vibrational spectra of the isolated tautomers of the 2-oxopyrimidine molecule, 2-pyrimidinol and 2-pyrimidinone (see Figure 1-1)

1.1 Tautomerism of Monooxopyrimidines

Before discussing the theoretical studies it is worth examining the tautomeric behavior of the system in question. Nowak et al.[1] studied the IR and UV spectra of various monooxopyrimidines in the gas phase, in low temperature inert matrices, and in various liquid solvents. They found that the tautomeric behavior of the 2-oxopyrimidines was different from that for the 4-oxopyrimidines. For the 4-oxopyrimidines in the gas phase and isolated in inert matrices they found comparable concentrations of the keto (oxo) and enol (hydroxo) forms, whereas 2-oxopyrimidines were found to exist predominantly in the enol form. In liquid solvent systems both 2- and 4-oxopyrimidines existed predominantly in the keto form. Czerminski et al.[2] studied autoassociation and tautomerism of 2-oxo-5-X pyrimidines (X=H,Cl,Br) finding similar results regardless of X. The

Figure 1-1. Molecular structures of 2-pyrimidinol, 2-pyrimidinone, cytosine and uracil.

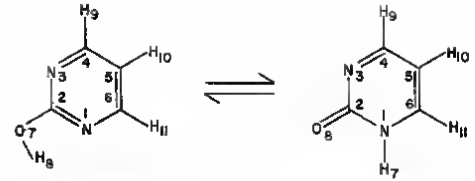

2 – pyrimidinol

2-pyrimidinone

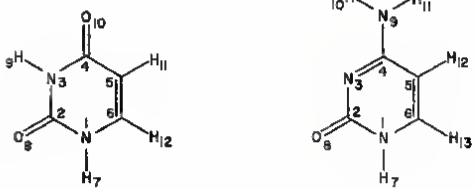

uracil

cytosine

latter studies were made under various conditions: in a dilute Ar matrix, more concentrated in an Ar matrix, in KBr pellets, as crystalline films (10 and 300° K), and in an amorphous film (10° K). The results from these studies of IR spectra obtained for 2-oxopyrimidine are shown in Figure 5 of Reference 2. The results for the 2-oxo-5-halogenated systems were similar. The compounds all existed as enol tautomers when isolated in low temperature inert matrices (Figure 5a of Reference 2). This conclusion was evident from the absence of a strong carbonyl stretch absorption band around 1700 cm^{-1}, and from the appearance of strong bands near 3580 cm^{-1} where the hydroxyl stretch is observed in inert matrices and gaseous pyrimidines and purines.[1,3-4] When the matrix was annealed and/or enriched, hydrogen bond association and enol to keto tautomerism took place. This conclusion followed from the appearance of C=O stretch absorption near 1650 cm^{-1} as well as from the strong broad bands for hydrogen bonded associates in the 3300-2200 cm^{-1} region. The KBr pellets, crystalline films (10 and 300° K), and amorphous films (10° K) showed the strong absorption in the carbonyl region near 1700 cm^{-1}, indicating the keto form as predominant. Furberg and Solbakk[5] determined from x-ray crystallographic methods that 2-oxopyrimidine existed in the solid as the keto form only, consistent with the above mentioned results from the IR spectra. Czerminski et al.[2] elucidated a possible mechanism for the tautomeric transition on going from isolated molecules to form the crystalline solid.

In our present study we shall concentrate on the experimental results from the dilute Ar matrix at 10° K. Before trying to understand more complicated matters such as tautomeric transitions, media effects, and perturbations due to molecular associations, we need full understanding of the spectra of each particular tautomeric form of the isolated monomers. The study of 2-oxopyrimidine in the dilute Ar matrix is such a case, since only the enol form occurs. In this study we shall work with a more detailed and better resolved and still unpublished spectrum of 2-oxopyrimidine in the dilute Ar matrix than is shown in Figure 5a of Reference 2. This spectrum has been provided to us by the Institute of Physics of the Polish Academy of Sciences.[6]

We will carry out theoretical calculations of the IR spectrum for each one of the tautomeric species of the 2- oxopyrimidine molecule. The calculations will be compared mainly with the above mentioned experimental spectrum of 2-oxopyrimidine in an Ar matrix.

1.2 Theoretical Perspective

Quantum mechanical calculations utilize extensively molecular orbital methods (MO). The two major approaches may be classified as semiempirical and *ab initio* methods. The first may utilize a simplified Hamiltonian, but is characterized by the use of experimental results to evaluate parameters used in the calculations. The second one uses the correct Hamiltonian and evaluates all parameters by

mathamathical methods, avoiding use of experimental results. We will be concerned here with ab initio studies using Hartree-Fock (HF) self-consistent field (SCF) calculations.

In this approach the wavefunction of the system is written as the Slater determinant formed from a set of occupied spin-orbitals. These spin-orbitals are just products of ordinary molecular orbitals (MO) and spin functions for each electron. The molecular orbitals are themselves written as linear combinations of atomic orbitals (AO). Each atomic orbital is expressed as a linear combination of simple basis functions. The energy corresponding to this wavefunction is then minimized by adjusting coefficients in these linear combinations so as to obtain a HF SCF wavefunction for the electronic ground state for a particular nuclear arrangement.

Various basis functions have been used in the past. The earliest ones were Slater type orbitals (STO) used as approximations to atomic orbitals.[7] The MO SCF calculations use either minimal or extended basis sets. In theory an infinite number of AOs can be used to construct a MO, but during calculations approximations have to be made. A minimal basis set of AOs consists only of occupied inner and valence shells, whereas an extended basis set also includes unoccupied higher shell AOs.

Because of computational difficulties with STOs (some integrals cannot be readily evaluated by the computer), most workers have replaced them with linear combinations of Gaussian functions.[8] Among the minimal basis sets used one

can find the STO-KG types (K=2-6).[9] A review by Pople[8] stated that results using STO-3G and STO-4G basis sets agreed quite well with calculations based on exact STOs studies. A better description of the wavefunction is provided by a linear combination of Gaussian functions called split valence basis sets. The number of functions is doubled for the valence shell to provide extra flexibility to the molecular orbitals. Among these one can usually find the 3-21G,[10] 4-21,[11] and 4-31G[12] basis sets as commonly used ones. The extended basis sets are those including polarization functions in the description of the wavefunction. Commonly used extended basis sets[13-16] are 3-21G*, 6-31G*, and 6-31G**.

It is expected that as the size of the basis set is increased the predictions from this wavefunction will be better. It is expected that additional improvements will result from including corrections to the wavefunction due to configuration interaction, i.e., linear combinations of Slater determinants. As far as geometry optimizations and force field evaluations are concerned, these expectations are generally fulfilled. But the high cost and complexity of these calculations on polyatomic molecules have limited such studies. It is beyond the scope of the present work to evaluate basis sets and correlation effects. The reader may find several reviews which deal with these aspects in more depth.[8,17-19]

In the present work we shall look almost exclusively at results from studies with small basis sets such as STO-3G and 4-31G at the HF SCF level connected with the prediction and interpretation of IR spectra of polyatomic molecules. We have classified these results as geometry optimisation, choice of reference state, determination of frequencies, scaling of force fields, and determination of intensities. These subjects are discussed in more detail in the following sections.

1.2.1 Geometry Optimization

The main goal of geometry optimization studies is the determination of the geometry of a chemical system at the minimum of its potential energy curve A given point on this potential curve or surface is the sum of the electronic energy and of the nuclear repulsion energy at a given nuclear arrangement of the system. In the past the points along these curves were determined from calculations of the energy made at each separate point and the equilibrium geometry was determined by fitting them to given functions. These explorations were carried out partially by varying certain parameters while holding others constant. With recent improvements in programming direct analytical calculations of energy derivatives have been carried out,[20] so that the energy of the system can be minimized with respect to all variables simultaneously. Thus quite valuable theoretical equilibrium geometries have been determined.

Popie[8] reviewed at some length geometry predictions at the Hartree-Fock level. He pointed out that at the time of his review most work was done at this level. For large molecules (around 10 atoms) most studies have been done with minimal basis sets. For smaller molecules larger basis sets have been used. The effects of higher levels of approximation such as configuration interaction have been studied to a very small extent for large molecules. It is claimed that HF theory using minimal basis sets (such as STO-3G) has been moderately successful in determining equilibrium geometries for closed shell systems. Bond lengths and angles are usually given with an accuracy of 0.03 A and 4^{o} respectively. Use of split valance basis sets (such as 4-31G) improved predictions of bond length but not bond and dihedral angles. Polarization functions added to split valence basis sets (such as 6-31G*) improved the prediction of the angles and gave equilibrium geometries close to the Hf limit. The bond lengths were systematically underestimated by 0.01-0.02 A. Very few predicted geometries with corrections for electron correlation have been studied. It seems that no major improvements are obtained as compared to the above mentioned basis sets.

1.2.2 Choice of Reference State

The potential energy, V, of a chemical system can be written as a power series expansion in the displacement coordinates as

$$V(x_1,x_2,\ldots,x_{3M}) = V_0 + \Sigma(\partial V/\partial x_i)_0 * \Delta x_i +$$

$$0.5 * \Sigma(\partial^2 V/\partial x_i \partial x_j)_{0,0} * \Delta x_i \Delta x_j + \ldots \qquad (1\text{-}1)$$

where $x_1, x_2, \ldots, x_{3M}$ are the cartesian coordinates of the M nuclei. The first term, V_0, is the potential energy of the molecule at equilibrium. The second term vanishes at the equilibrium point. The third term is the only one considered in the harmonic approximation since higher order derivatives are neglected. Thus

$$V(x_i,x_j,\ldots,x_{3M}) = 0.5 * \Sigma F_{ij} * \Delta x_i \Delta x_j \qquad (1\text{-}2)$$

where $F_{ij} (= \partial^2 V/\partial x_i \partial x_j)$ are known as the force constants. This approximation for the potential energy function is acceptable for small displacements near the equilibrium position as in low amplitude vibrations.

From the force constants the IR frequencies can be obtained. In theoretical calculations a given molecule will be distorted slightly from the equilibrium configuration in order to determine the force constants. This implies a priori knowledge of the equilibrium configuration. The choice of this configuration that we can call reference state is a controversial topic. Different criteria are used to select it. Several typical examples are cited below.

Some workers have utilized experimental equilibrium geometries as reference states.[20-26] In some cases better force constants were obtained than with theoretically determined reference states. Usage of experimental geometries shortened the computations since there was no need for geometry optimization calculations.

Others preferred theoretical reference states and the choices were various. Pulay et al.,[11] and Blom and Altona[27] have used empirically corrected SCF geometries. They evaluated the equilibrium geometry with a given basis set and then utilized empirical corrections to approximate it to experimental observations. They claimed that the experimental geometry is suspected of giving random errors in the evaluation of force constants. Experimental geometries could be different depending on the experimental technique employed. Further still most of them are vibrational averages which are different from true equilibrium geometries. This randomness is reflected significantly in the evaluated force constants. Fogarasi and Pulay[19] pointed out that for small molecules it is better to use high quality theoretical calculations for the determination of the equilibrium geometry. Then determine the force constants
at a lower theoretical level, e.g., SCF, as demonstrated by the work of Meyer and Rosmus on diatomic hydrides.[28]

Another group of researchers used theoretically determined equilibrium geometries as reference states without any modifications at all.[17,29-31] They evaluated the

theoretical ground state with a given level of theory, e.g., a given basis set. Then they determined the force field at the same level of theory using this geometry. Thus we have examples such as the work by Nishimura et al.[30] on uracil. They optimized uracil at the HF SCF level with an STO-3G basis set. Then they determined the force field at the same level of theory with this geometry. Pople went so far as saying that it makes no sense to depart from this approach.[17,32] These workers claim that in this way a more systematic approach of vibrational studies can be carried out, and data could be easily compared between different groups. This is akin to the concept of "theoretical modal chemistry" which uses a uniform level of theory throughout.[8,33] In a recent review by Hess and Schaad[34] on ab initio calculations of vibrational spectra they pointed out that this procedure is at least equivalent to the other mentioned choices of reference state.

1.2.3 Determination of Vibrational Frequencies

The vibrational frequencies are determined from the force constants (Equation 1-2) at the harmonic approximation. The force constants are determined in turn by numerical or analytical gradients of the potential energy.[20,25] Most of the work on medium to large polyatomic systems has been carried out at the Hartree-Fock SCF level with minimal basis sets. This is mainly due to the large cost of computer time.

These calculations usually overestimate the force constants and frequencies when compared to experimental results. Hess and Schaad,[34] reviewing an impressively large number of molecules, concluded that frequency errors are usually in the 5-10% range for Hartree-Fock SCF calculations with minimal basis sets. Pople et al.[29] carried out HF SCF calculations with 3-21G and 6-31G* basis sets on 37 small to medium sized molecules (3-10 first row atoms). They concluded that theoretical frequencies exceeded experimental ones by 150 cm^{-1} (about 12%) at the 3-21G level. Expansion of the basis set to 6-31G* (including d functions on atoms other than hydrogen) did not improve agreement with experiment. Other researchers concluded that usage of double sets or split valence basis sets give frequencies that are larger than experimental ones by 5-15%.[11,19,23,29,35-37]

Fogarasi and Pulay[19] provided us with detailed observations on the results from calculations with minimal basis sets (STO-3G) and medium sized ones (3-21G, 4-31G, 4-21) for force constants of medium to large molecules. They pointed out that diagonal terms of force fields from minimal basis set calculations were much overestimated when compared with medium sized basis sets. The STO-3G off-diagonal force constants showed random variations whereas medium sized basis sets cases were more systematic. For medium sized basis sets they found that diagonal stretching and bending force constants were systematically overestimated by 10-15% and 20-30% respectively. For off-diagonal force constants

the deviations were less systematic; large force constants were in error by 10-30%, and small ones had absolute errors in the 0.05-0.10 aJ/Å^n values.

1.2.4 Scaling of Force Fields

As seen in the previous section HF SCF calculations on medium to large molecules give frequencies that are usually overestimated when compared to experimental values. This discrepancy is usually attributed to the usage of small basis sets and lack of electron correlation. This attitude is in turn due to computer limitations and high cost. Because it is not possible to do exact calculations on medium to large chemical molecules many researchers have systematically determined force fields at the HF SCF level with small basis sets, and then scaled them so as to approximate them to the "true experimental force field." Various scaling approaches have been carried out.

A theoretical force field can be visualized as a matrix containing diagonal and off-diagonal values of force constants in a given coordinate system. The most usual coordinate system in scaling procedures is the internal coordinate set, e.g., bond stretches, angular deformations, etc. The researcher can vary any one of the matrix elements so as to fit his theoretical force field to experimental observations. Two major types of variations have been carried out: diagonal elements only, and all elements of the force field.

Among the examples in which variation only of diagonal elements were considered we find several interesting examples. Pulay and Meyer[37] scaled the theoretical force fields of ethene, ethylene, and acetylene. They reduced all diagonal stretching force constants by 10%, and those for all bendings by 20%. With this simple adjustment they reproduced experimental frequencies within 20-30 cm^{-1} (1.5-5.9% accuracy). Other researchers[38-42] have fitted the diagonal elements of the force field to experimental frequencies with excellent results. Fogarasi and Pulay[19] pointed out several disadvantages with these scaling procedures. They claimed that unless the calculated off-diagonal force constants are grossly in error, different force fields can be made to fit experimental frequencies analogously. They said that in the study of formaldoxime by Pouchan et al.,[42] the same agreement was obtained with experiment by scaling STO-3G and 4-31G force fields in spite of these two being significantly different. In this way the relative values of diagonal theoretical force constants were lost completely, and misassignments of experimental bands could not be detected.

Scaling of all the elements of the force field seems a more logical approach. Blom and Altona[27] scaled the 4-31G force fields of ethane, propane, and cyclopropene. They separated the diagonal force constants in the following groups: C-C stretching, C-H stretching, bendings and rockings, torsions, CH_2 wagging (in cyclopropane). All the off-diagonal elements were placed in one group. Then by

standard iterative procedures[43-44] they found scaling factors to multiply these groups by so as to obtain best fit with experimental results. In this way they came up with five (six for cyclopropane) scaling factors for the force constants. They were able to reproduce experimental frequencies to about 10 cm^{-1} (1% accuracy). Various other calculations along these lines gave similar results.[19]

Further scaling can be carried out by finding more conversion constants. The work by Wiberg et al.[31] on pyridine corrected all the 4-31G force field diagonal elements with individual scaling factors. The off-diagonal elements were divided into four groups (one for each of the symmetry groups of C_{2v} pyridine), and a single scaling constant for each different group. The following equation (Equation 1-3) shows how Pulay and coworkers[19,45-46] scaled their theoretical force field, F^{th}, by

$$F = C^{0.5} * F^{th} * C^{0.5} \qquad (1-3)$$

where the conversion constants of the diagonal matrix C gave the force field F which best fitted experimental results. In this way the diagonal elements of F^{th} such as Fii and Fjj were multiplied by Cii and Cjj respectively. Off-diagonal elements such as Fij were multiplied by the geometric mean, $[Cii*Cjj]^{0.5}$. Fogarasi and Pulay[19] argued that this approach was more physically significant than conversions of the type made by Blom and Altona[27] which made force constants coupling different coordinates share the same scaling

constants. Hipps and Foshuste[47] have utilized the arithmetic mean instead of the geometric one discussed here for scaling coupling force constants. A good reproduction of experimental frequencies has been obtained by these approaches.

As we have seen conversion constants have been utilized to obtain the best fit between theoretical and experimental results. A different philosophy of scaling has been adopted by other investigators[30,45-49] which we will shall call upgrading. In this case conversion constants are utilized to convert a lower level theoretical force field into a higher level one. For example Nishimura et al.[30] determined the force field of uracil at the HF SCF level with an STO-3G basis set. Then they utillzed 4-31G/STO-3G conversion constants to upgrade the STO-3G force field into one which should resemble a force field evaluated at the HF SCF level with a 4-31G basis set. The conversion was done by Equation 1-3 where F^{th} was the STO-3G force field, and F was the upgraded or "near 4-31G" one. The conversion constants C were obtained from comparisons of previous calculations at the STO-3G and 4-31G levels for urea, acrolein, and formamide.[30,50] It was emphasized that no attempts were made to fit theoretical results to experimental observations. There are various reasons for applying this upgrading technique, primarily the cost of the calculations. As the size of the molecule increases so does the complexity of the calculation and the cost. By upgrading low level force

fields such as those from STO-3G calculations, better quality force fields can be obtained at reasonable prices. Another important reason to use this approach is to know how far *ab initio* calculations can help in understanding chemical systems without referring to experimental observations. In this fashion purely theoretical predictions may be utilized to deduce experimental results.

1.2.5 Determination of Vibrational Intensities

Predicted IR spectra should include the intensities of the bands as well as the frequencies and normal modes. Unluckily there is less knowledge available about intensities than on force constants. This is quite evident on studies at the HF SCF level on medium to large polyatomic systems.[17,19,34] Pogarasi and Pulay[19] stated that, from the data available, fairly large basis sets, including polarization functions, were necessary to obtain reasonable values for predicted intensities (reliable to within 50%). They further stated that calculations using smaller basis sets can be considered to give correct qualitative predictions, i.e., they could differentiate between weak, medium, and strongly absorbing bands.

In actual calculations of band intensities, the derivatives of the dipole moment of a molecule with respect to a coordinate system are evaluated first. These dipole moment derivatives are then transformed into derivatives with respect to normal modes via a transformation matrix (the L matrix, see Chapter 2). This transformation matrix in

turn is obtained from the diagonalization of the calculated force field. Thus it can be said that the values of the calculated band intensities depend on the interaction between the calculated dipole moment derivatives and the calculated force field. Person reviewed these tranformations in great detail.[51]

Mehre et al [17] compared ab initio calculations of electric dipole moments with experimental ones. They focused mainly on comparisons of magnitudes since experimental data on signs and directions of dipole moments are scarce and have considerable uncertainty. They considered studies on a series of diatomic, small polyatomic, hypervalent, hydrocarbon, and monosubstituted benzene molecules at the HF SCF level with STO-3G, 3-21G, 3-21G*, and 6-31G* basis sets. In general they claimed moderate success with 3-21G* and 6-31G* basis sets, and recommended caution with STO-3G basis set results. Among their results they pointed out that for diatomic and small polyatomic systems the STO-3G, 3-21G, 3-21G*, and 6-31G* basis sets gave calculated dipole moments larger than experimental ones by 0.5, 0.49, 0.34, and 0.30 D respectively. For larger compounds containing heteroatoms these errors in calculated dipole moments for STO-3G, 3-21G, 3-21G*, and 6-31G* basis sets were 0.43, 0.44, 0.34, and 0.30 D respectively. For hydrocarbon compounds these deviations for STO-3G, 3-21G, and 6-31G* basis sets were 0.10, 0.06, and 0.07 D respectively. For monosubstituted benzenes the deviation for STO-3G basis set was 0.5 D.

The effect of electron correlation on the calculation of dipole momenta has been briefly considered.[17] As discussed above it was indicated[52] that near the HF limit the magnitudes of electric dipole momenta were in error by a few tenths of a debye. This discrepancy was significant since magnitudes of most dipole moments are within 0-5 D. This error then was particularly significant for molecules with very small dipole momenta such as carbon monoxide. The experimental dipole moment of CO is 0.11 D in the direction $^{-}CO^{+}$. The dipole moment calculated at near HF limit was 0.27 D in the $^{+}CO^{-}$ direction. Inclusion of electron correlation in the calculations corrected the near HF prediction of the magnitude and predicted the sign of the dipole moment in CO in the right direction.[17]

It is clear that the above mentioned observations on calculated dipole moments provide us only with approximate trends. More work is needed in order to have more precise knowledge. The calculation of dipole moments is subject also to a decision on the reference state. This has been pointed out by Mehra et al[17] who used experimental or calculated geometries on different occasions. They pointed out that in order to evaluate the reproduction of experimental dipole moments by different basis sets, two sources of error should be distinguished: limitations of the theory in describing charge distribution, and improper choice of molecular geometry.[17]

As far as the theory on calculations of IR band intensities is concerned, the situation is more complex than for dipole moment cases. As previously pointed out, little is known about *ab initio* calculations of IR intensities for large molecules. From the conclusions on dipole moments it becomes clear that future studies need to consider how the differences between calculated dipole moment derivatives and experimental ones differ from corresponding differences for dipole moments. Further still the choice of reference state and the interplay between these derivatives and force fields has to be faced in the light of band intensities observations.

1.3 Aims of the Present Work

The primary goal of this study is to interpret the experimental IR spectrum of 2-oxopyrimidine measured in a dilute Ar matrix at 10° K. In order to do so reliable spectra for 2-pyrimidinol and 2-pyrimidinone have been calculated. The decision of the level of theory to be used in these calculations was based on the limitations of available knowledge and programming costs. Secondary goals are considerations about the effect of different coordinate systems, convergence, integral threshold, and choice of reference state in the scaling (upgrading) of force fields, and the nature of predicted IR spectra (frequencies, normal modes, and intensities).

Chapter 2 summarizes the theory used in *ab initio* calculations, and the usage of the latter in the determination of frequencies, normal modes, and intensities

of IR fundamental bands for the present study. Chapter 3 is concerned with an accurate calculation of the IR spectrum of 2-pyrimidinol. This spectrum is used to assign the experimental fundamental bands of 2-pyrimidinol in the low temperature dilute Ar matrix IR spectrum of 2-oxopyrimidine.

Chapters 4 and 5 are concerned with the effect of coordinate system, convergence, integral threshold, and choice of reference state on the scaling of force fields and the nature of calculated IR frequencies, normal modes and intensities. Simple statistical approaches have been introduced to evaluate the quality of the calculated IR spectrum. Chapter 6 is concerned with the calculation of the IR spectrum of 2-pyrimidinone. Some calculations for uracil have been considered in order to help in these considerations.

As a more generalized aim the results of the present work will be used in the future for the interpretation of IR spectra of halogenated oxopyrimidines and of spectra of nucleic bases, particularly cytosine (Figure 1-1). The advantage of examining the IR spectrum of the low temperature dilute Ar matrix of the 2-oxopyrimidine molecule is that it provides a rare opportunity of studying exclusively the IR spectrum of the hydroxo (enol) tautomer of 2-oxopyrimidine (i.e. 2-pyrimidinol). This in turn can be utilized in helping with the interpretation of the IR spectra of nucleic bases. Spectra of these compounds are often made up of contributions from different tautomeric

forms of the nucleic base. A case in point is the spectrum of cytosine. One of the tautomeric forms of this nucleic base is very similar to the structure of 2-pyrimidinol.

The statistical approaches introduced in Chapters 4 and 5 are given with the intent of emphasizing that evaluation of the quality of a predicted IR spectrum in terms only of band frequencies is not necessarily sufficient. The observations are understood as simple trends and should be taken as qualitative only. In future work there should be more concern in considering simultaneously the predicted frequencies, normal modes, and intensities of the IR bands.

CHAPTER 2
THEORY

In this chapter we shall outline the methods of calculation used for the prediction and interpretation of IR spectra. We shall divide the discussion into two parts ab initio calculations and vibrational spectra. The first one considers the ab initio molecular orbital calculations, and the second one, the usage of such results in the calculation of the frequencies, normal modes, and intensities of the vibrational spectra.

2.1 Ab Initio Calculations

All the calculations were done by the restricted Hartree-Fock self-consistent field method (RHF SCF) with STO-3G and 4-31G basis sets. The molecules under consideration were 2-pyrimidinol and 2-pyrimidinone. The programs used were GAUSSIAN 76[53] and GAUSSIAN 82 [32] GAUSSIAN 76[53] was used with the Amdahl 470 computer at the North East Regional Data Center (NERDC), and GAUSSIAN 82[32] with the VAX-780 of the Quantum Theory Project (QTP), Department of Chemistry (University of Florida). These programs were used at various times for different purposes. The reasons for the choice of one over the other were due to factors such as cost, time of installation, relation to time of computation, and nature of the computations. This section is organized

in two parts: GAUSSIAN 82[32] calculations and GAUSSIAN 76[53] calculations.

2.1.1 GAUSSIAN 82 Calculations

Various types of calculations were done with the GAUSSIAN 82 program.[32] They are divided under three headings: geometry optimizations, RHF SCF 4-31G calculations, and RHF SCF STO-3G calculations. The first one is concerned with the determination of the equilibrium geometries of both tautomers of 2-oxopyrimidine. The second one looks at the determination of the force field and atomic polar tensors of 2-pyrimidinol with a 4-31G basis set. The third one considers the determination of the force fields of both tautomers of 2-oxopyrimidine with an STO-3G basis set.

2.1.1.1 Geometry optimizations

The BFGS optimization procedure described by Head and Zerner[54] (installed as a GAUSSIAN 82[32] subroutine) was used with its default parameters for all optimizations. This subroutine performs simultaneous optimization of all variables by analytic gradient methods. All calculations were done at the RHF SCF level.

The equilibrium geometries for both tautomers of 2-oxopyrimidine were determined with an STO-3G basis set. The equilibrium geometry of 2-pyrimidinol was also determined with a 4-31G basis set. The initial guesses for the STO-3G optimization of both tautomers were those published from the MINDO/3 calculations by Czerminski et al.[55] The STO-3G optimized geometries are given in Chapters 4 and 5. The initial guess for the 4-31G optimization of

2-pyrimidinol was the geometry optimized with the STO-3G basis set. The 4-31G optimized geometry of 2-pyrimidinol is given in Chapter 3.

2.1.1.2 RHF SCF 4-31G calculations

The subroutine FORCE of GAUSSIAN 82[32] was used to determine the cartesian force field and the atomic polar tensors (APT) of 2-pyrimidinol. The calculation was done at the RHF SCF level with a 4-31G basis set. The default parameters of GAUSSIAN 82[32] were used (including convergence = 10^{-9} and integral threshold = 10^{-10}).

This subroutine was done a total of 56 times. One was for the reference state which was at the above mentioned 4-31G optimized geometry (Section 2.1.1.1), and the remaining 55 were done for each of the displaced geometries. Each atom of the reference state was displaced one at a time in the +x,-x,+y,-y, and +z direction by 0.005 A. The cartesian forces and the dipole moments were calculated for the reference state and each of the displaced geometries.

Each run of FORCE subroutine yielded a 1 x 33 matrix of cartesian forces acting on each atom. An element of this matrix can be called f_{ij}^{+} where i stands for a given atom, j for one of the three cartesian coordinates (x,y,z), and + for a positive displacement. Similarly f_{ij}^{-} stands for a -j displacement of atom i. From these matrices a 33 x 33 cartesian force field, F_x, was constructed by

$$F_{ij} = [(f_{ij}^{-} - f_{ij}^{+})] * 15.5691/[2(0.005/0.529167)] \qquad (2\text{-}1)$$

where F_{ij} was an element of F_x matrix in mdyn/A. Similarly from the dipole moment components of each run of FORCE subroutine we got the 3 x 33 polar tensor matrix, P_x, which was a juxtaposition of the 3 x 3 APTs of the atoms of the molecule under investigation:

$$P_x = \begin{matrix} \partial p_x/\partial x_1 & \partial p_x/\partial y_1 & \partial p_x/\partial z_1 & \partial p_x/\partial x_2 & \cdots \\ \partial p_y/\partial x_1 & \partial p_y/\partial y_1 & \partial p_y/\partial z_1 & \partial p_y/\partial x_2 & \cdots \\ \partial p_z/\partial x_1 & \partial p_z/\partial y_1 & \partial p_z/\partial z_1 & \partial p_z/\partial x_2 & \cdots \end{matrix} \qquad (2\text{-}2),$$

where the first three columns of P_x pertained to atom 1, the next three to atom 2, and so forth. Each of the components of P_x were calculated in units of e by

$$\partial p_x/\partial x_i = \Delta p_x/\Delta x_i = [\, p_x(x_o + 0.005) - p_x(x_o - 0.005)] * \{4.80324/(2(0.005))\} \qquad (2\text{-}3),$$

and so forth. Thus the APTs, P_x, were the derivatives of the dipole moment with respect to cartesian displacements of the atoms. The cartesian force field, F_x (converted to internal symmetry coordinates) and the APTs, P_x, of 2-pyrimidinol are given in Chapter 3.

2.i.i.3 RHF SCF STO-3G calculations

The subroutine FREQ of GAUSSIAN 82[32] was used to determine the cartesian force fields of both tautomers of 2-oxopyrimidine. The calculations were done at the RHF SCF level with an STO-3G basis set. The default parameters of the subroutine were used. The reference geometry was the optimised STO-3G geometry of Section 2.i.i.i. This subroutine evaluated the entire force field by analytic gradient techniques. No APTs could be determined with this subroutine. The only necessary input was the reference state. It was possible to use this subroutine because the basis set utilized was small (STO-3G). This subroutine could not be used with bigger basis sets such as 4-31G due to computer limitations. This was the reason why subroutine FORCE was used to evaluate the 4-31G force field of 2-pyrimidinol (Section 2.1.1.2) instead of subroutine FREQ.

2.i.2 GAUSSIAN 76 Calculations

Diagonal force constants and atomic polar tensors for various reference states (Chapters 4 - 6) of both tautomers were calculated at the RFH SCF level with 4-31G basis sets using the GAUSSIAN 76 program.[53] The reference states of

2-pyrimidinol were the 4-31G and STO-3G optimized geometries (Section 2.1.1.1), and two possible crystal structures (Chapter 5). The reference states of 2-pyrimidinone were the STO-3G optimized geometry (Section 2.1.1.1) and the crystal structure (Chapter 6). The default parameters of the GAUSSIAN 76[53] program were used. The convergence was $5 * 10^{-5}$, and the integral threshold was 10^{-6} at all times. The only exception was the determination of the diagonal force constants and APTs of 2-pyrimidinol at a convergence of 10^{-8} (reference state is 4-31G optimized geometry -- see Chapter 5).

For a given reference state the energies and dipole moment components of the ground state and displaced geometries were evaluated. From the energies the force constants were determined, and from the dipole moments, the APTs. It should be mentioned that all calculations done with GAUSSIAN 76[53] were carried out in W coordinates. This is a set of coordinates described by Chin,[56] who wrote a series of programs in these coordinates that could be used in conjunction with GAUSSIAN 76 [53] In the present study we call them W coordinates although Chin[56] used a different nomenclature. These coordinates are the mass weighted, molecule fixed, symmetry adapted, principal cartesian coordinates.[56] They are based on a molecule fixed coordinate system which translates and rotates along with the molecule. In this way the vibrational motions of the molecule are separated from translational and rotational ones

(Eckart-Sayvatz conditions) [57] For no other major reason than simplicity in computations at that time we used these coordinates.

For a given reference state displacements in the positive and negative directions were made for each coordinate, and the energy and dipole moment components were calculated, one point at a time, for the reference state and for each displaced geometry. The diagonal force constants of the force field in W coordinates, F_w, were determined by

$$F_{wi} = [\, E(x_o + \Delta x) + E(x_o - \Delta x) - 2E(x_o) \,] * \{ 4.3598/(0.01)^2 \} \qquad (2\text{-}4)$$

where the ith diagonal force constant F_{wi} i of the force field was given in mdyn/A using displacements Δwi of 0.01 $\mu^{0.5}$-A. The terms $E(x_o + \Delta x)$ and $E(x_o - \Delta x)$ stood for the energies in Hartrees of the positively and negatively displaced geometries, and $E(x_o)$ was the energy of the reference state in the same units. The F_w matrix could be converted to cartesian coordinates (X coordinates) by suitable transformations (see Section 2.2.1).

The dipole moment derivatives were evaluated in W coordinates in a manner analogous to Equation 2-3 (but displacing by Δwi) to form the P_w matrix. The P_w matrix was converted to cartesian APTs, P_x, by

$$F_X = F_W * U * M^{0.5} \qquad (2\text{-}5)$$

where F_X was in units of e, U was the coordinate transformation matrix[56] (between W and X coordinates), and M was a diagonal matrix containing the masses of the atoms in emu. In this fashion the diagonal elements of F_W, and the APTs, P_X, could be obtained for each reference state. The results of these calculations are shown in Chapters 5 and 6.

2.2 Vibrational Spectra

This part deals with the use of ab initio calculations of force constants and APTs in the evaluation of frequencies, normal coordinates, and intensities. All the calculations were done on our H-100 microcomputer using Chin's programs.[56] This study is divided in four different sections: interconversion of coordinates, method to determine frequencies, determination of intensities, and interpretation.

2.2-1 Interconversion Of Coordinates

As proposed by Pulay and coworkers[11,19] we decided to use symmetrized internal coordinates, S coordinates, for the determination of IR frequencies from force constants. The S coordinates were obtained by applying projection operator techniques[58] to get linear combinations of internal coordinates corresponding to the irreducible representations of the symmetry group of the molecule. All the molecules

coneidered in the preeent work heve C_s eymmetry. The correaponding S coordinates wara dafinad according to tha recommendations by Pulay and collaboratora.[11,19]

The *ab initio* calculeted force conetenta end force fielde were expreaaed either in W or X (carteaian) coordinatea. Since the calculetions covered in the following eectione were done in S coordinetee, it wee importent to convart forca fialds in W and X coordinatas, F_w and F_x, into force fialds in S coordinates, F_s. Thaaa interconveraiona were carried out by the following reletionshipe (in matrix notation):

$$F_s = A^t * F_x * A \tag{2-6}$$

$$F_x = B^t * F_s * B \tag{2-7}$$

$$F_w = U * M^{-0.5} * F_x * M^{-0.5} * U^t \tag{2-8}$$

$$F_x = M^{0.5} * U^t * F_w * U * M^{0.5} \tag{2-9}$$

$$F_w = U * M^{-0.5} * B^t * F_s * B * M^{-0.5} * U^t \tag{2-10}$$

$$F_s = A^t * M^{0.5} * U^t * F_w * U * M^{0.5} * A \tag{2-11}$$

where U wea the coordinate tranaformation matrix mentioned in Equetion 2-5 end U^t wes ite trenepoee, M wee the diegonel metrix containing the maaaa of the atoma in emu, and A end

B were coordinate transformation matrices B (between S and X coordinates), and A^t and B^t were their corresponding transposed matrices.

The A and B matrices are quite important relationships. Their construction has been explained by several authors.[57,59] To determine them the first step carried out was to calculate the B_i matrix which transforms X (cartesian) to R (internal) coordinates:

$$R = B_i * X \qquad (2\text{-}12)$$

where B_i was a (3N + a) * 3N matrix, N was the number of atoms of the molecule, and a was any whole number (number of redundancies plus six). Thus B_i could be redundant. To eliminate such redundancy and utilize the symmetry of the molecule the following was used:

$$S = H * R \qquad (2\text{-}13)$$

where B was a (3N-6) * (3N + a) matrix which symmetrized the internal coordinates, R, to give the corresponding S coordinates. In a similar fashion the B_i matrix was transformed by

$$B = H * B_i \qquad (2\text{-}14)$$

where B transformed X into S coordinates (not redundant).

This can be seen more clearly by combining Equations 2-12 through 2-14

$$S = R * B_i * X$$
$$= B * X \qquad (2\text{-}15)$$

The A matrix is a form of inverse matrix of B because it is a rectangular matrix[59] (A*B=E and B*A=E, where E is the identity matrix). The following relationship was used (further explanations on the A matrix can be found in references 57 and 59):

$$A = M^{-1} * B^t * G^{-1} \qquad (2\text{-}16)$$

where M^{-1} was the inverse of the mass matrix M, and G^{-1} was the inverse of the kinetic energy matrix G. The G matrix is defined in the immediate next section.

2.2.2 Method to determine Frequencies

In accordance with Wilson et al.[59] the G matrix was defined as

$$G = B * M^{-1} * B^t \qquad (2\text{-}17).$$

Furthermore

$$G * F * L = L * A \qquad (2\text{-}18)$$

where F was the force field (in S coordinates in our case), L was the transformation matrix which related S coordinates

to normal coordinates and Λ was a diagonal matrix of the eigenvalues λ_i which were related to the normal vibration freguencies ν_i by

$$\lambda_i = 4\pi^2 c^2 \nu_i^2 \qquad (2\text{-}19)$$

or

$$\nu_i(cm^{-1}) = 1303.1 * \lambda_i^{0.5} \qquad (2\text{-}20)$$

where c was the speed of light in cm/sec, ν_i was a particular wavenumber in cm^{-1} for the fundamental band related to the λ_i eigenvalue of the diagonal Λ matrix.

It can be seen that the frequencies of fundamental bands could be obtained by the solution of Equation 2-18. In our calculations we followed the solution of the GF matrix of Equation 2-18 as explained by Miyazawa which included asymmetry considerations.[60] These methods have been worked by various autors[5] and have been detailed by Scott-Lebron.[61]

2 2.3 Determination of Intensities

To determine the intensities of bands the APTs, P_x, as formulated by Person and Newton were used[62] (see Equation 2-2). The IR intensity, I_i, of a given nondegenerate band was given by[62-64]

$$I_i(km/mole) = 974.9 * |\partial p/\partial Q_i|^2 \qquad (2\text{-}21)$$

where $|\partial p/\partial Q_i|$ was the absolute value of the dipole moment derivative with respect to the ith normal coordinate.

The APTs, P_x, were related to $\partial p/\partial Q_i$ by

$$P_Q = P_x * A * L \qquad (2\text{-}22)$$

where A and L were as previously defined. The P_Q was a 3 * (3N-6) matrix (for non linear molecule with N atoms) containing the dipole moment components with respect to normal coordinates (1 through 3N-6)

$$P_Q = \begin{matrix} \partial p_x/\partial Q_1 & \partial p_x/\partial Q_2 & \cdots & \partial p_x/\partial Q_{3N-6} \\ \partial p_y/\partial Q_1 & \partial p_y/\partial Q_2 & \cdots & \partial p_y/\partial Q_{3N-6} \\ \partial p_z/\partial Q_1 & \partial p_z/\partial Q_2 & \cdots & \partial p_z/\partial Q_{3N-6} \end{matrix} \qquad (2\text{-}23).$$

Equation 2-5 could be used to convert any set of APTs in W coordinates, P_w, to P_x. Once the matrix P_x was obtained it could be used to calculate P_Q, which in turn gave the intensities of the bands in km/mole via Equation 2-21.

2.2.4 Interpretation

In the present work the normal coordinates for fundamental modes were explained in S coordinates. These coordinates have helped us to visualize the normal vibration corresponding to a given fundamental band.

Two methods were used to analyze these results. The first one was derived by Morino and Kuchitsu[65] and is referred to as the "MK method." The second one was derived by Keresztury and Jalsovsky[66] and is referred to as the "KJ method."

The "MK method" rationale was as follows. For the eigenvalue λ_k of the kth normal coordinate,

$$\lambda_k = \Sigma L_{kl}{}^t * F_{lj} * L_{jk}$$

$$= \Sigma F_{lj} * L_{lk} * L_{jk} \qquad (2\text{-}24),$$

Since the potential energy, V, was given (in matrix notation) by

$$V = 0.5 * Q^t * A * Q \qquad (2\text{-}25),$$

it followed that the potential energy distribution of the kth normal mode, $V(Q_k)$ was

$$V(Q_k) = 0.5 Q_k{}^2 \Sigma F_{lj} * L_{lk} * L_{jk} \qquad (2\text{-}26).$$

Morino and Kuchitsu[65] assumed that the product $F_{lj}L_{lk}L_{jk}$ was significant only when l=j. Thus only the $F_{ii}L_{ik}{}^2$ terms were evaluated determine the potential energy

distributions (PEDs). The percentage measuring the contribution to the kth normal coordinate from the ith symmetry coordinate was given by PED_{ik},

$$PED_{ik} = (F_{ii} * L_{ik}^{2} / \lambda_k) * 100 \qquad (2\text{-}27)$$

where F_{ii} was the diagonal force constant associated with the ith symmetry cordinate, and λ_k was the eigenvalue of the kth normal coordinate. The rationale used in the "KJ method" was the same with the difference that no assumptions were made as in the "MX method", i.e., all terms in Equation 2-26 were considered. Thus the "KJ method" is more theoretically justified than the "MX method."

The PEDs give information about the contribution of each symmetry coordinate to a given normal mode. In this fashion one can determine which S coordinate contributes to a given band. In our calculations contributions less than 10% were not reported. Both methods have given similar results for the in-plane vibrations of the tautomers of 2-oxopyrimidine. The "KJ method" seems to be more accurate for out-of-plane modes where the assumptions made in the "MX method" plus the low eigenvalues could lead to complications.

CHAPTER 3
INTERPRETATION OF THE IR SPECTRUM OF 2-PYRIMIDINOL

This chapter is concerned with the interpretation of the IR spectrum of 2-oxopyrimidine in a low temperature Argon matrix. The experimental and theoretical techniques connected with this spectrum are outlined first. Following this the experimental fundamental bands are assigned by comparison with the theoretical calculations of the spectrum. Consequently the chapter is divided into four sections: experimental techniques, theoretical techniques, assignment of bands, and summary.

3.1 Experimental Techniques

The experimental work was carried out by M. J. Nowak, H. Rostkowska, and K. Szczepaniak.[6] A paper on these results is in preparation.[6] Details of the technique have been previously outlined.[2,67] A simple summary is presented in this section.

The 2-oxopyrimidine vapor and the matrix gas were condensed on a CsI window cooled to about 10^{o} K. The matrix gas to solute ratio was about 1000:1. The IR spectrum (frequencies and absorbances) was recorded on a Perkin Elmer 580B spectrophotometer for the 4000-400 cm^{-1} region at a 1 cm^{-1} resolution.

Table 3-1 lists the experimental frequencies and integrated relative absorbances (R.A.s) obtained from the above mentioned spectrum. The R.A.s were calculated by integration of the bands in the experimental spectrum with a compensating polar planimeter of fixed arm (Keuffel and Esser Co., Model # 620000). These R.A.s are expressed in units such that the integrated absorbance of the experimental fundamental ν_1 was assumed to be the same as the intensity calculated for ν_1 (= 1380 km/mole). The upper parts of Figures 3-1 and 3-2 represent the experimental spectrum tabulated in Table 3-1. The R.A.s are drawn as stickbars to facilitate future comparisons with theoretical results. This "stickbar representation" is used throughout the rest of this dissertation. As mentioned before (Introduction), this spectrum is known to be due to absorption predominantly by the 2-pyrimidinol tautomer with some trace absorption by the 2-pyrimidinone tautomer.[6]

3.2 Theoretical Techniques

Calculations were carried out for 2-pyrimidinol. The geometry was optimized with GAUSSIAN 82[32] using a 4-31G basis set (See Chapter 2). Using this optimized geometry as reference state, the force constants and APTs were evaluated with GAUSSIAN 82[32] using the 4-31G basis set (Chapter 2). From these results the frequencies, PEDs, and intensities of the fundamental bands were determined using the methods outlined in Section 2.2.

TABLE 3-1
EXPERIMENTAL RESULTS AND ASSIGNMENT OF THE IR SPECTRUM MEASURED IN A DILUTE AR MATRIX FOR 2 -OXOPYRIMIDINE AT 10° K

Wavenumber[a,b]	R.A.[c]	Assignment[d]	PED[e]
3584	49.9	ν1	100S8
3574	88.1	ν1	
3088	1.1	ν2	12S9,75S10,12S11
3053	10.1	ν3	52S9,47S11
3034	1.5	ν4	35S8,24S10,40S11
3013	3.8	"Region a"	
2987	2.2	"Region a"	
1722.5	8.1	"Region b"	
1678	8.7	"Region b"	
1668	10.8	"Region b"	
1632	3.7	"Region b"	
1627	3.0	"Region b"	
1600.5	3.0	"Region b"	
1580	48.2	ν5	21S2,10S3,23S5,14S6,11S18
1564	48.0	ν5	
1573	81.2	ν6	17S1,11S3,28S4,13S17
1464.5	58.2	ν7	12S2,10S5,21S7,15S17,12S18
1458	5.1	"Region c"	
1445	2.5	"Region c"	
1434.5	164.5	ν8	13S1,27S18,28S18
1417	2.2	"Region d"	
1380	2.4	"Region d"	
1351.5	7.0	ν9	16S3,14S7,40S17
1328	66.8	ν10	22S16,11S17,36S18
1225	5.7	ν11	45S16,16S18
1215	28.8	ν11	
1211	7.8	ν11	
1200	21.6	ν11	
1186	11.4	ν11	
1168	17.5	ν12	32S3,34S6,20S18
1088	2.0	ν13,ν14	19S2,43S5,12S18 (ν13)

---

continued

TABLE 3-1 continued

Wavenumber[a,b]	R.A.[c]	Assignment[d]	PED[e]
1084.5	3.2	ν13,ν14	15S1,54S4 (ν14)
1079.5	7.1	ν13,ν14	
1075	4.7	ν13,ν14	
871	13.3	ν16	20S1,22S2,27S7,11S14
810	32.2	ν22	39S20,40S23,15S26
793	3.7	ν23	26S20,10S25,50S26,12S7
641.5	5.2	ν17	68S13,18S14
564	26.5	ν24	34S20,20S22,32S23,12S24
558	20.6	ν25	86S24
536	2.8	ν25	
523	12.9	ν25	
512	7.1	ν25	
502	15.4	ν25	
457.5	17.0	ν18	80S15

[a]Experimental wavenumbers (cm^{-1}) determined by M. J. Nowak, H. Rostkowska, and K. Szczepaniek (Reference 6).

[b]Experimental frequency measured at the peak of band.

[c]Experimental integrated relative absorbances measured with a planimeter in units such that the integrated absorbance of the two peaks assigned to experimental ν1 is assumed to be equal to the calculated ν1 intensity (= 138 Km/mole). The experimental results are obtained from Reference 6.

[d]Assigned fundamentals correspond to 2-pyrimidinol. "Region a," "Region b," "Region c," and "Region d," correspond to unassigned weak peaks of experimental spectrum that could be combination bands of 2-pyrimidinol, traces of 2-pyrimidinone and impurities (for further explanation see Section 3.3). Bands ν15, ν18, ν20, and ν21 have negligible absorption. Bands ν26 and ν27 have negligible absorption, and/or are beyond studied experimental range of frequencies.

[e]Potential Energy Distribution (%) calculated by KJ method (Reference 56) using the 4-31G optimized force field of 2-pyrimidinol (Table 3-3). For example, 32S3 of ν12 means 32% contribution of S3 symmetrized internal coordinate (S coordinate) to ν12 fundamental mode. The S coordinates are detailed in Table 3-4.

Figure 3-1. Comparison between the experimental Ar matrix spectrum of 2-oxopyrimidine and the unscaled predicted IR spectrum of 2-pyrimidinol for the 4000 - 3000 reciprocal cm region. The EXPT spectrum is redrawn from that for the isolated 2-oxopyrimidine sample in dilute Ar matrix at 10 K (Reference 6). The CALC spectrum is the unscaled set of predictions from the full 4-31G study (Table 3-7). The term a in the EXPT spectrum stands for "Region a" (see Table 3-1).

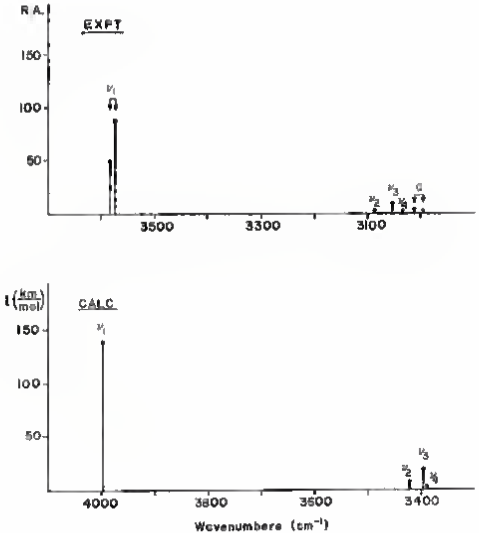
R.A.
EXPT
150
100
50
3500
3300
3100
I (km/mol)
CALC
150
100
50
4000
3800
3600
3400
Wavenumbers (cm⁻¹)

Figure 3-2. Comparison between the experimental Ar matrix spectrum of 2-oxopyrimidine and the unscaled predicted IR spectrum of 2-pyrimidinol for the 2000 - 200 reciprocal cm region. The EXPT spectrum is redrawn from that for the isolated 2-oxopyrimidine sample in dilute Ar matrix at 10 K (Reference 6). The CALC spectrum is the unscaled set of predictions from the full 4-31G study (Table 3-7). The terms b, c, and d in the EXPT spectrum stand for "Region b," "Region c," and "Region d" respectively (see Table 3-1).

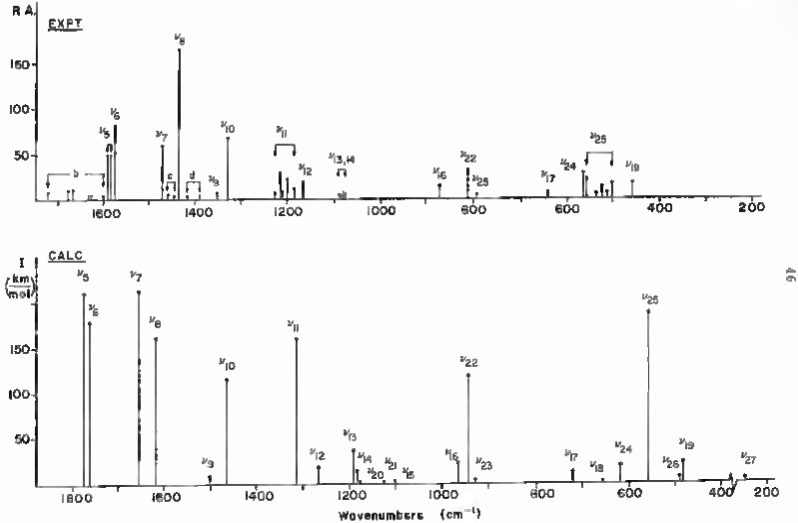
R.A.
EXPT
150
100
50
1600
1400
1200
1000
800
600
400
200
CALC
I
(km/mol)
Wavenumbers (cm⁻¹)

Table 3-2 gives the 4-31G optimized geometry of 2-pyrimidinol in terms of coordinates defined in Figure 3-3. The 4-31G force field in S coordinates, F_S, is shown in Table 3-3. The S coordinates used for 2-pyrimidinol are given in Table 3-4. Table 3-5 shows the APTs in accordance to the orientation indicated in Table 3-6.

Table 3-7 gives the unscaled wavenumbers (cm^{-1}) and intensities (km/mole) predicted for the fundamental bands from the above mentioned force field and set of APTs. The PEDs are given in Table 3-8 for both PED methods described in Chapter 2. The bottom parts of Figures 3-1 and 3-2 show a stickbar plot of the unscaled predicted spectrum, to be compared with the experimental spectrum.

3.3 Assignment of Bands

In order to compare the experimental and the theoretical spectra to reach an assignment of bands, it is useful to scale the calculated wavenumbers. This can be done because it is known that predicted wavenumbers are too high by about 10% (see Introduction). Consequently the calculated spectrum is modified slightly to obtain Figures 3-4 and 3-5. The experimental results shown in these figures are identical to those shown in Figures 3-1 and 3-2. The modification is in the calculated spectrum. All the predicted wavenumbers are multiplied by a constant factor of 0.9 (Table 3-7), leaving the intensities untouched.

This modification of predicted wavenumbers is done only for assignment purposes. It has proven to be quite

TABLE 3-2
OPTIMIZED GEOMETRY OF 2-PYRIMIDINOL
AT THE HF SCF LEVEL WITH A 4-31G BASIS SET

i	r_i(A)[a]	i	θ_i(degrees)[a]
1	1.322	12	117.8
2	1.320	13	125.2
3	1.327	14	117.2
4	1.384	15	122.1
5	1.379	16	116.4
6	1.330	17	121.4
7	1.337	18	117.0
8	0.953	19	112.4
9	1.069	20	121.7
10	1.068	21	121.9
11	1.069	22	116.5
		23	117.8
		24	116.2
		25	121.7
		26	122.1

[a]Bond lengths, r, and Angles, θ, are according to Figure 3-3. The geometry was optimized by the BFGS procedure of Head and Zerner (References 32 and 54).

Figure 3-3. Structure, atom numbering and in-plane internal coordinates of 2-pyrimidinol used in this work. The out-of-plane internal coordinates are the out-of-plane bends and torsions given in Table 3-4.

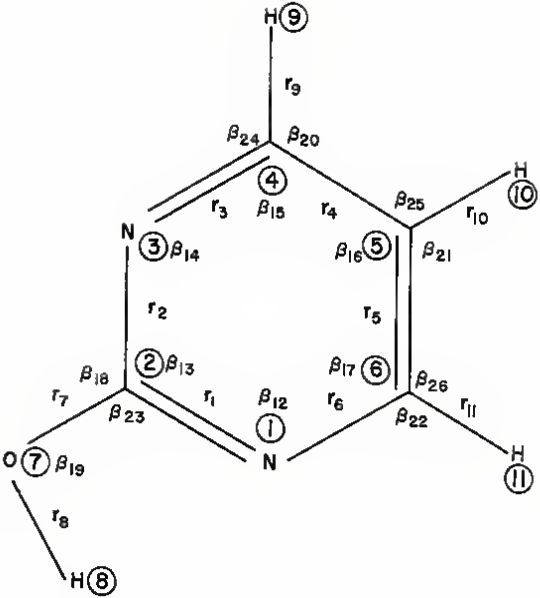
H 9
r9
β24
β20
4
r3
β15
r4
β25
r10
H 10
N 3 β14
β16 5
β21
r2
r5
β18
2 β13
β17 6
β26
r7
r1
β12
r6
r11
β23
β22
1
O 7 β19
N
H 11
r8
H 8

TABLE 3-3
FORCE CONSTANTS FOR 2-PYRIMIDINOL
IN SYMMETRIZED INTERNAL COORDINATES S
EVALUATED AT THE HF SCF LEVEL WITH A 4-31G BASIS SET

	S1[a,b,c,d]	S2	S3	S4	S5	S6
S1	8.90201					
S2	1.29878	8.92856				
S3	-.75255	.95023	8.83356			
S4	.72709	-.75839	1.14173	7.93078		
S5	-.76238	.76198	-.66902	.90288	8.15218	
S6	.95745	-.75171	1.01109	-.68362	1.12944	8.72396
S7	.84444	.90138	-.08341	-.06585	-.15368	-.04195
S8	-.08873	-.05268	-.00633	.01163	-.00189	-.00117
S9	-.01695	-.01912	.20865	.08835	-.00001	-.02863
S10	-.02918	-.03137	-.01774	.06409	.06532	-.01681
S11	-.02536	-.01439	-.02835	-.00846	.08560	.19956
S12	.35143	.34070	.23403	.00660	-.01436	-.20842
S13	.54593	-.46613	.01695	.06288	-.37403	.46933
S14	.17844	-.37366	-.56756	.37299	.14079	-.32839
S15	-.65215	.54017	-.08242	.08953	-.07933	.08317
S16	-.07127	.06073	-.00376	.02506	-.01831	.00751
S17	.03076	-.04073	-.36224	-.16025	-.01762	-.00316
S18	-.03879	.03936	.00278	-.18340	.18557	-.00027
S19	.03426	-.02910	-.00492	-.01658	-.15622	.35361

---

continued

TABLE 3-3 continued

	S7	S8	S9	S10	S11	S12
S7	7.91528					
S8	.03642	6.93739				
S9	.01867	-.00120	6.31931			
S10	.00075	-.00096	.01360	6.38005		
S11	.01605	-.00276	.00229	.01357	6.31713	
S12	.23673	-.00808	.00529	-.11521	.08425	1.70170
S13	.24604	-.01362	-.00673	.05342	.02429	.01515
S14	-.37339	.02201	.02147	-.09266	.08548	-.00640
S15	.11380	.08132	.00918	.00140	-.00888	-.02262
S16	.49751	.29046	.00167	-.00215	-.00182	.02196
S17	-.00971	-.00064	.01156	-.00448	.00749	-.01526
S18	-.00343	-.00100	.00162	.00067	-.00184	-.00117
S19	.00839	-.00259	-.00771	.00398	-.01263	.01456

	S13	S14	S15	S16	S17	S18	S19
S13	1.67077						
S14	-.16276	1.83607					
S15	-.06862	-.00657	1.37391				
S16	.00651	-.00108	.16156	.83260			
S17	.04143	.07959	-.01220	-.00322	.69191		
S18	-.09422	-.05470	-.00692	-.00224	.01008	.60824	
S19	.00831	-.00521	-.01425	-.00219	-.01193	.00968	.66520

---

continued

TABLE 3-3 continued

	S20	S21	S22	S23	S24	S25	S26	S27
S20	.36881							
S21	-.02987	.30688						
S22	.06021	-.00981	.34371					
S23	-.16468	-.09061	.15987	.87296				
S24	.00630	-.00177	-.01384	-.02474	.06653			
S25	-.15087	.16175	.02646	-.00342	.00212	.64188		
S26	.19043	-.08513	.15924	-.04509	.00110	-.07352	.57952	
S27	-.15199	-.09172	-.13847	-.00939	.00127	-.02982	.08223	.63842

[a]The reference geometry is the 4-31G optimized geometry of 2-pyrimidinol (Table 3-2).

[b]The symmetrized internal coordinates are defined in Table 3-4.

[c]The units are md/A for stretch-stretch, md for bend-stretch, and md-A for the rest.

[d]The force field is symmetrized where the interaction between in-plane and out-of-plane force constants is zero, and $F_{ij} = F_{ji}$.

TABLE 3-4
SYMMETRIZED INTERNAL COORDINATES FOR 2-PYRIMIDINOL

In-plane[a,b]

S1	= $\Delta r1$	= rN1C2
S2	= $\Delta r2$	= rC2N3
S3	= $\Delta r3$	= rN3C4
S4	= $\Delta r4$	= rC4C5
S5	= $\Delta r5$	= rC5C6
S6	= $\Delta r6$	= rC6N1
S7	= $\Delta r7$	= rC2O
S8	= $\Delta r8$	= rOH
S9	= $\Delta r9$	= rC4H
S10	= $\Delta r10$	= rC5H
S11	= $\Delta r11$	= rC6H
S12	= $(1/6)^{0.5}\{\Delta\beta12-\Delta\beta13+\Delta\beta14-\Delta\beta15+\Delta\beta16-\Delta\beta17\}$	= δIR
S13	= $(1/12)^{0.5}\{2\Delta\beta12-\Delta\beta13-\Delta\beta14+2\Delta\beta15-\Delta\beta16-\Delta\beta17\}$	= δIIR
S14	= $(1/2)\{\Delta\beta13-\Delta\beta14+\Delta\beta16-\Delta\beta17\}$	= δIIIR
S15	= $(1/2)^{0.5}\{\Delta\beta18-\Delta\beta23\}$	= δC2O
S16	= $\Delta\beta19$	= δCOH
S17	= $(1/2)^{0.5}\{\Delta\beta20-\Delta\beta24\}$	= δC4H
S18	= $(1/2)^{0.5}\{\Delta\beta21-\Delta\beta25\}$	= δC5H
S19	= $(1/2)^{0.5}\{\Delta\beta22-\Delta\beta26\}$	= δC6H

---

continued

TABLE 3-4 continued

Out-of plane[a,b]

$S20 = (1/6)^{0.5}\{\Delta\tau1-\Delta\tau2+\Delta\tau3-\Delta\tau4+\Delta\tau5-\Delta\tau6\}$	$= \tau I\Theta$
$S21 = (1/2)\{\Delta\tau I-\Delta\tau3+\Delta\tau4-\Delta\tau6\}$	$= \tau II\Theta$
$S22 = (1/12)^{0.5}\{-\Delta\tau1+2\Delta\tau2-\Delta\tau3-\Delta\tau4+2\Delta\tau5-\Delta\tau6\}$	$= \tau III\Theta$
$S23 = \Delta\gamma O\Delta$	$= \gamma O$
$S24 = (I/2)^{0.5}\{\Delta\tau7+\Delta\tau\Delta\}$	$= \tau OH$
$S25 = \Delta\gamma H9$	$= \gamma H9$
$S26 = \Delta\gamma HI0$	$= \gamma H10$
$S27 = \Delta\gamma H11$	$= \gamma H11$

[a]The nomenclature and numbering follow Figure 3-3. The recommendations of Pulay et al. (Reference 11) are carried out.

[b]The atoms involved in torsions are: $\tau1$=6123, $\tau2$=1234, $\tau3$=2345, $\tau4$=3456, $\tau5$=4561, and $\tau6$=5612.

TABLE 3-5
ATOMIC POLAR TENSORS FOR 2-PYRIMIDINOL
EVALUATED AT THE HF SCF LEVEL WITH A 4-31G BASIS SET

N1[a,b,c]

-.50124	.21353	0
-.35140	-1.08300	0
0	0	-.44553

O7

-.27401	.10323	0
.06516	-1.67432	0
0	0	-.64123

C2

.39693	-.09379	0
-.05204	2.19208	0
0	0	.59127

H8

.23131	-.07765	0
-.02949	.49910	0
0	0	.45802

N3

-.45981	-.12835	0
.36158	-1.03260	0
0	0	-.40389

H9

.02322	.07622	0
.07175	.04747	0
0	0	.09993

C4

.72660	.24381	0
-.08096	.59477	0
0	0	.12908

H10

.09895	-.00274	0
-.00369	-.05791	0
0	0	.18321

C5

-.87720	.01853	0
-.01445	-.07804	0
0	0	.21652

H11

-.02853	-.06734	0
-.06973	.05286	0
0	0	.10410

C6

.71044	-.28551	0
.09882	.53548	0
0	0	.14157

[a]Units are in electrons (e).

[b]The atom numbering is given in Figure 3-3; the coordinate system orientation is the principal cartesian coordinates of Table 3-6.

[c]The reference geometry is the 4-31G optimized geometry of 2-pyrimidinol (Table 3-2).

TABLE 3-6
PRINCIPAL CARTESIAN COORDINATES, GROUND STATE ENERGIES, AND GROUND STATE DIPOLE MOMENTS OF 2-PYRIMIDINOL AT THE 4-31G OPTIMIZED GEOMETRY

	X[a]	Y[a]	Z[a]
N1	1.158530	-.251557	0
C2	-.024006	-.843013	0
N3	-1.186380	-1.218328	0
C4	-1.161310	1.108035	0
C5	.025131	1.820646	0
C6	1.186947	1.077612	0
O7	-.052523	-2.179809	0
H8	.820612	-2.561703	0
H9	-2.111279	1.598478	0
H10	.038884	2.888357	0
H11	2.153680	1.534123	0

ENERGY (AU)[b]

= -337.04834994 (10^{-9} CG, 10^{-10} IT, 4-31G BS)[c]

= -337.04836268 (10^{-8} CG, 10^{-6} IT, 4-31G BS)[d]

= -337.04836254 ($5 * 10^{-5}$ CG, 10^{-6} IT, 4-31G BS)[d]

DIPOLE (DEBYES)[b]

= 3.7388 (10^{-9} CG, 10^{-10} IT, 4-31G BS)[c]

= 3.7384 (10^{-8} CG, 10^{-6} IT, 4-31G BS)[d]

= 3.7388 ($5 * 10^{-5}$ CG, 10^{-6} IT, 4-31G BS)[d]

[a]Principal cartesian coordinates in A. The 4-31G optimized geometry is shown in Table 3-2. The atom numbering is shown in Figure 3-3.

[b]The terms CG, IT, and BS stand for the convergence, integral threshold, and basis set respectively, that were used in the corresponding calculation.

[c]The calculation was performed with GAUSSIAN 82 (Reference 32).

[d]The calculation was performed with GAUSSIAN 76 (Reference 53).

TABLE 3-7
CALCULATED FREQUENCIES AND INTENSITIES FOR
2-PYRIMIDINOL AT THE HF SCF LEVEL WITH A 4-31G BASIS SET

ν	Calculated[a,b] Frequency (cm^{-1})	Calculated[a,b] Intensity (km/mole)	Calculated[a,c] Frequency *0.9 (cm^{-1})
1	3997.9	138.0	3598.1
2	3423.2	7.2	3080.9
3	3397.9	20.0	3058.1
4	3391.4	2.9	3052.3
5	1785.2	209.1	1606.7
6	1762.3	178.4	1586.0
7	1650.8	211.7	1485.7
8	1616.3	160.9	1454.7
9	1500.7	9.7	1350.7
10	1462.3	115.0	1316.1
11	1312.9	159.1	1181.6
12	1266.9	17.5	1140.2
13	1190.6	36.1	1071.5
14	1184.4	14.3	1066.0
15	1102.3	2.2	992.0
16	962.6	22.8	866.3
17	721.0	10.4	646.9
18	657.7	0.4	592.0
19	482.1	22.5	433.9
20	1178.4	1.0	1060.6
21	1156.4	0	1040.6
22	941.2	117.7	847.1
23	928.8	3.2	835.9
24	617.9	19.0	556.1
25	555.4	185.8	499.9
26	489.5	5.5	440.6
27	256.4	4.5	230.8

[a]The 4-31G force field (Table 3-3) and 4-31G APTs (Table 3-5) were used.

[b]Correspond to unscaled results.

[c]Correspond to scaled results.

TABLE 3-8
PERCENTAGE POTENTIAL ENERGY DISTRIBUTION FOR 2-PYRIMIDINOL BY THE MK AND KJ METHODS AT THE HF SCF LEVEL WITH A 4-31G BASIS SET

	MK METHOD[a,b]	KJ METHOD[a,b]
1	100S8	100S8
2	12S9,75S10,12S11	12S9,75S10,12S11
3	52S9,47S11	52S9,47S11
4	36S9,25S10,40S11	35S9,24S10,40S11
5	24S2,11S3,25S5,17S6,10S13,13S19	21S2,10S3,23S5,14S6,11S19
6	20S1,14S3,31S4,11S14,16S17	17S1,11S3,28S4,13S17
7	12S2,11S5,24S7,16S17,13S18	12S2,10S5,21S7,15S17,12S18
8	13S1,10S7,27S18,30S19	13S1,27S18,28S19
9	10S3,13S7,37S17	16S3,14S7,40S17
10	12S7,25S16,12S17,35S19	22S16,11S17,36S19
11	47S16,15S18	45S16,16S18
12	17S1,17S2,48S3,5OS6,21S18	32S3,34S6,20S18
13	12S1,28S2,54S5,10S16,10S18	19S2,49S5,12S18
14	22S1,56S4	15S1,54S4
15	64S12	59S12
16	15S1,17S2,25S7,14S14	20S1,22S2,27S7,11S14
17	72S13,22S14	69S13,18S14
18	14S7,12S13,50S14	18S7,15S13,57S14
19	85S15	80S15
20	15S20,44S25,48S26,42S27	37S25,41S26,36S27
21	58S25,55S27	54S25,52S27
22	77S20,69S23,25S26	39S20,40S23,15S26
23	38S20,13S23,22S25,46S26,28S27	26S20,10S25,50S26,12S27
24	28S20,10S21,33S22,39S23,13S24, 18S26	34S20,20S22,32S23,12S24
25	15S22,87S24	86S24
26	92S21,25S22	83S21,20S22
27	19S21,67S22	16S21,60S22,17S23

[a]The MK and KJ methods detailed in Chapter 2 (References 65 and 66). The 4-31G force field (Table 3-3) and unscaled frequencies (Table 3-7) are used in the methods

[b]The asymmetrized internal coordinates of Table 3-4 are used. As in example of Table 3-1, 100S8 for ν_1 mode means 100% contribution by S8 coordinate to ν_1 fundamental mode. This nomenclature is used in all future PED tables and explanations.

helpful in similar situations.[48,67,68] Thus the assignment can be carried out using Figures 3-4 and 3-5.

The fundamental bands in the experimental spectrum are split in various instances, e.g., fundamental ν5 (Figures 3-4, 3-5). We shall not attempt to define the exact causes for this experimental splitting. In general, band splitting is due to matrix effects, hydrogen bonding, Fermi resonance, tunneling, and rotational isomerism. Further complications are found when tautomerism and polymeric aggregation are taking place significantly. As mentioned in Section 1.1 many of these effects can be discarded as far as this dilute Ar matrix spectrum is concerned. The 2-oxopyrimidine system is known to be only in the monomeric 2-pyrimidinol form.[2,6] One can safely rule out tautomerism, hydrogen bonding and polymeric aggregation.[2,6] Hence Fermi resonance, rotational isomerism, and matrix effects are considered to be major reasons for the experimental band splitting observed here.

In the experimental spectrum of 2-oxopyrimidine small bands that could not be easily explained have been grouped together as "region a," "region b," "region c," and "region d" respectively (see Figures 3-1, 3-2, 3-3, and 3-4). Possible explanations for the absorption in these regions are combinations and/or overtones of fundamental bands of 2-pyrimidinol, the presence of traces of 2-pyrimidinone, and possibly impurities.

We now concentrate on specific regions of the experimental spectrum and compare the absorption there

Figure 3-4. Comparison between the experimental Ar matrix spectrum of 2-oxopyrimidine and the frequency-scaled predicted IR spectrum of 2-pyrimidinol for the 4000 - 3000 reciprocal cm region. The EXPT spectrum is redrawn from that for the isolated 2-oxopyrimidine sample in dilute Ar matrix at 10 K (Reference 5). The CALC spectrum is the frequency-scaled set of predictions from the full 4-31G study (Table 3-7). The scaling constant is 0.9 for all calculated frequencies. The term a in the EXPT spectrum stands for "Region a" (see Table 3-1).

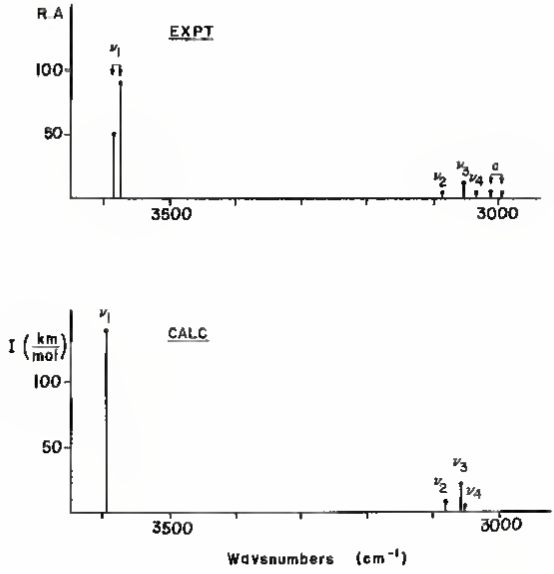
R.A
EXPT
100
50
ν_1
ν_2
ν_3
ν_4
a
3500
3000
I $\left(\frac{km}{mol}\right)$
CALC
100
50
ν_1
ν_2
ν_3
ν_4
3500
3000
Wavsnumbers (cm^{-1})

Figure 3-5. Comparison between the experimental Ar matrix spectrum of 2-oxopyrimidine and the frequency-scaled predicted IR spectrum of 2-pyrimidinol for the 2000 - 400 reciprocal cm region. The EXPT spectrum is redrawn from that for the isolated 2-oxopyrimidine sample in dilute Ar matrix at 10 K (Reference 6). The CALC spectrum is the frequency-scaled set of predictions from the full 4-31G study (Table 3-7). The scaling constant is 0.9 for all calculated frequencies. The predicted band at 256.4 reciprocal cm (fundamental mode 27 of Table 3-7) is not shown in the CALC spectrum. The terms b, c, and d in the EXPT spectrum stand for "Region b," "Region c," and "Region d" respectively (see Table 3-1).

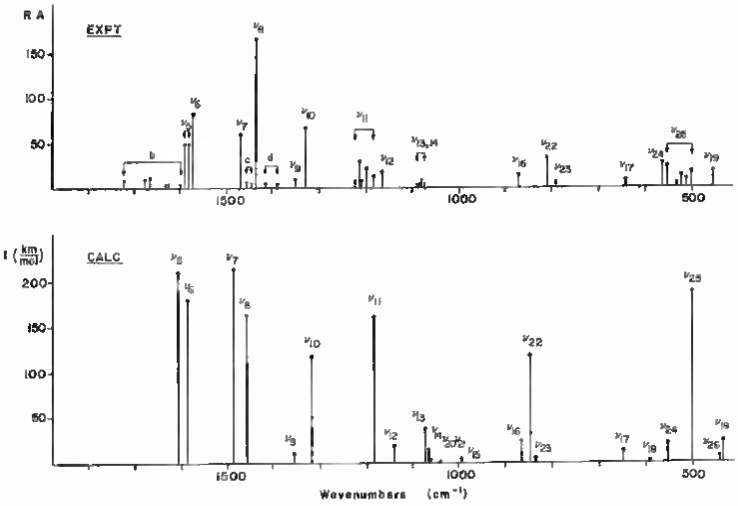
R A
EXPT
150
100
50
ν8
ν6
ν5
ν7
ν10
ν11
ν13,14
ν12
ν9
ν16
ν22
ν23
ν17
ν24
ν26
ν19
b
c
d
1500
1000
500
I (km/mol)
CALC
200
150
100
50
ν8
ν6
ν7
ν11
ν25
ν10
ν22
ν9
ν12
ν13
ν16
ν23
ν17
ν18
ν24
ν26
ν19
1500
1000
500
Wavenumbers (cm⁻¹)

with the theoretical predictions to make the assignments. The PEDs by the "KJ method" (Table 3-8) are used to describe the normal modes of the fundamental bands.

3.3.1 Region 4000-2000 cm^{-1}

Two bands around 3600 cm^{-1} and a series of weak bands around 3100-3000 cm^{-1} are seen experimentally in this region (see Figure 3-4). Based on our prediction for ν_1 the two experimentally observed bands around 3600 cm^{-1} are assigned to a split ν_1 O-H stretching mode. Possible reasons for the splitting are matrix effects, tunneling, and rotational isomerism. The first three experimental weak bands observed around 3100-3000 cm^{-1} are assigned to the C-H stretching modes ν_2, ν_3, and ν_4 respectively. Mode ν_2 is due to a mixture of all three C-H stretches where rC5H is predominant. Mode ν_3 is a 1:1 combination of C4H and C6H stretches. Mode ν_4 corresponds to a roughly equal combination of all in-plane C-H stretches. The bands in "region a" (3013 - 2997 cm^{-1}) are probably due to combination bands involving ν_5 and ν_6 modes which have strong absorptions. These results are consistent with the assignments based on characteristic frequencies.[69] In this region the assignments for other purine and pyrimidine bases[1-4] are similar to the ones proposed here. No other fundamentals are expected in this region for 2-pyrimidinol.

3.3.2 Region 2000-1400 cm^{-1}

In this region (Figure 3-5) the experimental absorption bands assigned to the ν_5 through ν_8 fundamentals are observed. These bands are commonly referred to as

breathing vibrations of aromatic rings.[69] The weak experimental bands of "region b" (1722.5 - 1600.5 cm^{-1}), "region c" (1458 - 1445 cm^{-1}), and "region d" (1417 - 1390 cm^{-1}) are also seen here. By comparing the upper and lower parts of Figure 3-5 it can be seen that the assignment of experimental bands is straightforward. The only complication concerns the ν5 mode. The calculated intensities for the ν5 and ν6 fundamentals are roughly equal. Thus the experimental doublet assigned to ν5 is believed to be due to splitting of the band by Fermi resonance so that the experimental intensity for ν5 is the sum of the intensities of bands in the doublet. The ratio between the calculated intensities for ν7 and ν8 is opposite to the one observed for the corresponding experimental bands. This fact can be attributed to the limitations of the level of theory and basis set used in the calculation. It is possible that because of these limitations the aromatic electronic delocalization is not properly explained. This in turn would affect the values of force constants and intensities. The PED results (Table 3-8) indicate that modes ν5 through ν8 are due to in-plane bends and ring stretches. Bands in "region b" (Figure 3-5) are probably due to C=O stretches of 2-pyrimidinone tautomer and/or to combination bands of 2-pyrimidinol.[2,69] Similarly bands in "region c" and "region d" are probably combination bands[69] of lower frequency modes of 2-pyrimidinol.

Various other pyridine and pyrimidine systems show similar breathing modes and combination bands in this region.[69] A point of interest is the split ν5 band. Since many combination bands are possible near this band, Fermi resonance seems a plausible reason for the splitting. The latter explanation is preferred over matrix effect or rotational isomerism arguments. This is inferred from the fact that the normal coordinates (PEDs) for all breathing modes are similar and all should be split for the same reasons.

3.3.3 Region 1400-1000 cm^{-1}

A series of experimental absorption bands are observed in this region (Figure 3-5). From comparison of calculated spectra with observed, the assignment of ν9 and ν10 fundamentals is straightforward. These bands are due mostly to couplings of in-plane C-H bends with the C-O stretch and to a lesser extent with the COH bend. The ν11 and ν12 fundamentals are harder to assign. We believe that ν11 fundamental in the experimental spectrum is split into five bands. The reason is because the intensity calculated for ν11 is too high to be explained by one of the low intensity bands observed in this part of the spectrum. The PED table shows that ν11 is predominantly the in-plane COH bending. This band may be expected to be quite sensitive to the environment of the molecule. The ν12 band has no contribution from in-plane δCOH, and is expected to be a single band quite in agreement with our calculations.

Four weak experimental bands are observed around 1100 cm^{-1} (Figure 3-5). Calculations in this area predict two in-plane fundamentals, ν_{13} and ν_{14}, and two very weak out-of-plane fundamentals, ν_{20} and ν_{21}. The corresponding experimental bands are so weak and close to each other that we assign them to the ν_{13} and ν_{14} fundamentals. Based on the calculated intensities for the out-of-plane fundamentals ν_{20} and ν_{21} we do not expect that they be seen at all in the experimental spectrum. The PED table shows that ν_{13} and ν_{14} are due mostly to in-plane ring stretches, and ν_{20} and ν_{21} to out-of-plane H bends, γH's.

The splitting of the experimental ν_{11} fundamental is of particular interest. To explain it in terms of Fermi resonance or combination bands does not seem right. This is evident by looking at the experimental out-of-plane ν_{25} fundamental. This band is due mostly to out-of-plane torsion involving the O and H atoms of the hydroxyl bond, τOH. The absorption assigned to ν_{25} displays a very similar pattern to that for ν_{11} band which is due to in-plane δCOH. Since Fermi resonance or combination bands (not possible at all in the ν_{25} area) cannot explain the structure for the ν_{25} band it could be argued that they also do not explain either the analogous ν_{11} band. This leaves us with matrix interaction, tunneling, and rotational isomerism (i.e., in-plane or out-of-plane rotamers of the OH group) as the most probable reasons for the splitting of the ν_{11} band. The OH group can be visualized as subject to various orientations with respect to the ring, and/or interactions within the matrix.

3.3.4 Region 1000-200 cm^{-1}

In this region a few experimental low frequency in-plane fundamentals and most of the experimental out-of-plane fundamentals are observed (Figure 3-5). A weak band predicted for ν15 around 1000 cm^{-1} due to in-plane ring bends, δR1, is not seen experimentally. In the 500-800 cm^{-1} portion of the spectrum the experimental bands are assigned as ν16, ν22, and ν23 respectively based on the correasponding predicted bands in this region. Halogenation studies,[6] which replaced H10 of 2-pyrimidinol by Br or Cl, showed that the experimental 871 cm^{-1} band of the spectrum of 2-pyrimidinol remains unchanged throughout halogenation. This was not the case for the 810 cm^{-1} band. From the PED results (Table 3-8) ν22 is shown to depend more on the coordinates of the molecule in the region immediately adjacent to H10; hence it is sensible to assign it to the band observed experimentally at 810 cm^{-1}.

The assignment of the remaining experimental fundamentals is rather straightforward by comparison with the calculated spectrum. The major difficulty occurs for the ν25 fundamental due to the out-of-plane torsion TOH. This split band has been already explained in connection with discussion of the ν11 fundamental involving th in-plane bend of the COH group. The predicted ν27 band cannot be compared to experimental results, since the experimental study did not cover the region below 400 cm^{-1}.

3 4 Summary

Table 3-1 summarizes the assignment and interpretation of the IR spectrum of 2-oxopyrimidine in a dilute low temperature Argon matrix. For purposes of simplifying these results Table 3-9 is constructed. This table provides a direct comparison of experimental to calculated spectra for 2-pyrimidinol. The experimental frequencies are the assigned fundamentals, disregarding peaks from regions a, b, c, and d. For split bands such as v5 the average of the split band frequencies is listed as the experimental value. For v13 and v14 the same frequency is reported. The experimental absorbances are the R.A.s reported in Table 3-1. For split bands the R.A.s are added so as to give the total R.A. for the fundamental. For v13 and v14 the R.A. values are assumed to be equal.

The calculated frequencies reported in Table 3-9 are the calculated scaled frequencies (multiplied by the single scaling constant of 0.9) as described in Table 3-7. The calculated R.A.s of Table 3-9 are the unscaled calculated intensities (Table 3-7) multiplied by a conversion constant. We call this conversion constant the absorbance-intensity conversion constant. The absorbance-intensity conversion constant for the in-plane case is the ratio of the sum of in-plane experimental R.A.s to the sum of the in-plane calculated intensities (Table 3-7). It is equal to 0.577 (=772.1/1338.0). Similarly the absorbance-intensity conversion constant for the out-of-plane modes is 0.360

(=121.2/336.6) The unobserved ν27 is not taken into account. This conversion constant is essentially the product of the cell path length, the molute concentration and a scaling constant averaged over the number of considered fundamentals. Thus the usage of this conversion constant can hardly be called scaling of the absorbances. It is used to enable us to have a more proper comparison of the band absorbances. This method can only be used after the assignment of the experimental spectrum has been made. Figure 3-6 shows the plot of the results of Table 3-9

The agreement shown in Figure 3-6 and Table 3-9 show that the relationship between experimental and calculated spectra is quite satisfactory The only significant modification of the calculated results is the multiplication of all frequencies by a single scaling constant, 0.9. The discrepancies that were seen between the R.A.s and the intensities of Figures 3-4 and 3-5 are minimized by the usage of the absorbance-intensity conversion constants. The methods used in the construction of Table 3-9 will be useful in future chapters.

It is interesting that the absorbance-intensity conversion constant used for the out-of-plane modes is smaller than for the in-plane modes. This is consistent with previous findings in calculations of intensities of large molecules at the HF SCF level with small basis sets. It was found that in general out-of-plane intensities are predicted to be much higher in comparison to experimental values than are those predicted for the in-plane intensities.

In short it can be said that the assignment is satisfactory, and in good agreement with literature results throughout the entire IR region. The usage of the 4-31G basis set at the RHF SCF level is rewarding. It shows that this level of theory can be used reliably for large molecules like 2-pyrimidinol. Figures 3-1 and 3-2 which compare the experimental frequencies and intensities to the unscaled calculated spectrum of 2-pyrimidinol could have been just as well used for assignment purposes as were Figures 3-4 and 3-5. These figures are included in this chapter to show that with the 4-31G basis set at the RHF SCF level quite satisfactory unscaled results are obtained. The usage of 0.9 as a scaling constant for frequencies is done exclusively to ease the work of assignment of experimental spectra. This is quite different from procedures to fit calculated to experimental spectra by statistical methods.

TABLE 3-9
COMPARISON OF
EXPERIMENTAL AND CALCULATED SPECTRA OF 2-PYRIMIDINOL

ν	Experimental Fraquancy[a,b]	Experimental R A[a,c]	0.9*Calculated Frequency[a,d]	Calculated R.A.[a,e]
1	3579.0	138.0	3598.1	79.6
2	3088	1.1	3080.9	4.2
3	3053	10.1	3058.1	11.5
4	3034	1.5	3052.3	1.7
5	1587.0	97.2	1606.7	120.7
6	1573	81.2	1586.0	102.9
7	1469.5	59.2	1485.7	122.2
8	1434.5	164.5	1454.7	92.8
9	1351.5	7.0	1350.7	5.6
10	1329	66.8	1316.1	66.4
11	1207.4	75.5	1181.6	91.8
12	1160	17.5	1140.2	10.1
13	1082	8.5	1071.5	20.8
14	1082	8.5	1066.0	8.3
15	--	0	992.0	1.3
16	871	13.3	866.3	13.2
17	641.5	5.2	648.9	6.0
18	--	0	592.0	0.2
19	457.5	17.0	433.9	13.0
20	--	0	1060.6	0.4
21	--	0	1040.8	0
22	810	32.2	847.1	42.4
23	793	3.7	835.9	1.2
24	564	26.5	556.1	6.8
25	526.2	58.8	499.9	66.9
26	--	--	440.6	2.0
27	--	--	230.8	1.6

[a] The plot is given in Figure 3-6.

[b] Experimental frequencies in cm^{-1} of fundamental modes of 2-pyrimidinol as assigned in Chapter 3 (from Table 3-1).

[c] Experimental integrated relative absorbances of fundamental modes of 2-pyrimidinol are from Table 3-1.

[d] Frequencies in cm^{-1} copied from Table 3-7.

[e] Calculated intensities for 2-pyrimidinol at the HF SCF level with a 4-31G basis set (of Table 3-7) multiplied by absorbance-intensity conversion constants (0.577 for in-plane modes, and 0.360 for out-of-plane modes as explained in Section 3.4).

Figure 3-6. Comparison of experimental to calculated spectra of 2-pyrimidinol. The EXPT values correspond to analysis of experimental results (Table 3-9). The CALC values correspond to analysis of full 4-31G study (Table 3-9).

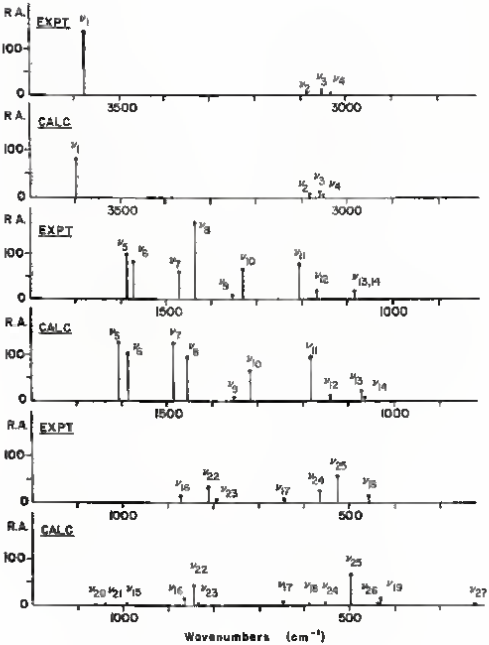
R.A.
EXPT
100
0
3500
3000
CALC
1500
1000
500
Wavenumbers (cm⁻¹)

CHAPTER 4
EFFECT OF UPGRADING THE FORCE FIELD IN DIFFERENT COORDINATE SYSTEMS ON PREDICTED IR SPECTRUM OF 2-PYRIMIDINOL

As discussed in Chapter 1 it is customary to upgrade or scale force fields. No consistent study has been carried out on the effect on predicted IR spectra of choosing different coordinate systems for the scaling of force constants. The purpose of this chapter is to study this effect. The presentation will be divided in three major sections: methods, survey of results, and conclusions.

4.1 Methods

The optimized geometry of 2-pyrimidinol calculated at the HF SCF level with an STO-3G basis set (Section 2.1.1.1) was utilized as reference state to evaluate the force field for this molecule at the HF SCF level with an STO-3G basis set (Section 2.1.1.3). Table 4-1 gives this optimized geometry. Table 4-2 shows this force field expressed in symmetrized internal coordinates (S coordinates).

This STO-3G force field was upgraded by scaling according to Equation 1-3 where F^{th} was this STO-3G force field; C was the diagonal matrix of scaling constants chosen to be the ratios of the diagonal force constants of the 4-31G force field (Table 3-3) to the corresponding values of the STO-3G force field (Table 4-2). For example for S1 the conversion constant was 8.90281/8.86576 = 1.0042. These conversion constants, also referred to as scaling constants,

TABLE 4-1
OPTIMIZED GEOMETRY OF 2-PYRIMIDINOL
AT THE HF SCF LEVEL WITH AN STO-3G BASIS SET

i	r_i(A)[a]	i	θ_i(degrees)[a]
1	1.357	12	114.3
2	1.381	13	128.5
3	1.349	14	113.8
4	1.390	15	123.4
5	1.384	16	117.2
6	1.352	17	122.9
7	1.381	18	114.9
8	0.969	19	103.7
9	1.089	20	120.8
10	1.079	21	121.5
11	1.088	22	118.2
		23	118.8
		24	118.0
		25	121.4
		26	121.0

[a]Bond lengths, r, and Angles, θ, according to Figure 3-3. The geometry was optimized by the HFGS procedure of Head and Zerner (References 32 and 54).

TABLE 4-2
FORCE CONSTANTS FOR 2-PYRIMIDINOL
IN SYMMETRIZED INTERNAL COORDINATES S
EVALUATED AT THE HF SCF LEVEL WITH AN STO-3G BASIS SET

	S1[a,b,c,d]	S2	S3	S4	S5	S6
S1	8.86576					
S2	1.50876	8.69719				
S3	-1.10107	1.21220	8.57506			
S4	1.03951	-1.17687	1.54227	8.96455		
S5	-1.18176	1.05178	-1.09015	1.42294	8.22658	
S6	1.23338	-1.10415	1.32587	-1.10825	1.53006	8.43410
S7	.68538	.72887	-.15541	-.04507	-.12037	-.12242
S8	-.08887	-.03737	.00163	.02001	-.00275	-.00630
S9	-.01153	.00558	.11772	-.04775	.00376	-.03200
S10	-.00352	-.00775	-.03240	-.03305	-.03210	-.03625
S11	-.00473	-.00471	-.03384	.00558	-.04819	.11627
S12	.41017	.40662	.26764	.02181	.00262	.24900
S13	.60456	-.47346	.03831	.00884	-.35478	.51826
S14	.13685	-.42485	-.64181	.32821	.08658	-.37815
S15	-.53146	.44269	-.04655	.05840	-.04424	.04814
S16	-.10648	.06855	.00826	.01860	-.02136	.00668
S17	.02709	-.04601	-.30842	.16567	.00381	.00428
S18	-.03442	.03356	.00917	-.20034	.20258	-.00875
S18	.04066	-.02484	-.00504	-.00324	-.16448	.30203

---

continued

TABLE 4-2 continued

	S7	S8	S9	S10	S11	S12
S7	8.49432					
S8	-.32324	10.16835				
S9	.01071	-.00121	7.48348			
S10	-.03560	.00282	-.00791	7.69100		
S11	.01090	-.00107	-.00240	.00863	7.48874	
S12	.12292	-.01429	.08174	-.09967	.08238	1.70342
S13	.16552	-.02047	-.06850	.03296	.01623	.01319
S14	-.23223	.02215	.02122	-.05805	.07061	-.01194
S15	.03145	.14216	.00127	.00247	-.00614	-.02273
S16	.60720	.24900	.00309	.00038	-.00005	.03664
S17	-.00072	-.00221	-.00936	-.01517	.00558	-.01813
S18	-.00215	-.00114	.01643	.00067	-.01635	-.00054
S19	.00302	-.00314	-.00550	.01520	.00919	.01834

	S13	S14	S15	S16	S17	S18	S19
S13	1.68339						
S14	-.08394	1.76964					
S15	-.12472	-.03348	1.22572				
S16	.00214	-.02737	.22877	1.32672			
S17	.04188	.09159	-.02111	-.00802	.74423		
S18	-.09698	-.05582	-.00377	-.00287	.01264	.65009	
S19	.09969	-.01084	-.02139	-.00316	-.01537	.01260	.74085

---

continued

TABLE 4-2 continued

	S20	S21	S22	S23	S24	S25	S26	S27
S20	.41816							
S21	-.03432	.32777						
S22	.06093	.00539	.32568					
S23	- 19659	-.09543	.16032	.77648				
S24	.01022	.00370	-.01387	-.03633	.07261			
S25	-.18931	.21048	.01743	-.01353	.00485	.68333		
S26	.21864	-.09638	.17845	-.04518	.00359	- 08667	.62538	
S27	-.18908	-.11174	-.17616	-.01204	.00195	-.02568	-.09231	.68171

[a]The reference geometry is the STO-3G optimized geometry of 2-pyrimidinol (Table 4-1).

[b]The symmetrized internal coordinates are defined in Table 3-4.

[c]The units are md/A for stretch-stretch, md for bend-stretch, and md-A for the rest.

[d]The force field is symmetrized where the interaction between in-plane and out-of-plane force constants is zero, and $F_{ij} = F_{ji}$.

TABLE 4-3
THE 4-31G/STO-3G SCALING CONSTANTS
FOR 2-PYRIMIDINOL USED IN THE SC, XCD, AND WCD METHODS

S	C_s	C_{xd}	C_{wd}
1	1.0042	.9788	.9794
2	1.0266	.9830	.9777
3	.9226	.9340	.9381
4	.8847	.8951	.8810
5	.8836	.8943	.9072
6	.9247	.9342	.9306
7	.9318	.8886	.8889
8	.8789	.8577	.8513
9	.8438	.8552	.8578
10	.8295	.8298	.8442
11	.8436	.8539	.8546
12	.9990	.9165	.9155
13	.9925	.9271	.9512
14	1.0375	.9044	.9083
15	1.1209	.9360	.9851
16	.6728	.8195	.8313
17	.9297	.8675	.8579
18	.9356	.9356	.8745
19	.9249	.8685	.8631
20	.8820	1.0054	.9869
21	.9363	.9934	1.0211
22	1.0554	.9743	.9779
23	1.1243	1.2008	1.2605
24	.9163	.9255	.9390
25	.9393	.9509	.9779
26	.9257	.9303	.9347
27	.9365	.9476	.9620

Note: The scaling constants correspond to the methods of Section 4.1.

are given as the C_e values of Table 4-3. From the C values and the F^{th} force field, F was obtained. Force field F is referred to as a "near 4-31G" force field.

This "near 4-31G" force field was then used to calculate bond frequencies and potential energy distribution (PEDs) of 2-pyrimidinol by the method to determine frequencies and the "MK method" respectively of Chapter 2. The band intensities were calculated via Equation 2-22 where the L matrix from this "near 4-31G" force field was used together with the atomic polar tensors (APTs) of 2-pyrimidinol evaluated at the HF SCF level with a 4-31G basis set (Table 3-5). This whole process is defined by the name "SC method" which stands for the "symmetrized internal coordinate method." The frequencies, PEDs, and intensities obtained by this method are given in Tables 4-4, 4-5, and 4-6 respectively under the SC heading.

Similarly we considered other prescriptions for upgrading the STO-3G force field expressed in other coordinate systems. The "WC method" and the "XC method" were done with an F^{th} force field (Equation 1-3) calculated for W and X coordinate displacements respectively. The W coordinates were the ones described in Chapter 2, and the X coordinates were the cartesian coordinates. The F^{th} force field used with the WC and XC methods was the same STO-3G force field of Table 4-2 expressed in W and X displacement coordinates respectively. These coordinate interconversions are shown in Equations 2-6 through 2-11.

TABLE 4-4
PREDICTED BAND FREQUENCIES OF 2-PYRIMIDINOL
OBTAINED FROM THE FORCE FIELDS OF VARIOUS SCALING METHODS

ν	4-31G	XC	XCD	SC	WC	WCD	STO-3G
1	3997.9	3953.6	3952.4	4001.1	3937.0	3937.4	4267.6
2	3423.2	3440.7	3437.9	3429.8	3465.2	3458.9	3760.8
3	3397.9	3431.8	3428.2	3406.7	3438.6	3432.4	3707.4
4	3391.4	3415.0	3411.8	3398.0	3413.0	3422.4	3701.8
5	1785.2	1836.8	1821.6	1834.8	1838.4	1825.6	1908.9
6	1762.3	1809.7	1799.3	1809.0	1807.3	1796.3	1887.6
7	1650.8	1670.1	1668.7	1690.6	1676.6	1663.3	1756.1
8	1616.3	1628.7	1632.1	1648.2	1614.6	1621.1	1704.9
9	1500.7	1510.8	1503.3	1499.1	1514.1	1504.1	1624.8
10	1462.3	1476.4	1469.0	1466.6	1478.3	1466.6	1549.6
11	1312.9	1331.1	1335.0	1315.6	1328.0	1329.6	1409.1
12	1266.9	1251.8	1244.1	1234.6	1223.9	1224.4	1291.7
13	1190.6	1179.1	1193.1	1200.6	1179.0	1191.2	1263.6
14	1184.4	1073.6	1059.9	1091.2	1078.8	1059.8	1100.3
15	1102.3	994.9	990.1	992.7	994.4	988.7	1020.4
16	962.6	919.6	929.3	954.3	916.6	929.1	962.0
17	721.0	714.0	707.1	737.0	719.2	714.8	737.3
18	657.7	604.3	608.8	640.6	602.2	610.7	639.4
19	482.1	436.4	440.0	473.3	446.4	449.8	455.8
20	1178.4	1172.8	1150.1	1149.9	1170.6	1162.1	1189.3
21	1156.4	1150.1	1132.6	1126.0	1150.0	1144.4	1164.4
22	941.2	953.3	936.7	925.1	959.7	943.6	956.0
23	928.8	922.0	898.6	849.2	919.9	897.4	881.4
24	617.9	618.6	622.8	604.8	614.1	629.7	602.2
25	555.4	565.1	563.9	561.0	571.3	568.2	574.3
26	489.5	490.4	477.9	471.2	488.8	483.1	480.2
27	256.4	260.1	254.2	257.3	260.1	255.4	253.3

Note: Frequencies are in cm^{-1}. The various methods of scaling are described in Section 4.1. See text (Section 4.1) for definitions of method symbols heading each column.

TABLE 4-5
PREDICTED POTENTIAL ENERGY DISTRIBUTIONS
OF 2-PYRIMIDINOL IN FUNDAMENTAL BANDS
OBTAINED FROM THE FORCE FIELDS OF VARIOUS SCALING METHODS

ν	4-31G	XC	XCD	SC	WC	WCD	STO-3G
1	100S8	100S8	100S8	100S8	100S8	100S8	100S8
2	12S9	34S9	32S9	79S10	77S10	83S10	94S10
	75S10	42S10	45S10	10S11	14S11		
	12S11	22S11	22S11				
3	52S9	47S9	49S9	53S9	72S9	75S9	51S9
	47S11	51S11	50S11	46S11	27S11	22S11	48S11
4	36S9	18S9	19S9	37S9	20S9	16S9	46S9
	25S10	56S10	53S10	20S10	22S10	14S10	49S11
	40S11	26S11	28S11	43S11	58S11	70S11	
5	24S2	27S2	21S2	16S2	25S2	22S2	17S2
	11S3	21S5	11S3	15S3	23S5	24S5	23S5
	25S5	13S16	23S5	18S5	13S16	15S6	14S6
	17S6		17S6	20S6		10S19	15S16
	10S13		11S19	14S19			13S19
	13S19						
6	20S1	12S1	20S1	23S1	15S1	20S1	13S1
	14S3	24S3	14S3	15S2	24S3	18S3	16S3
	31S4	21S4	27S4	26S4	21S4	25S4	26S4
	11S14	19S6	12S17	12S17	16S6	13S17	13S16
	16S17	10S14			10S14		17S17
		14S17			14S17		
7	12S2	13S5	13E5	13S1	15S5	10S1	17S5
	11S5	12S16	14S7	10S2	13S16	15S5	16S16
	24S7	27S18	20S18	34S7	22S18	21S7	22S18
	16S17			10S17		11S18	
	13S18						
8	13S1	18S1	16S1	10S3	18S1	10S1	16S1
	10S7	30S7	23S7	10S6	30S7	17S7	31S7
	27S18	10S18	17S18	34S18	21S19	21S18	12S18
	30S19	19S19	18S19	19S19		16S19	19S19
9	10S3	48S16	51S16	13S3	44S16	49S16	40S16
	13S7	30S17	28S17	11S6	34S17	27S17	31S17
	37S17	12S19	12S19	12S7		15S19	16S19
				25S17			
				12S19			

---

continued

TABLE 4-5 continued

v	4-31G	XC	XCD	SC	WC	WCD	STO-3G
10	12S7	10S3	11S3	31S16	11S3	11S3	13S3
	25S16	20S7	10S6	24S17	22S7	10S6	12S6
	12S17	10S12	17S7	30S19	24S19	16S7	15S7
	35S19	15S17	16S17			19S17	17S17
		19S19	20S19			18S19	17S19
11	47S16	16S16	15S16	40S16	17S16	15S16	11S16
	15S18	20S17	21S17	22S18	19S17	20S17	17S17
		11S18	10S18	11S19	22S19	24S19	13S18
		25S19	25S19				21S19
12	17S1	19S3	20S3	21S3	16S3	15S3	18S3
	17S2	21S6	22S6	24S6	19S6	19S6	21S6
	48S3	44S18	44S18	16S16	54S18	53S18	46S18
	50S6			34S18			
	21S18						
13	12S1	27S4	26S4	26S4	27S4	S6S4	28S4
	28S2	29S5	27S5	28S5	27S5	27S5	27S5
	54S5	12S17	13S17	10S17	16S17	14S17	11S17
	10S16	12S19	12S19	10S19	11S19	11S19	10S19
	10S18						
14	22S1	16S1	15S1	11S3	13S1	16S1	12S1
	56S4	11S3	11S3	69S12	66S12	12S3	10S3
		62S12	70S12			70S12	74S12
15	64S12	62S1	64S1	67S1	66S1	64S1	71S1
		62S2	62S2	55S2	58S2	60S2	61S2
		43S3	43S3	46S3	44S3	42S3	45S3
		59S4	58S4	56S4	57S4	59S4	55S4
		52S5	53S5	54S5	53S5	50S5	52S5
		47S6	48S6	46S6	43S6	47S6	47S6
16	15S1	17S2	20S2	24S2	20S2	22S2	26S2
	17S2	26S7	28S7	24S7	25S7	27S7	24S7
	25S7	17S12	13S14	14S14	15S12	12S14	12S14
	14S14	14S14			13S14		
17	72S13	70S13	71S13	64S13	70S13	71S13	70S13
	22S14	21S14	19S14	23S14	21S14	18S14	21S14
18	14S7	16S7	15S7	17S7	17S7	16S7	15S7
	12S13	15S13	12S13	16S13	15S13	11S13	14S13
	50S14	55S14	57S14	49S14	56S14	58S14	56S14
19	85S15	92S15	90S15	11S13	93S15	10S13	89S15
				85S15	10S16	88S15	

---

continued

TABLE 4-5 continued

ν	4-31G	XC	XCD	SC	WC	WCD	STO-3G
20	15S20 44S25 48S26 42S27	44S25 48S26 37S27	41S25 40S26 38S27	52S25 49S26 29S27	100S25 22S26	60S25 44S26 24E27	37S25 53S26 40S27
21	58S25 55S27	55S25 60S27	58S25 59S27	47S25 69S27	24S26 98S27	42S25 73S27	61S25 56S27
22	77S20 69S23 25S26	74S20 54S23 47S26	27S20 28S23 71S26	13S23 16S25 70S26 18S27	29S20 32S23 68S26	26S20 30S23 71S26	22S25 69S26 25S27
23	38S20 13S23 22S25 46S26 28S27	76S20 21S23 30S25 25S26 31S27	140S20 51S23 28S25 29S27	151S20 78S23 20S25 18S27	122S20 51S23 23S25 29S27	133S20 57S23 27S25 29S27	175S20 59S23 14S25 14S27
24	28S20 10S21 33S22 39S23 13S24 18S26	16S20 15S21 32S22 63S23 11S24 18S26	17S20 15S21 36S22 69S23 23S26	25S20 12S21 44S22 56S23 25S26	22S20 13S21 36S22 64S23 21S26	23S20 15S21 34S22 61S23 24S26	15S21 17S22 42S23 56S24 10S26
25	15S22 87S24	14S22 85S24	92S24	11S22 91S24	10S22 88S24	93S24	40S22 42S23 44S24 13S26
26	92S21 25S22	92S21 23E22	102S21 28S22 10S25	102S21 27S22 10S25	100S21 21S22	102S21 28S22 10S25	104S21 28S22 11S25
27	19S21 67S21	22S21 71S22	24S21 82S22	27S21 70S22	21S21 81S22	23S21 84S22	21S21 70S22

Note: The various methods of scaling are described in Section 4.1. The PEDs are defined in the symmetrized internal coordinates of Table 3-4.

TABLE 4-6
PREDICTED BAND INTENSITIES OF 2-PYRIMIDINOL OBTAINED FROM THE FORCE FIELDS WITH VARIOUS SCALING METHODS AND THE 4-31G ATOMIC POLAR TENSORS OF 2-PYRIMIDINOL

ν	4-31G	XC	XCD	SC	WC	WCD	STO-3G
1	138.0	139.9	141.7	141.2	140.7	141.8	141.7
2	7.2	10.4	10.1	6.9	7.8	6.4	4.6
3	20.0	21.2	21.1	21.4	19.0	19.8	21.0
4	2.9	.8	.9	3.9	4.4	5.9	6.1
5	209.1	122.9	161.5	233.0	125.9	149.4	104.7
6	179.4	242.7	205.5	159.9	249.9	221.9	191.9
7	211.7	39.8	98.4	310.7	41.3	144.0	61.3
8	160.9	357.4	309.1	79.3	346.4	264.7	402.0
9	9.7	227.3	230.5	10.2	221.2	219.4	259.3
10	115.0	4.7	1.1	100.4	15.4	0	.9
11	159.1	66.2	64.2	129.4	69.2	66.2	55.2
12	17.5	16.9	14.9	49.9	7.6	10.0	11.9
13	36.1	.4	.3	0	.4	.3	0
14	14.3	0	.2	1.6	.2	.2	1.1
15	2.2	33.1	32.9	36.1	34.3	33.5	29.9
16	22.9	21.5	24.4	21.3	23.1	23.4	16.3
17	10.4	10.3	9.9	9.2	9.3	9.2	10.3
18	.4	.1	.1	.4	.1	.1	.1
19	22.5	23.4	22.6	25.4	23.1	22.9	21.6
20	1.0	.1	0	.2	.1	0	.3
21	0	0	0	0	.1	0	0
22	117.7	113.0	95.7	73.7	97.4	95.8	56.5
23	3.2	.1	16.5	39.9	14.8	16.4	56.5
24	19.0	17.9	9.6	11.3	7.9	6.4	122.2
25	185.9	181.9	199.3	196.2	191.9	202.0	89.1
26	5.5	17.5	10.8	10.8	19.5	11.1	9.0
27	4.5	6.1	4.7	4.5	5.0	4.9	4.0

Note: The intensities are in km/mole. The methods are described in Section 4.1. The APTs are calculated at HF SCF level with 4-31G basis set (Table 3-5).

The 4-31G diagonal values used to evaluate the 4-31G/STO-3G scaling constants were obtained from the diagonal values of the 4-31G force field of 2-pyrimidinol (Table 3-3) expressed in W or X coordinates. These 4-31G diagonal values in W or X coordinates were divided by the corresponding diagonal values of the STO-3G force field (Table 4-2), F^{th} of Equation 1-3, in W or X coordinates respectively. Thus the 4-31G/STO-3G scaling constants which made up the diagonal C matrix of Equation 1-3 were obtained. In this way the "near 4-31G" force field, F of Equation 1-3, in W or X coordinates was obtained. In order to simplify the discussion, the conversion constants for the WC and XC methods are not included in the present work. They can be calculated from available data by Equations 2-6 through 2-11. Using the "near 4-31G" force field in W or X coordinates and the 4-31G APTs (Table 3-5) the band frequencies, PEDs, and intensities of 2-pyrimidinol were calculated in the same way as for the "SC method," and these values are included in Tables 4-4 through 4-6.

It should be realized that although scaling in the SC, WC, and XC methods was done via Equation 1-3, the F^{th} force field to be upgraded was a matrix with a different degree of diagonality in each case. In order to eliminate (to some extent) this differing factor, two other methods were devised, the "WCD method" and the "XCD method."

In the case of the "WCD method" the "near 4-31G" force field obtained from the "WC method" was converted from W into S coordinates (via Equations 2-6 through 2-11). Then

the diagonal values of this "converted near 431-G" force field were divided by the corresponding diagonal values of the STO-3G force field in S coordinates (Table 4-2) to give 4-31G/STO-3G scaling constants. These constants are referred to as C_{wd} and are given in Table 4-3. Using Equation 1-3 with the C_{wd} values defining the C matrix, the STO-3G force field in S coordinates (Table 4-2) for F^{th}, the "near 4-31G" force field, F, in S coordinates corresponding to the "WCD method" was obtained. Using this "near 4-31G" force field and the 4-31G APTs (Table 3-5) the band frequencies, PEDs, and intensities of 2-pyrimidinol were calculated in the same way as for the previously described SC, XC, and WC methods. For the "XCD method" the prescriptions were identical except that X coordinates were used. The C_{xd} values of Table 4-3 correspond to the 4-31G/STO-3G scaling constants used in this method. The scaling constants and results from the WCD, XCD, and SC methods can be directly compared since they involve the upgrading of the identical F^{th} force field expressed in S coordinates, i.e., they upgrade a force field with the same degree of diagonality.

Tables 4-4 and 4-5 show the band frequencies and PEDs of 2-pyrimidinol obtained from the usage of the "near 4-31G" force fields for the various methods. These tables include two extra headings, STO-3G and 4-31G, which are added for comparison purposes. The STO-3G results were obtained by using the unscaled STO-3G force field of 2-pyrimidinol (Table 4-2) to determine band frequencies and PEDs by the

method to determine frequencies and the "MK method" of Section 2.2. The 4-31G results are taken directly from Tables 3-7 and 3-8. Table 4-6 shows the band intensities calculated for 2-pyrimidinol by the various methods using the 4-31G APTs from 2-pyrimidinol (Table 3-5).

4.2 Survey of Results

Figures 4-1 through 4-5 show the spectra predicted by the various methods considered in this chapter. These spectra are stickbar plots of Tables 4-4 and 4-6. The breakdown into the various spectral regions is arbitrary. These figures demonstrate that the various upgrading methods are not equally effective in imitating the 4-31G spectrum. For instance in Figure 4-1 it is deduced by visual inspection that, although all methods improve on the STO-3G results, the "SC method" seems to give the best agreement with 4-31G spectrum. Comparison of the performance of the various methods by visual inspection of the spectra tends not to be very objective. In order to achieve more objectivity in the comparison of the ability of the methods to imitate 4-31G spectrum simple statistical approaches are considered.

Table 4-7 contains a simple statistical analysis of the efficiency of the various methods in reproducing the 4-31G results. The efficiency is measured by the success in mimicking the band frequencies, PEDs, and intensities of 2-pyrimidinol evaluated at the HF SCF level with a 4-31G basis set, i.e., 4-31G results. The EF, EN, and EI terms

Figure 4-1. Comparison of calculated IR spectra (ν1 through ν4) from various scaling methods. The methods are elaborated in Chapter 4.

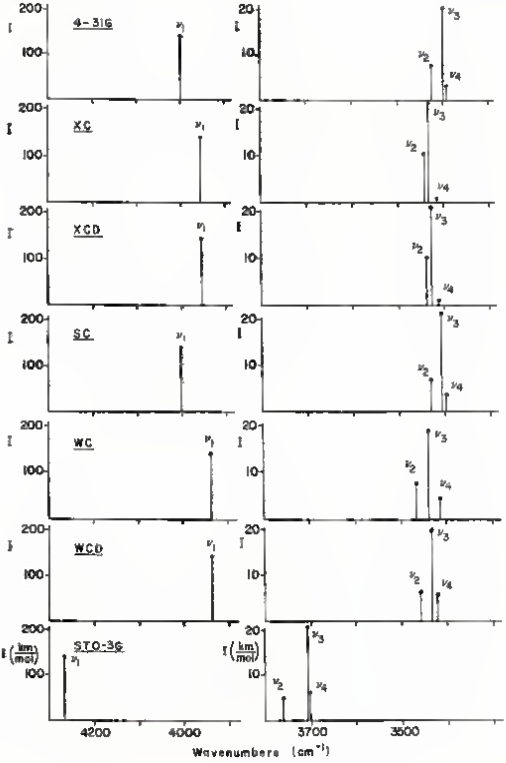
4-31G
XC
XCD
SC
WC
WCD
STO-3G
I
I (km/mol)
ν1
ν2
ν3
ν4
4200
4000
3700
3500
Wavenumbers (cm⁻¹)

TABLE 4-7
STATISTICAL ANALYSIS ON THE ABILITY OF THE VARIOUS METHODS TO MIMIC THE PREDICTED 4-31G RESULTS FOR THE ν1 THROUGH ν4 FUNDAMENTAL BANDS OF 2-PYRIMIDINOL

	XC	XCD	SC	WC	WCD	STO-3G
EF1	-44.3	-45.4	3.2	-60.9	-60.4	269.7
EF2	17.4	14.7	6.6	42.0	35.7	337.6
EF3	33.9	30.3	6.8	40.7	34.6	309.6
EF4	23.6	20.3	6.6	21.6	31.0	310.1
ΣEF	119.2	110.8	25.1	165.1	161.7	1226.9
EN1	0	0	0	0	0	0
EN2	65	60	18	16	32	43
EN3	9	6	2	40	46	2
EN4	63	57	9	37	61	44
ΣEN	137	123	29	93	141	89
EI1	9	3.7	3.2	2.7	3.8	3.7
EI2	3.2	2.9	-.3	.6	-.6	-2.6
EI3	1.2	1.1	1.4	-1.0	-.2	1.0
EI4	-2.1	-2.0	.9	1.5	2.9	3.2
ΣEI	7.4	9.7	5.8	5.6	7.7	10.5
FP	3	2	1	5	4	6
NP	5	4	1	3	6	2
IP	3	5	1	1	4	6
EPP	3	3	1	2	5	5

Note: The EF parameters are in cm^{-1}, the EI parameters in km/mole. All other parameters are unitless. The statistical terms are defined in Section 4.2. The predicted 4-31G results correspond to the full 4-31G study of Chapter 3.

measure deviations in frequency, normal modes, and intensities respectively from the 4-31G results. For instance SF1 is the difference in frequency between the v1 band predicted by a given method and the v1 band predicted from the 4-31G results (Table 4-4). The ΣEF, ΣEN, and ΣEI terms are the sum of the absolute values of the deviations of predicted frequencies (EFs), normal modes (ENs), and intensities (EIs) respectively for a given method for fundamentals v1 through v4. The FP is an assigned frequency parameter which helps one to judge the methods from the best (= 1) to the worst (=6) in their ability to mimic the 4-31G results on the basis of ΣEF values. Similarly NP and IP are the normal mode and intensity parameters based on grading the ΣEN and ΣEI values respectively. The EFF is the efficiency parameter which is used to grade the overall performance of a given method based on the FP, NF, and IF values.

Table 4-7 permits us to make a more objective and quantitative comparison of spectra of Figure 4-1 obtained by different methods than just a visual comparison. Similarly Tables 4-8 through 4-11 permit us to compare the performance of each of the methods for the spectra calculated in Figures 4-2 through 4-5 respectively. Table 4-12 summarizes these tables where the analyses is divided according to the symmetry of the molecule (in-plane and out-of-plane fundamental modes). In this table the EPIP, ENIP, and EIIP are the means of the ΣEF, ΣEN, and ΣEI values respectively for the in-plane fundamentals (v1 through v19). The EPOP, ENOP, and EIOP are the means of the ΣEF, ΣEN, and ΣEI

Figure 4-2. Comparison of calculated IR spectra (ν5 through ν8) from various scaling methods. The methods are elaborated in Chapter 4.

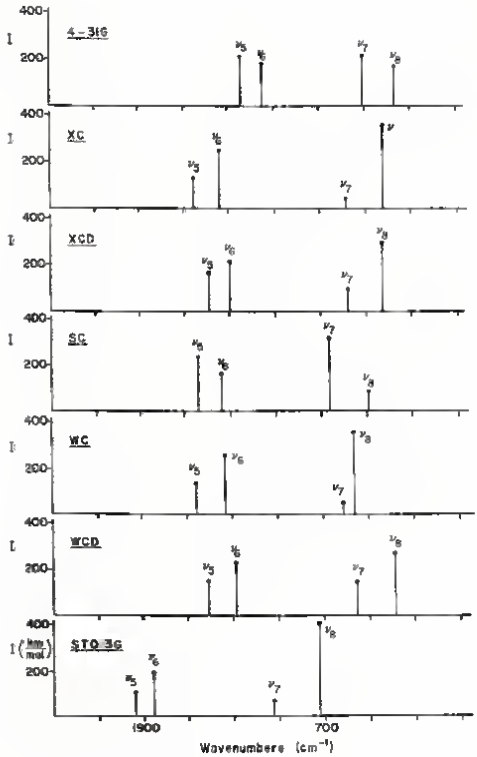
4-31G
XC
XCD
SC
WC
WCD
STO-3G
I
400
200
ν_5
ν_6
ν_7
ν_8
ν_3
1900
700
Wavenumbers (cm^{-1})

TABLE 4-8
STATISTICAL ANALYSIS
ON THE ABILITY OF THE VARIOUS METHODS
TO MIMIC THE PREDICTED 4-31G RESULTS FOR THE ν5 THROUGH ν8
FUNDAMENTAL BANDS OF 2-PYRIMIDINOL

	XC	XCD	SC	WC	WCD	STO-3G
EF5	51.8	38.3	49.6	53.2	40.3	123.7
EF6	47.4	37.1	46.8	45.1	34.1	125.3
EF7	19.3	17.9	39.0	25.8	12.8	105.3
EF8	12.3	15.8	31.9	-1.8	4.8	88.6
ΣEF	130.7	107.1	188.0	125.9	91.8	442.9
EN5	71	17	33	67	29	48
EN6	50	19	52	43	24	39
EN7	80	47	63	76	47	83
EN8	53	38	61	61	30	50
ΣEN	254	121	209	249	130	220
EI5	-86.2	-47.6	23.9	-83.3	-60.7	-104.4
EI6	64.3	27.1	-18.5	71.4	43.5	13.5
EI7	-171.9	-123.3	99.0	-170.4	-67.7	-150.4
EI8	196.5	147.2	-81.6	185.5	103.8	241.1
ΣEI	518.9	345.2	223.0	510.6	275.7	509.4
FP	4	2	5	3	1	6
NP	5	1	3	5	2	4
IP	5	3	1	5	2	4
EFF	8	2	3	4	1	5

Note: The EF parameters are in cm^{-1}, the EI parameters in km/mole. All other parameters are unitless. The statistical terms are defined in Section 4.2. The predicted 4-31G results correspond to the full 4-31G study of Chapter 3.

Figure 4-3. Compsrison of calculsted IR spectra (ν9 through ν15) from various scaling methods. The methods are elaborated in Chapter 4.

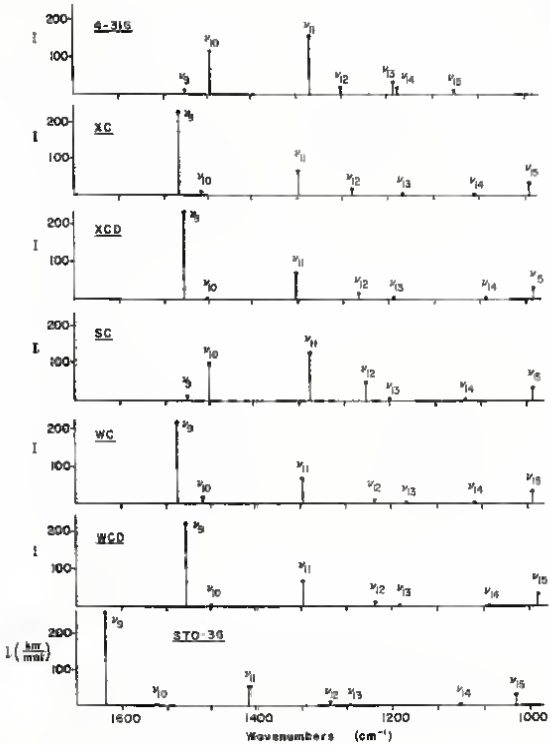
4-31G
XC
XCD
SC
WC
WCD
STO-3G
I
200
100
ν_9
ν_{10}
ν_{11}
ν_{12}
ν_{13}
ν_{14}
ν_{15}
ν_{16}
I (km/mol)
1600
1400
1200
1000
Wavenumbers (cm^{-1})

TABLE 4-9
STATISTICAL ANALYSIS ON THE ABILITY OF THE VARIOUS METHODS TO MIMIC THE PREDICTED 4-31G RESULTS FOR THE ν9 THROUGH ν15 FUNDAMENTAL BANDS OF 2-PYRIMIDINOL

	XC	XCD	SC	WC	WCD	STO-3G
EP9	10.0	2.6	-1.7	13.3	3.3	124.0
EP10	14.1	6.7	4.2	16.0	4.2	87.2
EP11	18.2	22.1	2.7	15.1	16.7	96.2
EP12	-15.1	-22.8	-32.3	-43.0	-42.4	24.8
EP13	-11.4	2.6	10.0	-11.6	.7	73.0
EP14	-110.9	-124.6	-93.2	-105.7	-124.7	-84.1
EP15	-107.3	-112.1	-109.6	-107.8	113.6	-81.8
ΣEP	287.1	293.3	253.7	312.4	305.6	571.1
EN9	90	95	39	70	97	85
EN10	72	70	35	69	74	76
ENII	80	83	25	86	91	76
EN12	115	113	116	130	130	118
EN13	136	138	132	141	138	126
ENI4	135	144	158	131	144	150
EN15	389	392	388	385	386	395
ΣEN	1017	1035	893	1012	1060	1026
EI9	217.6	220.8	.5	211.5	209.7	248.6
EI10	-110.3	-113.9	-14.6	-99.6	-115.0	-114.1
EI11	-92.9	-94.9	-30.7	-90.9	-92.9	-103.9
EI12	-.6	-2.7	31.4	-9.9	-7.5	-5.6
EI13	-35.7	-35.8	-36.1	-35.7	-35.8	-36.1
EII4	-14.3	-14.1	-12.7	-14.1	-14.1	-13.2
EI15	30.9	30.7	33.9	32.1	31.3	26.7
ΣEI	502.3	512.9	159.9	493.8	506.3	548.2
FP	2	3	1	5	4	6
NP	3	5	1	2	6	4
IP	3	5	1	2	4	6
EPF	2	4	1	3	5	6

Note: The EP parameters are in cm^{-1}, the EI parameters in km/mole. All other parameters are unitless. The statistical terms are defined in Section 4.2. The predicted 4-31G results correspond to the full 4-31G study of Chapter 3.

Figure 4-4. Comparison of calculated IR spectra (v16 through v19) from various scaling methods. The methods are elaborated in Chapter 4

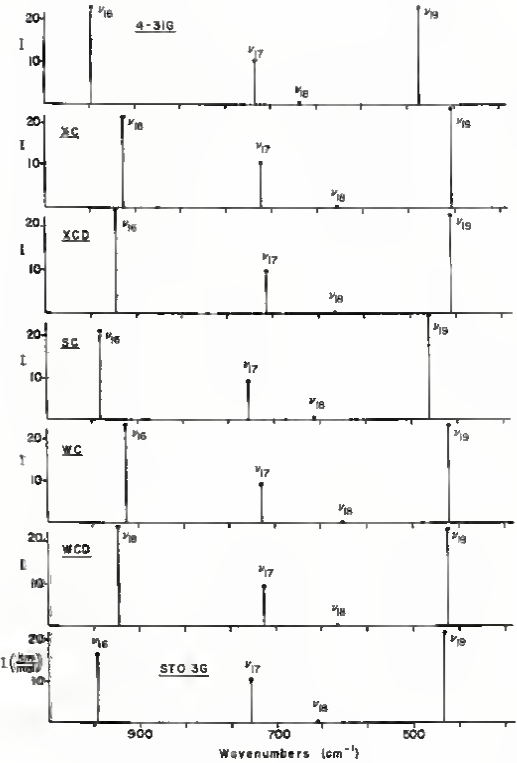
4-31G
XC
XCD
SC
WC
WCD
STO 3G
I
I (km/mol)
20
10
ν_{16}
ν_{17}
ν_{18}
ν_{19}
900
700
500
Wavenumbers (cm^{-1})

TABLE 4-10
STATISTICAL ANALYSIS ON THE ABILITY OF THE VARIOUS METHODS TO MIMIC THE PREDICTED 4-31G RESULTS FOR THE ν16 THROUGH ν19 FUNDAMENTAL BANDS OF 2-PYRIMIDINOL

	XC	XCD	SC	WC	WCD	STO-3G
EF16	-43.0	-33.2	-8.2	-46.0	-33.4	-.6
EF17	-7.0	-13.9	16.0	-1.8	-6.2	16.3
EF18	-53.4	-49.0	-17.2	-55.6	-47.1	-18.3
EF19	-45.7	-42.1	-8.8	-35.7	-32.3	-26.3
ΣEF	149.1	138.2	50.2	139.0	119.1	61.6
EN16	33	22	23	34	24	27
EN17	3	4	9	3	5	3
EN18	10	8	8	12	11	9
EN19	7	5	11	18	13	4
ΣEN	53	39	51	67	53	43
EI16	-1.3	1.6	-1.5	.3	.6	-6.5
EI17	-.1	-.6	-1.2	-1.1	-1.2	-.1
EI18	-.3	-.3	0	-.3	-.3	-.3
EI19	.9	.1	2.9	.6	.3	-.9
ΣEI	2.6	2.6	5.6	2.3	2.4	7.8
FF	5	3	1	4	2	6
NF	4	1	3	6	4	2
IF	3	3	5	1	2	6
EFF	5	1	3	4	2	6

Note: The EF parameters are in cm^{-1}, the EI parameters in km/mole. All other parameters are unitless. The statistical terms are defined in Section 4.2. The predicted 4-31G results correspond to the full 4-31G study of Chaptsr 3.

Figure 4-5. Comparison of calculated IR spectra (ν20 through ν27) from various scaling methods. The methods are elaborated in Chapter 4.

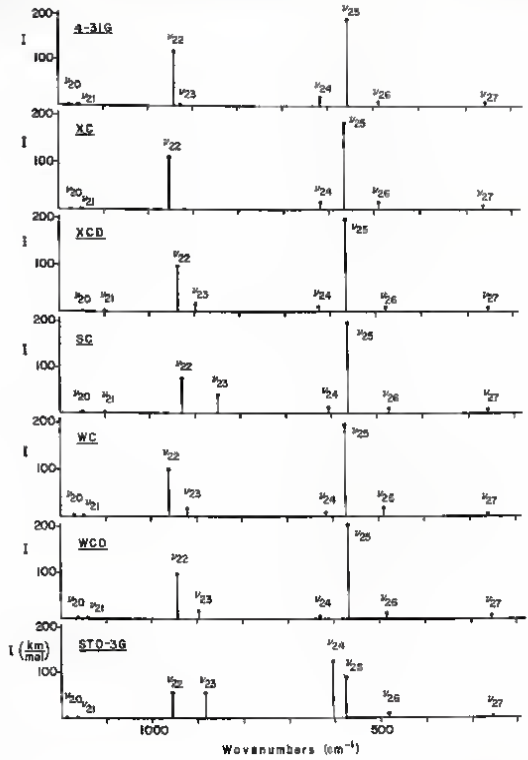
4-31G
XC
XCD
SC
WC
WCD
STO-3G
I
I (km/mol)
200
100
ν20 ν21 ν22 ν23 ν24 ν25 ν26 ν27
1000
500
Wavenumbers (cm⁻¹)

TABLE 4-11
STATISTICAL ANALYSIS ON THE ABILITY OF THE VARIOUS METHODS TO MIMIC THE PREDICTED 4-31G RESULTS FOR THE ν20 THROUGH ν27 FUNDAMENTAL BANDS OF 2-PYRIMIDINOL

	XC	XCD	SC	WC	WCD	STO-3G
EF20	-5.7	-28.3	-28.6	-7.9	-16.3	10.9
EF21	-6.3	-23.9	-30.4	-6.4	-12.0	8.0
EF22	12.1	-4.5	-12.1	18.4	2.3	14.8
EF23	-6.8	-30.2	-79.6	-8.9	-31.3	-47.3
EF24	.7	4.9	-13.1	-3.8	11.8	-15.7
EF25	9.7	8.4	5.6	15.9	12.8	18.9
EF26	.9	-11.7	-18.3	-.8	-6.4-9.3	
EF27	3.7	-2.2	.9	3.7	-1.0	-3.1
ΣEF	45.8	114.2	188.6	65.8	94.0	128.0
EN20	20	22	37	139	53	29
EN21	8	4	25	125	34	4
EN22	40	137	212	128	136	237
EN23	78	193	236	170	191	251
EN24	44	67	53	53	52	103
EN25	3	20	8	6	21	123
EN26	2	23	22	12	23	36
EN27	7	20	11	14	21	5
ΣEN	202	486	604	647	531	788
EI20	-.9	-1.0	-.8	-.9	-1.0	-.7
EI21	0	0	0	.1	0	0
EI22	-4.7	-22.0	-44.0	-20.3	-21.9	-61.2
EI23	-3.1	13.3	36.7	11.6	13.2	53.3
EI24	-1.1	-9.4	-7.7	-11.1	-12.6	103.2
EI25	-3.9	13.5	10.4	6.0	16.2	-96.7
EI26	12.0	5.3	5.3	14.0	5.6	2.5
EI27	1.6	.2	0	.5	.4	-.5
ΣEI	27.3	64.7	104.9	64.5	70.9	318.1
FP	1	4	6	2	3	5
NP	1	2	4	5	3	6
IP	1	3	5	2	4	6
EFF	1	2	5	2	4	6

Note: The EF parameters are in cm^{-1}, the EI parameters in km/mole. All other parameters are unitless. The statistical terms are defined in Section 4.2. The predicted 4-31G results correspond to the full 4-31G study of Chapter 3.

values respectively for the out-of-plane fundamentals (ν20 through ν27). The EFTOT, ENTOT, and EITOT are the means of the EEF, EEN, and EEI values respectively for all fundamentals (ν1 through ν27). The FFIE, NFIF, IeIF, and EFFIP are the frequency, normal mode, intensity, and overall parameters analogous to Tables 4-7 through 4-11 which help one to grade the performance of the various models regarding in-plane modes only. Similarly FFOF, NFOF, IFOF, and EFFOF are used to grade the performance of the models regarding out-of-plane modes only; and FFTOT, NFTOT, IFTOT, and EFFTOT are used to grade the performance of the models throughout all fundamental modes.

4.3 Conclusions

The various methods considered in this chapter gave predicted results of different quality for bend frequencies, normal modes, and intensities of 2-pyrimidinol. The reason for these differences did stem from the use of different coordinate systems in upgrading procedures. To actually judge as to how severe these differences are is hard to determine from the data presently available to us. The interesting fact is that the same force fields at the HF SCF level with 4-31G and STO-3G basis sets respectively were used in all the methods considered in this chapter. This finding alone shows us that there is the need to carry out further investigations on the selection of coordinate systems to be used in scaling procedures.

Within the scope of the statistical approaches used so far the trend in the deviations of the normal modes and intensities seems to be similar to the trend in the deviations in the band frequencies throughout the various methods applied to calculations for the in-plane modes. These results are not entirely without contradictions especially when one examines the out-of-plane results. Nonetheless it seems certain that the commonly used approach to consider only the comparison of band frequencies in the evaluation of the results of different scaling procedures for force fields is insufficient. It is possible that more sophisticated statistical analysis is needed to investigate the differences between the predicted spectra of the various methods. Ideally this analysis should look simultaneously at the differences in band frequencies, normal modes, and intensities.

The analysis in Table 4-12 for the in-plane results indicates that the best method is SC. For the out-of-plane results XC is the preferred method. All upgrading methods show an improvement over the "STO-3G method" which uses an unscaled force field at the HF SCF level with an STO-3G basis set. By judging the efficiency over all the fundamental modes (EFFTOT) it seems that SC is the method of choice.

Table 4-12 contains a few other parameters that have not been explained yet. The MDIF and MDOF parameters are the means of the absolute magnitudes of the differences between

the C_{xd} and C_{wd} values from the C_s values of Table 4-3 for the in-plane and out-of-plane modes respectively. The MIP and MOP parameters are the means of these differences for in-plane and out-of-plane modes respectively. The %DIAGIP and %DIAGOP are rough measures of the degree of diagonality of the in-plane and out-of-plane portion of the force field to be upgraded, i.e., the F^{th} force field of Equation 1-3. The %DIAGIP is the ratio of the sum of the absolute values of the diagonal elements of the in-plane force field F^{th} to the sum of the absolute values of all the in-plane elements of the force field, multiplied times 100. The %DIAGOP is the same corresponding ratio for the out-of-plane force constants.

The purpose of introducing these parameters is to show that there is some relationship between them and all the rest of statistical parameters concerning frequencies and normal modes in Table 4-12. The fact that XC and WC methods had values of the %DIAGIP AND %DIAGOP quite different from those for the SC and STO-3G methods was an important factor in the development of the WCD and XCD methods. Thus the XC and WC methods are not included in these immediate observations. On the other hand the SC, XCD, and WCD methods share the same values of the %DIAGIP and %DIAGOP. There seems to be a relationship between the errors for the predicted in-plane frequencies and for the normal modes predicted by these methods and the corresponding MDIP and MIP values. This same trend is harder to follow in the out-of-plane case. These observations could be roughly

interpreted as saying that the closer the scaling constants of a given method are to the C_s values the better the method will mimic the 4-31G band frequencies and normal modes. Notice that the band intensities are not included in this discussion because they depend not only on the force field but also on the APTs (Section 1.2.5).

Various observations are made in this chapter. The need exists to understand scaling methods more thoroughly. It seems that the more diagonal the force field to be upgraded is, the better the results that are obtained from scaling procedures. Thus a search could be suggested for coordinate systems that provide a high degree of diagonality for the force field to be scaled. The usage of other systems of conversion could be tried with perhaps the inclusion of the geometry of the molecule. As seen before band intensities and normal modes should be incorporated in statistical fitting of calculated to experimental spectra.

The philosophy used in this chapter is to try to imitate the spectrum of 2-pyrimidinol calculated at the HF SCF level with a 4-31G basis set using the results at the same level calculated with an STO-3G basis set. It is shown that such imitation is not easily achieved by the various methods attempted. Further still the relationships between these two levels of theory is not clearly understood as to their effect on predicted IR spectra. If this is true for this comparison between two rather similar results calculated with rather similar representations of the

TABLE 4-12
SUMMARY OF THE STATISTICAL ANALYSIS
ON THE ABILITY OF THE VARIOUS METHODS
TO MIMIC THE PREDICTED 4-31G RESULTS FOR THE ALL THE
FUNDAMENTAL BANDS OF 2-PYRIMIDINOL

	XC	XCD	SC	WC	WCD	STO-3G
EFIP	36.1	34.2	26.2	39.1	35.7	I21.2
EFOP	5.7	14.3	23.6	8.2	11.8	16.0
EFTOT	27.1	28.3	25.4	29.9	28.6	90.0
ENIP	76.9	69.4	62.2	74.8	72.8	72.5
ENOP	25.3	60.8	75.5	80.9	66.4	98.5
ENTOT	61.6	66.8	66.1	76.6	70.9	80.2
EIIP	54.3	45.8	20.6	53.3	41.7	56.6
EIOP	3.4	8.1	13.1	9.1	8.9	39.8
EITOT	39.2	34.6	18.5	39.9	32.0	51.6
FPIP	4	2	I	5	3	6
NPIP	6	2	1	5	4	3
IPIP	5	3	1	4	2	6
EPFIP	5	2	1	4	3	5
FPOP	1	4	6	2	3	5
NPOP	1	2	4	5	3	6
IPOP	1	2	5	2	4	6
EPFOP	1	2	5	3	4	6
FPTOT	2	3	1	5	4	6
NPTOT	1	3	2	5	4	6
IPTOT	4	3	1	5	2	6
EPFTOT	2	3	1	5	4	6
MDIP	--	.0489	0	--	-.0513	.0943
MIP	--	-.0267	0	--	-.0257	.0744
MDOP	--	.0467	0	--	.0623	.0803
MOP	--	.0264	0	--	.0429	.0354
%DIAGIP	33.1	61.6	30.5	61.6	61.6	61.6
%DIAGOP	35.2	46.1	45.1	46.1	46.1	46.1

Note: The EF parameters are in cm^{-1}, the EI parameters in km/mols. All other parameters are unitless. The statistical terms are defined in Section 4.2. The predicted 4-31G results correspond to the full 4-31G study of Chapter 3.

wavefunctions, the situation should be even more complex when a theoretical representation is scaled to fit experimental results. It is suggested that such comparisons between calculations from rather similar levels of theory (e.g., using 4-31G and STO-3G basis sets as here), be studied further in order to understand the theory of scaling of force fields

CHAPTER 5
EFFECT OF CONVERGENCE, INTEGRAL THRESHOLD, AND CHOICE OF REFERENCE STATE IN AB INITIO CALCULATIONS ON THE PREDICTED IR SPECTRUM OF 2-PYRIMIDINOL

There are many controversies surrounding various types of calculations in predictive IR work as discussed in Chapter 1. This chapter presents some of our findings in connection with these problems. The predicted IR results from ab initio calculations performed at different degrees of convergence and integral threshold are discussed. Similarly the effect of choosing different reference geometries in the evaluation of force fields and atomic polar tensors are considered. All the studies covered in this chapter are made exclusively on 2-pyrimidinol. The discussion is divided in three sections: convergence and integral threshold, reference geometry, and conclusions

5.1 Convergence and Integral Threshold

Ab initio calculations of diagonal force constants and atomic polar tensors of 2-pyrimidinol were carried out at the HF SCF level with a 4-31G basis set at two different convergence limits of the GAUSSIAN 76[53] program: 10^{-8} and $5 * 10^{-5}$. The integral threshold in both cases was 10^{-6}. Diagonal force constants and APTs evaluated at 10^{-8} convergence are referred to as HC force constants and HC atomic polar tensors respectively. Similarly for the $5 * 10^{-5}$ convergence, they are referred to as LC force constants

and atomic polar tensors respectively. The details of the ab initio calculations are given in Section 2.1.2. The reference geometry was at all times the 4-31G optimized geometry of 2-pyrimidinol (Tables 3-2 and 3-6).

By the "WCD method" explained in Chapter 4, the HC and LC diagonal force constants and the STO-3G force field of 2-pyrimidinol (Table 4-2) were used to give HC and LC "near 4-31G" force fields respectively. The scaling constants are given in Table 5-1, where C_{HC} and C_{LC} correspond to the HC and LC cases respectively. The HC and LC atomic polar tensors of 2-pyrimidinol are given in Tables 5-2 and 5-3 respectively.

Using the HC and LC "near 4-31G" force fields, the band frequencies of Tables 5-4, 5-5, and the normal modes of Table 5-8 were obtained. The 4-31G APTs (Table 3-5), the HC APTs, and the LC APTs of 2-pyrimidinol were used together with HC and LC "near 4-31G" force fields respectively to give the band intensities shown in Tables 5-4 and 5-5. Tables 5-6 and 5-7 are added for comparison purposes. The band frequencies in Table 5-6 are the unscaled frequencies obtained from the 4-31G force field of 2-pyrimidinol (Table 3-3). The band intensities of Table 5-6 are obtained from this 4-31G force field and the 4-31G APTs (Table 3-5), the HC APTs, and the LC APTs respectively. Similarly Table 5-7 shows the band frequencies and intensities obtained from the unscaled STO-3G force field of 2-pyrimidinol (Table 4-2), and the above mentioned APTs. In short, four different force fields (HC, LC, 4-31G, and STO-3G) were used in the

TABLE 5-1
THE 4-31G/STO-3G SCALING CONSTANTS
FOR 2-PYRIMIDINOL OBTAINED FROM TWO CONVERGENCE LEVELS

S	C_{HC}	C_{LC}
1	1.0403	1.1051
2	1.0221	1.0857
3	.9852	1.0318
4	.9182	.9579
5	.9401	.9991
6	.9656	1 0291
7	.9258	.9566
8	.8569	.8647
9	.8572	.8729
10	.8526	.8594
11	.8626	.8673
12	.9576	1.0035
13	1.0020	1.0629
14	.9435	.9890
15	1.0194	1.0881
16	.8400	.8634
17	.8708	.8821
18	.8932	.9084
19	.8782	.8914
20	1.0728	1.2458
21	1.0781	1.2809
22	1.0847	1.2314
23	1.2925	1.5268
24	.9597	1.4309
25	1.0170	1.1454
26	.9735	1.0698
27	1.0049	1.0963

Note: The HC and LC (10^{-8} and $5 * 10^{-5}$ convergence respectively) "near 4-31G" force fields by the "WCD method" are considered. Details given in Section 5.1

TABLE 5-2
ATOMIC POLAR TENSORS FOR 2-PYRIMIDINOL AT 10^{-8} CONVERGENCE
(HC APTS)

N1[a,b,c]			O7		
-.50238	.21197	0	-.27411	.10310	0
-.35099	-1.08208	0	.06497	-1.67436	0
0	0	.43665	0	0	-.65438

C2			H8		
.39590	-.09455	0	.23165	-.07805	0
-.05177	2.19262	0	-.02993	.50024	0
0	0	.62602	0	0	.45148

N3			H9		
-.46069	-.12766	0	-.02279	.07493	0
.36303	-1.03238	0	.07042	.04801	0
0	0	-.42893	0	0	.10682

C4			H10		
.72677	.24569	0	.09884	-.00236	0
-.07945	.59504	0	-.00263	-.05683	0
0	0	.14998	0	0	.18306

C5			H11		
-.87529	.01933	0	-.02888	-.06564	0
-.01347	-.07779	0	-.06943	.05210	0
0	0	-.24822	0	0	.09919

C6		
.71098	-.28676	0
.09924	.53542	0
0	0	.15163

EIFD = .03202[d]

EOFD = .16297[d]

[a]Units are in electrons (e)

[b]APTs were determined at HF SCF level with 4-31G basis set using 4-31G optimized geometry (Table 3-2) as reference state.

[c]The atom numbering is given in Figure 3-3; the coordinate system of orientation is the principal cartesian coordinates of Table 3-6.

[d]These terms are defined in Section 5.1.

TABLE 5-3
ATOMIC POLAR
TENSORS FOR 2-PYRIMIDINOL AT 5 * 10^{-5} CONVERGENCE
(LC APTS)

N1[a,b,c]			O7		
-.58352	-.15609	0	.03820	.23034	0
-.34984	-1.05713	0	.01290	-1.72256	0
0	0	-.42691	0	0	- 66645
C2			H8		
.04957	.05905	0	.23859	-.09701	0
-.12163	2.20169	0	- 02605	.36082	0
0	0	.61269	0	0	46013
N3			H9		
-.24471	-.08401	0	-.10427	.09576	0
.49868	-1.04122	0	.12669	.01629	0
0	0	-.40970	0	0	.12749
C4			H10		
.56205	.40217	0	.07813	.02024	0
-.22905	.80439	0	.01623	-.11940	0
0	0	.13605	0	0	-.18907
C5			H11		
-.94957	-.09688	0	-.11939	-.03867	0
-.11486	- 16981	0	-.07558	.04368	0
0	0	-.28337	0	0	.11956
C6					
1.03491	-.33491	0		EIFD = 4.36445[d]	
.21039	.68326	0			
0	0	.14145		EOPD = .19600[d]	

[a]Units are in electrons (e).

[b]APTs were determined at HF SCF level with 4-31G basis set using 4-31G optimized geometry (Table 3-2) as reference state.

[c]The atom numbering is given in Figure 3-3; the coordinate system of orientation is the principal cartesian coordinates of Table 3-6.

[d]The terms are defined in Section 5.1.

evaluation of frequencies and PEDs. For each force field three sets of APTs (4-31G, HC, and LC) were used in the evaluation of intensities.

Table 5-9 summarizes the statistical analysis performed on these results. The errors in frequencies, PEDs, and intensities are calculated in the same way as presented in Chapter 4. These errors are measured from the deviations of the various cases from 4-31G results for 2-pyrimidinol (Chapter 3). Since three sets of APTs are being considered, three measures of EIIP and EIOP are given. The MDIP, MOP, MDIP, and MDOP values are measured with respect to C_e scaling constants (Table 4-3) as was done in Chapter 4. These values can be compared to each other since the force field to be upgraded had the same diagonality in all cases. The statistical results for the "SC method" (Table 4-12) are added for comparison purposes.

Table 5-9 is a useful summary that shows the differences in prediction between the various considered methods and the 4-31G results of Chapter 3. Looking at the frequency results for HC and LC one can deduce that the higher the convergence the better the results. Nevertheless the actual difference in the EFIP for these two cases is not as large as the corresponding difference in EFOP. This suggests that convergence is more important for the determination of the out-of-plane force field than for the in-plane one. At least it can be said that the the effect of convergence is important for the out-of-plane modes where the use of C_{LC} scaling constants leads to a set of predicted

TABLE 5-4
PREDICTED BAND FREQUENCIES AND INTENSITIES FOR IR FUNDAMENTAL BANDS OF 2-PYRIMIDINOL FROM HC "NEAR 4-31G" FORCE FIELD AND 4-31G, HC, AND LC ATOMIC POLAR TENSORS

	Frequency[a] (cm^{-1})		Intenelties[b] (km/mole) 4-31G	HC	LC
1	3950.4		142.0	142.7	94.2
2	3476.7		6.6	6.4	25.4
3	3451.2		18.9	18.5	52.8
4	3439.2		6.7	6.7	23.6
5	1858.7		163.0	163.0	178.1
6	1832.4		231.6	231.8	230.6
7	1694.1		179.6	179.5	225.1
8	1648.6		206.5	206.2	162.4
9	1516.2		211.3	212.3	170.8
10	1490.0		.2	.2	9.9
11	1346.6		70.4	70.2	47.5
12	1242.4		9.9	9.8	2.9
13	1210.9		.4	.3	2.0
14	1084.7		.3	.3	3.4
15	1011.8		35.2	35.2	58.5
16	949.9		23.6	23.5	42.5
17	731.7		9.0	9.0	2.0
18	623.2		.1	.1	2.8
19	457.8		23.0	23.0	31.4
		ΣI[c]	1338.0	1338.8	1366.0
		ΣEI[c]	684.9	687.5	746.7
20	1181.3		.1	0	4
21	1166.9		0	0	0
22	963.6		101.8	107.9	119.1
23	927.2		10.3	12.4	9.7
24	647.0		6.1	5.8	3.7
25	575.3		199.0	192.1	203.6
26	499.1		14.6	16.4	16.8
27	267.0		4.7	3.8	3.0
		ΣI[c]	336.6	338.4	356.3
		ΣEI[c]	59.3	51.1	54.4

[a] Frequencies were predicted from HC "near 4-31G" force field by the "WCD method" (Section 5.1).

[b] Intenalties are predicted by usage of HC "neer 4-31G" force field and a given set of APTs: 4-31G APTs (Table 3-5), HC APTs (Table 5-2), and LC APTs (Table 5-3).

[c] The terms are defined in Section 5.1.

TABLE 5-5
PREDICTED BAND FREQUENCIES AND INTENSITIES FOR IR FUNDAMENTAL BANDS OF 2-PYRIMIDINOL FROM LC "NEAR 4-31G" FORCE FIELD AND 4-31G, HC, AND LC ATOMIC POLAR TENSORS

	Frequency[a] (cm^{-1})		Intensities (km/mole)[b] 4-31G	HC	LC
1	3968.7		142.1	142.8	94.3
2	3491.0		6.3	6.1	24.3
3	3462.9		18.5	18.1	51.3
4	3449.7		7.7	7.7	26.7
5	1907.3		166.7	166.7	178.1
6	1875.2		247.9	248.0	253.1
7	1730.3		179.6	179.4	221.1
8	1679.3		192.5	192.3	150.6
9	1534.9		206.0	207.0	165.2
10	1515.3		.6	.6	9.3
11	1367.0		67.5	67.3	44.3
12	1262.7		8.1	8.0	1.8
13	1234.9		.7	.6	2.0
14	1212.3		.3	.3	2.8
15	1040.0		35.7	35.6	58.7
16	973.0		25.7	25.6	45.1
17	752.6		8.8	8.8	1.9
18	637.8		.2	.2	2.9
19	472.4		23.3	23.4	31.7
		ΣI[c]	1337.8	1338.6	1366.1
		$\Sigma \varepsilon I$[c]	687.0	689.7	778.6
20	1244.4		.3	.3	1.0
21	1219.7		.1	0	.1
22	1027.8		112.6	121.2	127.9
23	989.1		.4	.2	1.0
24	715.9		121.8	117.5	115.1
25	684.8		91.4	88.9	101.4
26	544.4		5.4	6.6	6.6
27	286.3		4.6	3.9	3.1
		ΣI[c]	336.8	338.6	356.2
		$\Sigma \varepsilon I$[c]	206.3	204.3	195.5

[a]Frequencies are predicted from LC "near 4-31G" force field by the "WCD method" (Section 5.1).

[b]Intensities are predicted by usage of LC "near 4-31G" force field and a given set of APTs: 4-31G APTs (Table 3-5), HC APTs (Table 5-2), and LC APTs (Table 5-3).

[c]The terms are defined in Section 5.1.

TABLE 5-6
PREDICTED SAND FREQUENCIES AND INTENSITIES
FOR IR FUNDAMENTAL SANDS OF 2-PYRIMIDINOL FROM
4-31G FORCE FIELD AND
4-31G, HC, AND LC ATOMIC POLAR TENSORS

	Frequency[a] (cm^{-1})		Intensities (km/mole)[b] 4-31G	HC	LC
1	3997.9		138.0	138.7	91.5
2	3423.2		7.2	6.9	26.5
3	3397.9		20.0	19.7	62.2
4	3391.4		2.9	2.8	9.5
5	1785.2		209.1	209.2	227.9
6	1762.3		178.4	178.6	187.7
7	1650.8		211.7	211.6	253.3
8	1616.3		160.9	160.3	130.7
9	1500.7		9.7	9.7	10.8
10	1462.3		115.0	115.5	88.9
11	1312.9		159.1	159.6	119.8
12	1266.9		17.5	17.4	12.8
13	1190.6		36.1	36.1	46.1
14	1184.4		14.3	14.2	8.9
15	1102.3		2.2	2.2	12.3
16	962.6		22.8	22.7	41.6
17	721.0		10.4	10.4	2.1
18	657.7		.4	.4	3.0
19	482.1		22.5	22.6	30.7
		ΣI[c]	1337.9	1338.6	1366.1
		ΣEI[c]	0	3.1	349.1
20	1178.4		1.0	1.3	.5
21	1156.4		0	.1	.1
22	941.2		117.7	126.1	133.2
23	928.8		3.2	2.7	5.0
24	617.9		19.0	17.9	14.4
25	555.4		185.8	180.2	193.3
26	489.5		5.5	6.8	6.9
27	256.4		4.5	3.5	2.8
		ΣI[c]	336.7	338.6	356.2
		ΣEI[c]	0	18.3	33.1

[a] Frequencies are predicted from 4-31G force field (Table 3-3).

[b] Intensities are predicted by usage of 4-31G force field (Table 3-3) and a given set of APTs: 4-31G APTs (Table 3-5), HC APTs (Table 5-2), and LC APTs (Table 5-3).

[c] The terms are defined in Section 5.1.

TABLE 5-7
PREDICTED BAND FREQUENCIES AND INTENSITIES FOR IR FUNDAMENTAL BANDS OF 2-PYRIMIDINOL FROM STO-3G FORCE FIELD AND 4-31G, HC, AND LC ATOMIC POLAR TENSORS

	Frequency[a] (cm^{-1})		Intensities (km/mole)[b] 4-31G	HC	LC
1	4267.6		141.7	142.4	94.0
2	3760.8		4.6	4.5	17.9
3	3707.4		21.0	20.7	64.0
4	3701.6		6.1	6.0	19.0
5	1908.9		104.7	104.8	113.7
6	1887.6		191.9	192.2	181.9
7	1756.1		61.3	61.2	108.1
8	1704.9		402.0	401.6	365.5
9	1624.8		258.3	259.3	220.7
10	1549.6		.9	.9	11.8
11	1409.1		55.2	55.0	36.4
12	1291.7		11.9	11.8	4.4
13	1263.6		0	0	2.2
14	1100.3		1.1	1.1	9.8
15	1020.4		28.9	28.9	49.6
16	962.0		16.3	16.2	31.4
17	737.3		10.3	10.3	2.6
18	639.4		.1	.1	2.4
19	455.8		21.6	21.6	30.6
		ΣI[c]	1338.0	1338.6	1366.1
		ΣEI[c]	1075.9	1077.6	1084.2
20	1189.3		.3	.5	.1
21	1164.4		0	0	0
22	956.0		56.5	58.4	69.8
23	881.4		56.5	62.8	61.6
24	602.2		122.2	118.6	115.6
25	574.3		89.1	85.7	97.1
26	480.2		8.0	9.4	9.5
27	253.3		4.0	3.2	2.5
		ΣI[c]	336.6	338.6	356.2
		ΣEI[c]	318.1	324.3	298.5

[a]Frequencies are predicted from STO-3G force field (Table 4-2).

[b]Intensities are predicted by usage of STO-3G force field (Table 4-2) and a given set of APTs: 4-31G APTs (Table 3-5), HC APTs (Table 5-2), and LC APTs (Table 5-3).

[c]The terms are defined in Section 5.1.

TABLE 5-9
PREDICTED POTENTIAL ENERGY DISTRIBUTION
FOR IR FUNDAMENTAL BANDS OF 2-PYRIMIDINOL FROM
"NEAR 4-31G" FORCE FIELDS AT TWO CONVERGENCES

ν	HC CASE	LC CASE
1	100S9	100S9
2	10S9,92S10	94S10
3	79S9,16S11	92S9,12S11
4	10S9,13S10,77S11	11S10,91S11
5	22S2,10S3,24S5,16S6,10S19	24S2,24S5,16S6,10S13
6	22S1,17S3,25S4,11S17	24S1,19S3,24S4,10S6,10S14, 10S17
7	12S1,13S5,26S7	11S1,13S5,27S7
8	10S4,10S6,12S7,24S18,14S19	10S4,11S6,11S7,23S18,12S19
9	51S16,25S17,16S19	52S16,22S17,16S19
10	10S3,10S6,15S7,21S17,17S19	14S7,21S17,17S19
11	16S16,20S17,25S19	16S16,22S17,27S19
12	15S3,19S6,55S18	13S3,17S6,59S18
13	25S4,27S5,15S17,12S19	24S4,25S5,17S17,12S19
14	19S1,13S3,69S12	19S1,14S3,69S12
15	62S1,59S2,41S3,58S4,50S5,47S6	61S1,59S2,40S3,60S4,49S5, 47S6
16	24S2,27S7,12S14	22S2,29S7,12S14
17	72S13,17S14	72S13,17S14
18	16S7,10S13,59S14	16S7,10S13,59S14
19	99S15	99S15
20	64S25,43S26,21S27	93S25,29S26
21	37S25,78S27	10S25,14S26,95S27
22	39S20,35S23,70S26	100S20,65S23,48S26
23	12S20,45S23,29S25,31S27	67S20,15S23,31S25,29S26, 39S27
24	17S20,15S21,39S22,69S23, 25S25	11S20,11S21,10S22,29S23, 64S24
25	93S24	32S22,40S23,37S24,17S26
26	101S21,27S22,10S25	104S21,30S22,11S25
27	24S21,79S22	23S21,82S22

Note: The HC and LC "near 4-31G" force fields by the "WCD method" obtained from calculations at the two convergences of Section 5.1 are used. The "MK method" for PEDs is used (Section 2.2 4) The PEDs are defined in symmetrized internal coordinates (Table 3-4). See example of PED in Footnote a of Table 3-1

frequencies then is worse than that obtained utilizing an unscaled STO-3G force field. This is a form of warning that caution should be exercised in scaling procedures, where in some cases scaling a force field actually gives worst results than not scaling at all. The difference in the EPIP and EPOP values between the SC and HC methods is not large (they differ mainly in integral threshold values). This suggests that better integral thresholds improved the results but not by much. The trends concerning normal modes are harder to see since the statistical values are quite close to each other. The statistical values on the frequencies and normal modes are largely mimicked by the MDIP, MIP, MDOP, and MOP values.

The results for predicted intensities in Table 5-9 are more difficult to follow. One can begin by looking at the APTs of Tables 5-2 and 5-3. These tables show the IIPD parameter which stands for the sum of the absolute values of the differences between the in-plane components of the APTs and the corresponding components of the 4-31G APTs of 2-pyrimidinol (Table 3-5). Similarly IOPD is the sum of these deviations for the out-of-plane components. It is interesting to notice there is a large change in IIPD value between the HC and LC APTs, whereas a small one is seen for the IOPD case. The small IIPD for HC APTs suggests that integral threshold was not important for the in-plane case, since 4-31G and HC APTs had roughly the same convergence (10^{-9} and 10^{-8} respectively) but quite different integral thresholds (10^{-10} and 10^{-6} respectively). By similar

reasoning the large ΣIPD for the LC APTs (obtained at 5 * 10^{-5} convergence) suggests that convergence was quite important for the in-plane case. For the HC APTs the magnitude of the ΣOPD is similar to the ΣIPD perhaps suggesting again that integral threshold was not a significant parameter in these *ab initio* calculations. The ΣOPD values for HC and LC APTs are quite similar indicating that convergence was not as important as in the in-plane case (at least in the 10^{-8} to 5 * 10^{-5} convergence range).

Table 5-4 shows that the above mentioned observations on APTs are imitated rather closely by the predicted band intensities. The parameters ΣI and ΣEI in this table are the sum of the intensities and the sum of the absolute values of the deviations of the intensities from the corresponding 4-31G intensities (Table 3-7) respectively. For the in-plane modes both 4-31G and HC intensities were similar whereas LC showed a larger deviation. For the out-of-plane modes it seems there was no difference, or an element of randomness, between the ΣEI values. The same situation is observed in Tables 5-5 through 5-7.

Looking back at the errors in intensity values of Table 5-9, it can be seen that similar observations to the above mentioned ones are observed. For a given force field, HC for instance, the ΣIIP and ΣIOP values follow the same trends throughout the range of considered APTs. The logistics of understanding the statistical parameters of the intensities for various force fields with a given APT is more difficult to develop. For the in-plane modes results

TABLE 5-9
STATISTICAL ANALYSIS ON THE ABILITY OF VARIOUS FORCE FIELDS AND ATOMIC POLAR TENSORS FROM DIFFERENT LEVELS OF CONVERGENCE AND INTEGRAL THRESHOLD TO MIMIC THE PREDICTED 4-31G RESULTS FOR THE IE FUNDAMENTAL BANDS OF 2-PYRIMIDINOL

	APT	FORCE FIELD				
		HC	LC	STO-3G	4-31G	BC
EPIP		43.0	52.3	121.2	0	26.2
EPDP		13.3	73.5	16.0	0	23.6
ENIP		74.7	77.2	72.5	0	62.2
ENDP		66.4	79.4	98.5	0	75.5
EIIP	431G	36.0	36.2	56.6	0	20.8
EIDP	431G	7.4	25.8	39.8	0	13.1
EIIP	HC	36.2	36.3	56.7	.2	--
EIOP	HC	6.4	25.5	40.5	2.3	--
EIIP	LC	39.3	41.0	57.1	18.4	--
EIOP	LC	6.8	24.4	37.3	4.1	--
MDIP		.0468	.0600	0943	--	0
MIP		.0029	.0385	0744	--	0
MDDP		.0958	.2888	.0803	--	0
MDP		.0958	.2888	0354	--	0
FPIP		3	4	5	1	2
NPIP		4	5	3	1	2
IPIP		3	4	5	1	2
FPDP		2	5	3	1	4
NPDP		2	4	5	1	3
IPDP		2	4	5	1	3

Note: The EF and EI parameters are in cm^{-1} and km/mole respectively. The other parameters are unitless. The statistical terms, force fields, and APTs are described in Section 5.1 and Chapter 4. The predicted 4-31G results are from Chapter 3.

seemed to get better with force fields of higher convergence. We recall that band intensities were obtained from the interplay of force fields and APTs (Equation 2-22). Thus inetances could have occurred where the intensities calculated with a lower convergence force field were similar to the ones from a higher convergence force field. For example consider the rather close EIIP value for HC force field with HC APTs, and the value for LC force field with LC APTs. The reasons behind these observations on intensities predicted by various methods need be investigated further.

All the above mentioned observations on frequencies normal modes, and intensities predicted by the various methods are further summarized in the FP, NP, and IP parameters for in-plane and out-of-plane modes. In general it can be said that the higher the convergence and the integral threshold the better the results. Nonetheless in the range of studied convergences and integral thresholds, the convergence effect seems to be a much more critical one than the integral threshold.

5.2 Reference Geometry

Ab initio calculations of diagonal force constants and atomic polar tensors of 2-pyrimidinol were carried out at the HF SCF level with a 4-31G basis set using three reference geometries with the GAUSSIAN 76[53] program at $5 * 10^{-5}$ convergence and 10^{-6} integral threshold (see details in Section 2.1 2). The reference geometries are labelled as 3GG, XL1, and XL2. The force constants evaluated using these reference geometries are referred to as 3GG, XL1, and XL2

force constants respectively. Similarly APTs evaluated with these geometries are 3GG, XL1, and XL2 atomic polar tensors respectively. The 3GG geometry is the STO-3G optimized geometry of 2-pyrimidinol (Table 4-1). The XL1 and XL2 geometries are possible crystal structures of 2-pyrimidinol. The experimental geometry of 2-pyrimidinol crystal was not known because in the crystal the 2-pyrimidinone tautomer predominates.[2,5] The XL1 geometry was obtained by using crystallographic data for pyrimidine[70] together with the optimized geometry from a calculation with an STO-3G basis set for 2-pyrimidinol given previously in Table 4-1. The ring portion was determined from the crystallographic data, and the exocyclic components from the theoretical geometry. The XL2 geometry was determined by pursuing a more obstinate approach to estimate the "real" experimental geometry of 2-pyrimidinol. The ring portion and CH angles were obtained from the pyrimidine crystal,[70] the CH bond lengths from considerations on experimental work on benzene,[11,46,71,72] the CO and COH angles, the CO bond length from crystal work on 6-bromo-2-hydroxypyridine,[73] and the OH bond length from the considerations of Rogers for methanol and ethanol.[74] The XL1 and XL2 geometries are shown in Table 5-10.

By the "WCD method" explained in Chapter 4, the 3GG, XL1, and XL2 diagonal force constants and the STO-3G force field of 2-pyrimidinol (Table 4-2) were used to give 3GG, XL1, and XL2 "near 4-31G" force fields respectively. The scaling constants are given in Table 5-11 where C_{3GG}, C_{XL1},

TABLE 5-10
TWO POSSIBLE CRYSTAL GEOMETRIES OF 2-PYRIMIDINOL

	XL1	XL2		XL1	XL2
r_1(A)[a]			θ_1(degrees)[a]		
1	1.335	1.335	12	115.9	115.9
2	1.340	1.340	13	126.8	126.8
3	1.341	1.341	14	116.3	116.3
4	1.391	1.391	15	121.9	121.9
5	1.391	1.391	16	116.6	116.6
6	1.338	1.338	17	122.5	122.5
7	1.381	1.328	18	116.6	117.0
8	.989	.945	19	103.7	109.0
9	1.089	1.080	20	121.3	124.0
10	1.079	1.080	21	121.7	124.7
11	1.089	1.080	22	116.3	112.8
			23	116.3	116.2
			24	116.8	114.1
			25	121.7	118.7
			26	121.2	124.7

[a]Bond lengths, r, and Angles, θ, are according to Figure 3-3. Further details are given in Section 4.2

and C_{XL2} correspond to the 3GG, XL1, and XL2 respectively. The APTs evaluated with these reference geometries are given in Tables 5-12 through 5-14. Tables 5-15 through 5-17 show the corresponding orientation used in the calculation of these APTs.

Using the 3GG, XL1, and XL2 "near 4-31G" force fields, the band frequencies and normal modes of Tables 5-18 and 5-19 were obtained. The 3GG APTs were used together with the 3GG "near 4-31G" force field to give the 3GG intensities of Table 5-18. Similarly the XL1 APTs and XL1 "near 4-31G" force field gave the XL1 intensities of Table 5-18; and the XL2 APTs and XL2 "near 4-31G" force field gave the XL2 intensities of Table 5-18.

Table 5-20 summarizes the statistical analysis of these different calculations. The errors in frequencies, PEDs, and intensities are calculated in the same way as presented in Chapter 4. These errors are the deviations of the given parameter from the result for that parameter calculated with the 4-31G basis set for 2-pyrimidinol (Chapter 3). The MDIF, MIF, MDOF, and MOF values are measured with respect to C_s scaling constants (Table 4-3) as was done in Chapter 4. These values can be compared to each other since the force field to be upgraded had the same diagonality in all cases. The results of the LC and STO-3G methods with LC APTs from Table 5-9 are included in this table for comparison purposes. They had the same convergence and integral threshold as the 3GG, XL1, and XL2 calculations presented in Table 5-20.

TABLE 5-11
THE 4-31G/STO-3G SCALING CONSTANTS FOR 2-FYRINIDINOL
USING VARIOUS REFERENCE STATES

S	C_{3GG}	C_{XL1}	C_{XL2}
1	.8775	.8427	.6535
2	.9013	.8297	.6245
3	.9106	.8482	.6839
4	.8904	.8346	.6938
5	.9564	.8307	.7470
6	.9215	.8615	.7324
7	.8670	.8029	.7123
8	.7248	.7098	.8356
9	.7753	.7554	.7804
10	.8172	.7857	.7563
11	.7878	.7616	.7779
12	.8781	.8196	.6848
13	.8912	.8351	.6580
14	.8694	.7953	.6808
15	.9124	.8666	.6974
16	.8771	.8362	.8007
17	.8151	.7833	.7677
18	.8614	.8160	.7401
19	.8526	.8075	.7621
20	1.4749	.8894	.2017
21	1.5620	1.0397	.5438
22	1.4203	.9682	1.2601
23	1.4206	1.1930	1.1039
24	2.7268	2.1768	.2551
25	1.3701	1.1432	.5421
26	1.2151	1.0162	.6246
27	1.2197	1.0242	.6862

Note: The constants were obtained by the "WCD method." For further information see Section 5.2.

TABLE 5-12
ATOMIC POLAR TENSORS
FOR 2-PYRIMIDINOL WITH STO-3G OPTIMIZED GEOMETRY
(3GG APTS)

Ni[a,b,c]			O7		
-.77112	-.17313	0	.20826	.15557	0
-.22385	-1.02486	0	-.03166	-1.56421	0
0	0	-.42199	0	0	-.63121

C2			H8		
-.02362	.08224	0	.22188	-.10100	0
-.16551	2.00469	0	.03318	.39734	0
0	0	.57311	0	0	.43375

N3			H9		
-.12512	.20198	0	-.11429	.09634	0
.47983	-1.03705	0	.12394	.00194	0
0	0	-.38712	0	0	.13020

C4			H10		
.55079	.31895	0	.06732	.01192	0
-.24211	.81199	0	.01967	-.13198	0
0	0	.13469	0	0	.19193

C5			H11		
-.95774	-.16374	0	-.13246	-.05546	0
-.12560	-.15276	0	-.07493	.01729	0
0	0	-.29254	0	0	.12420

C6		
1.07611	-.37367	0
.20703	.67762	0
0	0	.14500

[a] Units are in electrons (e).

[b] The APTs were determined at HF SCF level with 4-31G basis set using 3GG geometry (Table 4-1) as reference state.

[c] The atom numbering is given in Figure 3-3; the coordinate system of orientation is the principal cartesian coordinates of Table 3-6.

TABLE 5-13
ATOMIC POLAR TENSORS
FOR 2-PYRIMIDINOL WITH CRYSTAL XL1 GEOMETRY
(XL1 APTS)

N1[a,b,c]			O7		
-.77839	-.18203	0	.18481	.15553	0
-.22287	-1.02888	0	-.04914	-1.55481	0
0	0	-.41848	0	0	-.83235

C2			H8		
.02884	.08410	0	.22532	-.08828	0
-.14018	2.01462	0	.03226	.39823	0
0	0	.57877	0	0	.43257

N3			H9		
-.17999	.19431	0	-.10890	.09381	0
.48903	-1.08185	0	.12525	.00489	0
0	0	-.39801	0	0	.13072

C4			H10		
.57814	.30715	0	.07382	.00458	0
-.25210	.81597	0	.01724	-.13289	0
0	0	.13326	0	0	.18922

C5			H11		
-.55941	-.13000	0	-.13225	-.05479	0
-.11117	-.13718	0	-.07407	.02072	0
0	0	-.27531	0	0	.12131

C6		
1.06440	-.38818	0
.20552	.87917	0
0	0	.13827

---

[a] Units are in electrons (e).

[b] The APTs were determined at RF SCF level with 4-31G basis set using XL1 geometry (Table 5-10) as reference state.

[c] The atom numbering is given in Figure 3-3; the orientation is the principal cartesian coordinates of Table 3-6.

TABLE 5-14
ATOMIC POLAR TENSORS
FOR 2-PYRIMIDINOL WITH XL2 GEOMETRY
(XL2 APTS)

N1[a,b,c]			O7		
-.77154	-.16484	0	.09946	.21673	0
-.24547	-1.01563	0	-.03703	-1.75854	0
0	0	-.43321	0	0	-.64832

C2			H8		
.03662	.07857	0	.23831	-.09486	0
-.11126	2.15597	0	.03277	.36030	0
0	0	.60640	0	0	.45372

N3			H9		
-.17159	-.10221	0	-.10264	.08257	0
.46782	-1.00261	0	.13150	.02213	0
0	0	-.41308	0	0	.13052

C4			H10		
.57188	.43283	0	.08158	.01184	0
-.24864	.78422	0	.03695	-.11913	0
0	0	.13453	0	0	.19160

C5			H11		
-.95924	-.07230	0	-.13034	-.01332	0
-.10403	-.16856	0	-.08151	.06189	0
0	0	-.29082	0	0	.12080

C6		
1.10479	-.37501	0
.15889	.67996	0
0	0	.14786

[a] Units are in electrons (e).

[b] The APTs were determined at HF SCF level with 4-31G basis set using XL2 geometry (Table 5-10) as reference state.

[c] The atom numbering is given in Figure 3-3; the coordinate system of orientation is the principal cartesian coordinates of Table 3-6.

TABLE 5-15
PRINCIPAL CARTESIAN COORDINATES, GROUND STATE ENERGIES, AND GROUND STATE DIPOLE MOMENTS OF 2-PYRIMIDINOL AT THE OPTIMIZED 3GG GEOMETRY

	X[e]	Y[a]	Z[a]
N1	1.210100	- .260898	0
C2	-.020087	-1.033453	0
N3	-1.237167	-.224995	0
C4	-1.171267	1.122394	0
C5	.024722	1.829727	0
C6	1.195156	1.091308	0
O7	-.059157	-2.213600	0
H8	.894939	-2.475541	0
H9	-2.125225	1.646604	0
H10	.038900	2.908934	0
H11	2.166678	1.581981	0

ENERGY (AU)[b]

= -333.24136065 (10^{-9} CG, 10^{-10} IT, STO-3G BS)[c]

= -337.03778011 ($5 * 10^{-5}$ CG, 10^{-6} IT, 4-31G BS)[d]

DIPOLE (DEBYES)[b]

= 2.6563 (10^{-9} CG, 10^{-10} IT, STO-3G BS)[c]

= 4.2169 ($5 * 10^{-5}$ CG, 10^{-6} IT, 4-31G BS)[d]

[a]Principal cartesian coordinates are in A. The optimized STO-3G geometry is used (Table 4-1) The atom numbering is shown in Figure 3-3.

[b]The term CG, IT, and BS stand for the convergence, integral threshold, and basis set respectively, that were used in the corresponding calculation.

[c]The calculation was performed with GAUSSIAN 82 (Reference 32).

[d]The calculation was performed with GAUSSIAN 76 (Reference 53).

TABLE 5-16
PRINCIPAL CARTESIAN COORDINATES, GROUND STATE ENERGY, AND GROUND STATE DIPOLE OF 2-PYRIMIDINOL AT THE CRYSTAL XL1 GEOMETRY

	x[a]	y[a]	z[a]
N1	1.179402	-.274446	0
C2	-.031853	-.835771	0
N3	-1.211295	-.199754	0
C4	-1.163656	1.140399	0
C5	.042631	1.833041	0
C6	1.202086	1.064570	0
O7	-.073677	-2.215837	0
H8	.880034	-2.479175	0
H9	-2.117187	1.665385	0
H10	.077209	2.911787	0
H11	2.186471	1.529133	0

ENERGY (AU)[b]

= -337.04190408 (5 * 10^{-5} CG, 10^{-6} IT, 4-31G BS)

DIPOLE (DEBYES)[b]

= 4.2332 (5 * 10^{-5} CG, 10^{-6}, 4-31G BS)

[a]Principal cartesian coordinates are in Å. The crystal XL1 geometry is shown in Table 5-10. The atom numbering is shown in Figure 3-3.

[b]The terms CG, IT, and BS stand for the convergence, integral threshold, and basis set used in the calculation. The calculation was performed with GAUSSIAN 76 (Reference 53).

TABLE 5-17
PRINCIPAL CARTESIAN COORDINATES, GROUND STATE ENERGY, AND GROUND STATE DIPOLE OF 2-PYRIMIDINOL AT THE CRYSTAL XL2 GEOMETRY

	X[a]	Y[a]	Z[a]
N1	1.177146	-.266502	0
C2	-.037250	-.642995	0
N3	-1.213091	-.200345	0
C4	-1.157904	1.139519	0
C5	.052266	1.625354	0
C6	1.207373	1.050366	0
O7	-.075668	-2.170436	0
H8	.608546	-2.503633	0
H9	-2.124760	1.620714	0
H10	.036406	2.905236	0
H11	2.212626	1.445159	0

ENERGY (AU)[b]

= -337.04469506 (5 * 10^{-5} CG, 10^{-6} IT, 4-31G BS)

DIPOLE (DEBYES)[b]

= 3.7967 (5 * 10^{-5} CG, 10^{-6}, 4-31G BS)

[a]Principal cartesian coordinates are in Å. The crystal XL2 geometry is shown in Table 5-10. The atom numbering is shown in Figure 3-3.

[b]The terms CG, IT, and BS stand for the convergence, integral threshold, and basis set used in the calculation. The calculation was performed with GAUSSIAN 76 (Reference 53)

Table 5-20 helps one to inspect the variations in results from the various cases with respect to the 4-31G results of Chapter 3. Looking at the frequency parameters in this table it can be seen that the different reference states gave different deviations. The LC results were the best in general. This is to be expected since the reference state in this case was the 4-31G optimized geometry (Table 3-2). The normal modes for all cases were approximately equivalent. The MDIP, MIP, MDOP, and MOP values mimic to a good extent the observations on frequencies and normal modes.

A set of new parameters is introduced in Table 5-20. These are MDR and MR which stand for the mean of the absolute values and the mean of the values respectively of the deviations of the bond lengths of a given geometry from the corresponding bond lengths of the 4-31G optimized geometry (Table 3-2) Similarly MDA and MA correspond to deviations in the angles. These are rough estimates of how close a given geometry was to the 4-31G optimized geometry (Table 3-2). One might have expected that the closer the geometry of the reference state was to the 4-31G optimized geometry, the closer the predicted IR results would have been to 4-31G results of Chapter 3, i.e., better statistical parameters of Table 5-20. It seems this was not the case. For example, XL2 was closer to the 4-31G optimized geometry than 3GG was. Nonetheless XL2 deviations in force constants

TABLE 5-18
PREDICTED BAND FREQUENCIES AND INTENSITIES OF 2-PYRIMIDINOL OBTAINED FROM FORCE FIELDS AND ATOMIC POLAR TENSORS EVALUATED WITH DIFFERENT REFERENCE STATES

	3GG		XL1		XL2	
ν	FREQ (cm^{-1})	I (km/mol)	FREQ (cm^{-1})	1 (km/mol)	FREQ (cm^{-1})	I (km/mol)
1	3631.6	62.1	3593.4	62.2	3899.8	81.2
2	3399.6	16.2	3332.3	17.2	3280.4	36.0
3	3290.4	56.1	3235.0	58.8	3271.7	60.2
4	2364.1	46.8	3221.4	41.8	3255.8	5.4
5	1803.8	135.8	1746.6	143.3	1633.2	31.2
6	1760.9	155.2	1706.0	177.4	1603.0	157.3
7	1625.3	80.7	1579.1	75.1	1496.6	115.2
8	1573.3	317.3	1532.4	315.6	1428.1	96.6
9	1468.1	236.8	1431.6	233.9	1396.1	606.1
10	1426.8	24.3	1390.3	10.9	1310.0	14.4
11	1302.2	34.8	1263.0	39.8	1199.2	35.3
12	1208.2	4.4	1172.7	4.2	1098.1	2.0
13	1176.9	1.1	1148.2	1.1	1070.4	3.1
14	1037.8	18.1	999.6	12.2	905.9	15.3
15	970.9	40.8	939.7	46.4	840.8	53.4
16	907.1	30.2	872.1	28.0	785.4	22.2
17	677.9	2.9	663.2	2.8	596.3	5.0
18	586.6	.5	568.4	.5	523.1	1.1
19	427.2	43.1	415.0	41.9	383.3	33.5
20	1334.9	.4	1239.4	.1	993.9	6.7
21	1270.8	0	1181.0	.3	889.1	6.7
22	1068.6	114.6	965.9	68.2	822.7	89.6
23	1052.3	8.6	859.1	65.0	687.6	5.0
24	886.7	197.5	790.4	182.6	451.9	9.1
25	713.4	1.6	602.0	3.3	336.4	.4
26	575.9	3.0	475.6	3 1	287.7	219.7
27	295.7	2.0	247.8	2.5	200.0	14.2

Note: See further details in Section 5.2.

TABLE 5-19
PREDICTED POTENTIAL ENERGY DISTRIBUTION FOR 2-PYRIMIDINOL IR FUNDAMENTAL BANDS OBTAINED FROM DIFFERENT REFERENCE STATES

	3GG	XL1	XL2
1	100S6	100S6	100S6
2	96S10	96S10	37S9
			43S10
			20S11
3	96S11	97S11	49S9
			47S11
4	98S9	97S9	14S9
			53S10
			34S11
5	14S2	14S2	12S2
	11S3	11S3	15S5
	33S5	32S5	43S16
	16S6	17S6	
	11S19	12S19	
6	15S1	17S1	16S3
	15S3	14S3	16S4
	30S4	30S4	14S6
	10S17	10S16	13S16
		11S17	21S17
			12S19
7	13S5	13S5	16S4
	17S16	19S16	23S5
	21S16	20S16	12S16
			31S18
8	16S1	16S1	12S1
	37S7	33S7	13S7
	14S19	15S19	17S17
			32S19
9	10S7	49S16	12S2
	52S16	21S17	37S7
	16S17	17S19	17S16
	16S19		24S17
10	13S6	10S3	14S3
	10S7	12S6	15S6
	25S17	13S7	15S7
	15S19	22S17	15S17
		15S19	19S19
11	12S16	12S16	13S17
	24S17	21S17	16S16
	26S19	27S19	20S19
12	16S6	12S3	12S3
	53S16	16S6	13S5
		53S16	22S6
			36S16
13	25S4	25S4	10S3
	21S5	23S5	32S4
	19S17	16S17	19S5
		10S19	

continued

TABLE 5-19 continued

	3GG	XL1	XL2
14	17S1	19S1	13S1
	10S3	13S3	10S3
	69S12	70S12	75S12
15	67S1	67S1	79S1
	67S2	63S2	54S2
	43S3	42S3	46S3
	60S4	58S4	52S4
	46S5	46S5	47S5
	50S6	45S6	41S6
16	12S1	25S2	41S2
	18S2	26S7	20S7
	25S7	10S12	10S14
	12S12	11S14	
	12S14		
17	74S13	73S13	68S13
	19S14	18S14	23S14
18	15S7	15S7	13S7
	12S13	11S13	17S13
	58S14	60S14	54S14
19	92S15	90S15	10S13
			89S15
20	109S25	97S25	38S26
	15S26	26S26	77S27
21	28S26	19S26	66S25
	96S27	93S27	20S26
			32S27
22	143S20	13S25	28S22
	59S23	73S26	91S23
	33S26	23S27	16S25
23	32S20	139S20	20S22
	23S25	93S23	52S23
	45S26	14S25	36S25
	38S27	16S27	66S26
24	100S24	99S24	22S20
			20S21
			86S22
			13S27
25	22S21	35S20	63S20
	51S22	14S21	84S21
	84S23	40S22	20S25
	24S26	50S23	16S26
		27S26	
26	101S21	105S21	99S24
	33S22	30S22	
	11S25	12S25	
27	17S21	22S21	69S20
	70S22	61S22	33S21
			24S22

Note: PEDs (MK) are in S coordinates (See Table 3-8).

and frequencies were greater than 3GG results. This suggests that approximate geometries used as reference states need not give approximate results. More is said about this later.

The errors in the intensities seen in Table 5-20 are more difficult to understand. This is a consequence of having used not only different "near 4-31G" force fields, but also different APTs. As mentioned before, it is difficult to evaluate the interplay between the force field and APTs that takes place in the evaluation of band intensities. The best results pertained to LC cases as expected. But this is not necessarily a fair comparison. A better comparison could be carried out by the transfer of APTs between reference states for intensity calculation purposes. This is not to be considered in the present work. The next section addresses this problem in a different way.

5.3 Conclusions

Convergence, integral threshold, and choice of reference state play a significant role in determining predictions of IR spectra. Cases are seen where poor convergence or choice of a reference state leads to results that are worse than unscaled ones, i.e., calculations with an STO-3G basis set. It is observed that in general the better the convergence and integral threshold the better the results. The similarity between trends in the EF and EN values and those in the MDIP, MIP, MDOP, and MOP values seems to be real.

TABLE 5-20
STATISTICAL ANALYSIS OF THE ABILITY OF VARIOUS STUDIES USING VARIOUS REFERENCE STATES IN REPRODUCING THE PREDICTED 4-31G RESULTS FOR 2-PYRIMIDINOL

	LC	3GG	XL1	XL2	STO-3G
EF1P	52.3	71.9	108.3	152.2	121.2
EFOP	73.5	134.3	52.7	181.8	16.0
EN1P	77.2	85.9	85.8	84.4	72.5
ENOP	79.4	111.9	152.5	160.1	98.5
EI1P	41.0	58.8	57.7	75.1	57.1
EIOP	24.4	47.1	57.9	57.7	37.3
MDIP	.0600	.0929	.1287	.2133	.0943
MIP	.0385	-.0631	.1108	-.1999	.0744
MDOP	.2888	.5866	.2385	.3636	.0803
MOP	.2888	.5866	.2167	-.3124	.0354
MDR	0	.024	.019	.011	.024
MR	0	.024	.019	.008	.024
MDA	0	1.9	1.3	1.8	1.9
MA	0	-1.0	.8	-.4	-1.0
FF1P	1	2	3	5	4
NF1P	2	5	4	3	1
IF1P	1	4	3	5	2
FFOP	3	4	2	5	1
NFOP	1	3	4	5	2
IFOP	1	3	5	4	2

Note: The EF and EI values are in cm^{-1} and km/mols respectively. The other terms in the table are unitless. They are defined in Section 5.2. The predicted 4-31 results correspond to the 4-31G studies of Chapter 3.

Calculations using similar reference states need not necessarily predict similar IR spectra. This indirectly contradicts researchers who use reference states close to the experimental geometry in the evaluation of force fields expecting predicted results close to experimental observations (see Introduction). On the other hand this indirectly supports researchers who use theoretically optimized reference states in the determination of force fields at the same level of theory. Our conclusions tend to make us side with the latter.

A small observation should be made at this point concerning XL2 calculations. The ab initio calculation of diagonal force constants in W coordinates (at the HF SCF level with a 4-31G basis set) with XL2 as reference state gave two small negative force constants (in the order of 0.05 md/A) for two out-of-plane modes. They were set equal to zero. This was the only case throughout all calculations carried out in the present work where negative force constants were seen. This can be interpreted in the sense that at least for fundamentals with very small frequencies it might be dangerous to use reference states such as experimental ones. It is paradoxical that the only case where this happened was for XL2, the geometry we expected to be closest to the experimental one.

Table 5-21 is constructed so as to permit a different comparison between the various cases treated in this chapter. So far all cases are compared to the 4-31G results of Chapter 3 during the statistical analysis. In this table

the comparisons are made with respect to experimental results. The calculated frequencies of a given case, e.g., HC predictions, were multiplied by 0.9 as was done in Chapter 3. These scaled frequencies were then compared to the experimental frequencies of Table 3-9. The EPIP and EPOP values were the means of the absolute values of the differences between the scaled frequencies of a given case and the corresponding experimental frequencies for in-plane and out-of-plane modes respectively. The calculated intensities of a given method were multiplied by the corresponding absorbance-intensity conversion constant (as was done in Section 3.4). These constants are labelled AICIP and AICOP, which correspond to in-plane and out-of-plane modes respectively. They are given in Table 5-21. These converted R.A.s are compared to the experimental R.A.s of Table 3-9. The EIIP and EIOP values are the mean of the absolute values of the deviations of the calculated R.A.s from the corresponding experimental R.A.s for the in-plane and out-of-plane modes respectively. The calculated R.A.s for 4-31G, SC, HC, and STO-3G cases involved the use of the 4-31G APTs (Table 3-5). For LC case the LC APTs were used. For the 3GG, XL1, and XL2 the 3GG, XL1, and XL2 APTs respectively were used.

Table 5-21 shows that the best approximation to experimental results came from the 4-31G case. This was followed by SC and HC methods. These results were the expected ones. Some randomness is observed in the analysis of the calculations of the out-of-plane results. These

TABLE 5-21
STATISTICAL ANALYSIS
ON THE ABILITY OF VARIOUS METHODS TO IMITATE
THE EXPERIMENTAL SPECTRUM OF 2-PYRIMIDINOL

	EFIP	EFOP	EIIP	EIOP	AICIP	AICOP
4-31G	14.6	26.6	15.1	7.2	.577	.360
SC	31.7	24.0	21.7	9.1	.577	.360
HC	42.2	31.4	25.1	7.8	.577	.360
STO-3G	121.9	20.5	27.6	12.6	.577	.360
LC	53.3	95.7	32.7	9.0	.565	.340
3GG	66.0	163.9	27.7	19.4	.591	.370
XL1	96.2	60.5	28.4	21.3	.586	.373
XL2	132.7	156.1	44.5	27.6	.562	.345

Note: The EF and EI terms are in cm^{-1} and km/mole respectively. The terms in the table are defined in Section 5.3. The experimental results are given in Table 3-9. The EFIP, EFOP, EIIP, and EIOP are out of 17, 4, 19, and 6 values respectively.

methods were all better than the STO-3G case. The results for the lower convergence studies (LC, 3GG, XL1, and XL2) did parallel to a large extent the observations made in the previous sections, thus giving them more validity. It can be said that to some extent the closer the predictions of a given method are to the 4-31G calculated results of Chapter 3, the closer these predictions are expected to be to experimental results. It is interesting to look at the absorbance-intensity conversion constants of Table 5-21. The AICIF values are rather similar for all the methods analyzed here. The same is true for the AICOF values. The average ratio of the AICIF to the AICOF value is 1.6 for a given method. This is in line with other observations where it was found that when the calculated out-of-plane intensities were compared with experimental results the calculated values were much larger for out-of-plane modes relative to experiment than for the in-plane modes.

CHAPTER 6
PREDICTION OF THE IR SPECTRUM OF 2-PYRIMIDINONE

This chapter is concerned with the prediction of the IR spectrum of 2-pyrimidinone. As seen in Chapter 1 there was no experimental spectrum for noninteracting, isolated 2-pyrimidinone molecules. In the gas phase and in dilute matrices the only tautomeric form present was 2-pyrimidinol. On the other hand the only tautomeric form present in the solid phase and in polar solutions was 2-pyrimidinone. The IR spectra of the latter system corresponded to molecular aggregates of various types. This fact in turn creates great difficulties in assigning fundamental bands. Hence the predicted spectra cannot be calibrated by comparison with experimental results.

This problem for 2-pyrimidinone is alleviated by the fact that there have been a great many experimental and calculational studies of the infrared spectra of uracil.[30,48,49,61,67] Based on the similarity in structure between the diketo form of uracil (Figure 1-1) and that of 2-pyrimidinone we expect to find similarity between calculated IR spectra for these two molecules. In this chapter we first examine the IR spectra of uracil to calibrate our calculations. This is followed by the calculation of the IR spectrum of 2-pyrimidinone. The chapter is divided in two sections: conclusions from uracil studies, and IR spectrum of 2-pyrimidinone

6.1 Conclusions from Uracil Studies

Nishimura et al [30] calculated the fundamental in-plane vibrational frequencies of the diketo tautomer of uracil with a "near 4-31G" force field. This force field was calculated by using Equation 1-3, where F^{th} was the force field of uracil in S coordinates calculated at the HF SCF level with an STO-3G basis set, C was a diagonal matrix containing 4-31G/STO-3G scaling constants, and F was the "near 4-31G" force field in S coordinates. These symmetrized internal coordinates are given in Table 6-1. The coovarsion constants 4-31G/STO-3G are given in Table 6-2 under C_{NTKM} label. This F^{th} force field was calculated using the optimized geometry of uracil at the HF SCF level with the STO-3G basis set. The 4-31G/STO-3G scaling constants were determined from calculations of force constants of some smaller model compounds similar to uracil at the HF SCF level with both 4-31G and STO-3G basis sets. These smaller molecules were "fragments" of uracil: urea, acrolein, and formamide.

Later on Chin et al [48] used these force constants[30] to repeat the calculation of the in-plane band frequencies, and PEDs, and extended the calculations to predict also the intensities of uracil. The APTs needed to calculate the intensities were determined at the HF SCF level with a 4-31G basis set using the GAUSSIAN 76 program[53] at a convergence of $5 * 10^{-5}$ and at an integral threshold of 10^{-6}. The reference state used in the calculation of these APTs was the geometry reported by Nishimura et al [30] based on x-ray

Figure 6-1. Structure, atom numbering and in-plane internal coordinates of uracil used in this work. The out-of-plane internal coordinates are the out-of-plane bends and torsions given in Table 6-1.

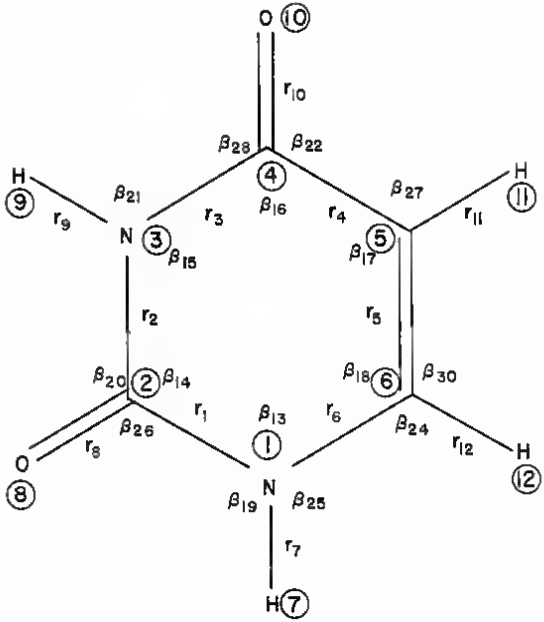
O 10
r10
β28
β22
H 9
β21
4
β27
H 11
r9
r3
β16
r4
r11
N 3
β15
5
β17
r2
r5
β20
2
β14
β18
6
β30
r1
β13
r6
β26
β24
r12
O 8
r8
1
H 12
N
β19
β25
r7
H 7

TABLE 6-1
SYMMETRIZED INTERNAL COORDINATES FOR URACIL

In-plane[a,b]

S1 = $\Delta r1$	= rN1C2
S2 = $\Delta r2$	= rC2N3
S3 = $\Delta r3$	= rN3C4
S4 = $\Delta r4$	= rC4C5
S5 = $\Delta r5$	= rC5C6
S6 = $\Delta r6$	= rC6N1
S7 = $\Delta r7$	= rN1H
S8 = $\Delta r8$	= rC2O
S9 = $\Delta r9$	= rN3H
S10 = $\Delta r10$	= rC4O
S11 = $\Delta r11$	= rC5H
S12 = $\Delta r12$	= rC6H
S13 = $(1/6)^{0.5}\{\Delta\beta13-\Delta\beta14+\Delta\beta15-\Delta\beta16+\Delta\beta17-\Delta\beta18\}$	= ΔIΘ
S14 = $(1/12)^{0.5}\{2\Delta\beta13-\Delta\beta14-\Delta\beta15+2\Delta\beta16-\Delta\beta17-\Delta\beta18\}$	= ΔIIΘ
S15 = $(1/2)\{\Delta\beta14-\Delta\beta15+\Delta\beta17-\Delta\beta18\}$	= ΔIIIΘ
S16 = $(1/2)^{0.5}\{\Delta\beta19-\Delta\beta25\}$	= δN1H
S17 = $(1/2)^{0.5}\{\Delta\beta20-\Delta\beta26\}$	= δC2O
S18 = $(1/2)^{0.5}\{\Delta\beta21-\Delta\beta27\}$	= δN3H
S19 = $(1/2)^{0.5}\{\Delta\beta22-\Delta\beta28\}$	= δC4O
S20 = $(1/2)^{0.5}\{\Delta\beta23-\Delta\beta29\}$	= δC5H
S21 = $(1/2)^{0.5}\{\Delta\beta24-\Delta\beta30\}$	= δC6H

---

continued

TABLE 6-1 continued

Out-of-plane[a,b]

$S22 = (1/6)^{0.5}\{\Delta\tau1-\Delta\tau2+\Delta\tau3-\Delta\tau4+\Delta\tau5-\Delta\tau6\}$	$= \tau I8$
$S23 = (1/2)\{\Delta\tau1-\Delta\tau3+\Delta\tau4-\Delta\tau6\}$	$= \tau II8$
$S24 = (1/12)^{0.5}\{-\Delta\tau1+2\Delta\tau2-\Delta\tau3-\Delta\tau4+2\Delta\tau5-\Delta\tau6\}$	$= \tau III8$
$S25 = \Delta\gamma H7$	$= \gamma B7$
$S26 = \Delta\gamma O8$	$= \gamma O8$
$S27 = \Delta\gamma H9$	$= \gamma H9$
$S28 = \Delta\gamma O10$	$= \gamma O10$
$S29 = \Delta\gamma H11$	$= \gamma H11$
$S30 = \Delta\gamma H12$	$= \gamma H12$

[a]The nomenclatura and numbering according to Figura 6-1. The recommandations of Pulay at al. (Reference 11) are carried out.

[b]The atoms involved in torsions are: τ1=6123, τ2=1234, τ3=2345, τ4=3456, τ5=4561, and τ6=5612.

TABLE 6-2
THE 4-31G/STO-3G SCALING CONSTANTS FOR URACIL

s	C_{NTKM}	C_{WG}
1	.96	.9381
2	.96	.9071
3	.96	.9289
4	.96	.9679
5	.82	.8376
6	.96	.8674
7	.87	.8092
8	.82	.8886
9	.87	.7886
10	.82	.8866
11	.82	.7761
12	.82	.8040
13	1.00	.8764
14	1.00	.8617
15	1.00	.8926
16	.91	.8556
17	1.08	.9443
18	.91	1.0344
19	1.08	.9628
20	.91	.8550
21	.91	.8339
22	--	1.6680
23	--	3.2203
24	--	1.4534
25	--	2.3812
26	--	1.0591
27	--	1.0048
28	--	1.1245
29	--	1.3635
30	--	1.5197

Note: Details are given in Section 6.1.

crystallographic data of 1-cyclohexyluracil (with a few modifications for NH and CH bonds). Their calculations were in essence the "SC method" reported in Chapter 4. They used their calculations to assign the in-plane experimental IR fundamental bands of uracil with considerable success. The experimental IR spectrum was obtained from investigations of uracil in a dilute Ar matrix at 10^{0} K.[67] In this matrix uracil was found[67] to be predominantly in the isolated diketo tautomeric form (Figure 1-1). These studies were reanalyzed and summarized by Scott-Lebron in his dissertation.[61]

We decided to reexamine these calculations in accordance with our procedures. The 4-31G/STO-3G scaling constants and APTs of uracil were calculated by using two sets of ab initio calculations. One set was calculated at the RHF SCF level with an STO-3G basis set using subroutine FREQ of GAUSSIAN 82[32] program (Chapter 2), at the geometry optimized at the same level of theory (Nishimura et al.[30]) as reference state, to obtain the force field. We refer to this force field as the "low field" of uracil. The other set was composed of the diagonal elements of the force field of uracil in W coordinates evaluated at RF SCF level with a 4-31G basis set using the GAUSIAN 76[53] program ($5 * 10^{-5}$ convergence, 10^{-8} integral threshold) with the crystal geometry[48] as reference state. We refer to this set as the "F_w constants" of uracil. Using the "low field" and the "F_w constants" the 4-31G/STO-3G scaling constants were calculated by the methods described in the discussion of the

WC and WCD methods of Chapter 4. The scaling constants for the WC work are not reported in the present work (they can be calculated using Equations 2-6 through 2-11). The scaling constants for WCD work are reported under C_{wd} in Table 6-2. The APTs of uracil were calculated at HF SCF level (with a 4-31G basis set) using GAUSSIAN 76[53] program (at $5 * 10^{-5}$ convergence, 10^{-6} integral threshold) using the crystal geometry[48] as reference state. We refer to them as the "crystal APTs" of uracil. The in-plane portion of the "low field" of uracil was the same as the force field of Nishimura et al.[30] The out-of-plane portion of the "low field" of uracil is given in Table 6-3. The "crystal APTs" were the same as those reported by Scott-Lebron.[61]

Tables 6-4 through 6-6 show the calculated frequencies, PEDs, and intensities of uracil. The NTKM results in these tables were calculated using the C_{NTKM} scaling constants (Table 6-2), the "low field," and the "crystal APTs" of uracil by the "SC method" of Chapter 4, i.e., the same way as the uracil calculations of Chin et al.[48] The WC results were calculated using the 4-31G/STO-3G scaling constants in W coordinate system (not reported in the present work), the "low field," and the "crystal APTs" by the "WC method" of Chapter 4. The WCD results were calculated using the 4-31G/STO-3G scaling constants C_{wd} (Table 6-2), the "low field," and the "crystal APTs" by the "WCD method" of Chapter 4. Finally the STO-3G calculations were made using the unscaled "low field" and the "crystal APTs."

TABLE 6-3
OUT-OF-PLANE FORCE CONSTANTS FOR URACIL
EVALUATED AT THE HF SCF LEVEL WITH AN STO-3G BASIS SET

	S22	S23	S24	S25	S26	S27	S28	S29	S30
S22	.26631								
S23	.01988	.14009							
S24	.13228	.01000	.33603						
S25	.10139	.09091	.01190	.11267					
S26	-.07973	-.04676	.07521	-.03460	.62833				
S27	.11259	-.05470	-.10138	.01391	-.03862	.13760			
S28	-.03468	.06655	.05619	-.00550	-.01561	-.05158	.74060		
S29	.21330	-.01587	.26131	.04364	-.00827	-.00022	-.02266	.57632	
S30	-.16938	-.03065	-.23396	-.02346	-.00449	-.01073	-.05033	-.17701	.65680

Note: The force constants are given in the symmetrized internal coordinates of Table 6-1. The units are in md-A. The reference geometry used in the evaluation of the force field was from Reference 30. The force field is symmetrized such that $F_{ij} = F_{ji}$.

TABLE 6-4
PREDICTED BAND FREQUENCIES OF URACIL FROM
THE FORCE FIELDS OF VARIOUS METHODS

ν	NTRM	WC	WCD	STO-3G
1	3867.4	3741.2	3729.6	4145.4
2	3842.6	3676.7	3658.4	4119.0
3	3412.0	3422.1	3344.9	3767.0
4	3367.3	3260.3	3313.7	3717.4
5	1965.4	2001.2	2005.4	2113.6
6	1941.4	1990.1	1983.2	2099.3
7	1856.2	1858.3	1852.2	2012.8
8	1642.9	1631.2	1627.3	1709.8
9	1559.0	1595.6	1595.3	1634.3
10	1543.2	1516.6	1506.1	1617.1
11	1538.4	1498.0	1496.8	1562.8
12	1388.7	1368.2	1371.3	1427.3
13	1301.6	1253.0	1255.7	1359.3
14	1172.1	1125.3	1134.6	1218.2
15	1072.7	1034.6	1022.4	1080.8
16	1032.8	1008.1	1016.6	1056.4
17	817.6	792.4	803.9	837.7
18	612.7	577.0	585.2	615.2
19	591.6	543.9	561.1	584.9
20	549.1	520.7	515.7	547.2
21	412.8	385.6	390.9	403.7
22	--	1422.0	1424.6	1177.2
23	--	1135.0	1071.0	920.1
24	--	1018.1	927.6	789.6
25	--	859.3	811.2	754.2
26	--	794.6	757.4	590.0
27	--	670.6	655.8	477.7
28	--	487.3	419.8	344.6
29	--	175.0	196.2	108.0
30	--	84.1	62.9	48.0

Note: The frequencies are in cm^{-1}. The methods are elaboreted in Section 6.1.

TABLE 6-5
PREDICTED POTENTIAL ENERGY DISTRIBUTION
FOR URACIL IR FUNDAMENTAL BANDS BY VARIOUS METHODS

S	NTKM	WC	WCD	STO-3G
1	100S7	99S7	100Z7	100S7
2	100S9	99S9	100S9	100S9
3	91S11	43S11	22S11	90S11
		55S12	77S12	
4	91S12	56S11	78S11	90S12
		43S12	22S12	
5	53S8	46S8	56S8	72S8
		30S10	11S18	
6	54S10	21S8	12S8	69S10
		39S10	64S10	
		16S18		
7	53S5	69S5	68S5	65S5
	10S6			12S10
	16S10			
	12S1			
8	22S6	13S3	16S8	22S6
	12S8	11S6	57S18	10S8
	29S16	17S8		38S16
		11S16		
		28S18		
9	11S1	16S6	22S6	59S18
	21S2	20S16	27S16	
	33S14	29S18	10S18	
10	14S1	13S1	14S1	19S16
	10S2	16S16	13S16	15S20
	14S3	13S20	14S20	38S21
	13S17	30S21	31S21	
	13S18			
11	24S16	15S1	12S1	21S1
	10S20	23S2	19S2	21S2
	26S21	14S16	10S3	11S3
		13S17	25S16	12S16
			12S17	12S17
12	21S3	11S2	13S2	24S3
	21S18	28S3	27S3	10S4
	19S20	16S18	10S18	17S18
		23S20	22S20	23S20
13	10S6	13S16	12S16	10S16
	14S16	24S20	26S20	23S20
	21S20	44S21	44S21	42S21
	43S21			
14	17S5	13S5	14S5	12S5
	37S6	37S6	40S6	44S6
	11S16	14S16	12S16	11S16
	24S20	20S20	21S20	19S20
15	17S13	22S1	16S1	77S1
		11S3	16S3	
		22S4	25S4	

continued

TABLE 6-5 continued

S	NTKM	WC	WCD	STO-3G
16	23S1	76S13	11S1	26S1
	12S2		68S13	12S2
	11S3			11S3
	20S4			22S4
	11S18			
17	18S1	17S1	17S1	18S1
	28S4	11S3	26S4	10S3
		25S4	12S13	28S4
		12S13		10S13
18	47S15	57S15	51S15	61S15
	14S18		14S18	
19	16S14	38S17	15S14	28S14
	11S15	32S18	11S15	30S17
	28S17		33S17	20S18
	19S18		20S18	
20	62S14	70S14	66S14	50S14
	15S15	16S15	14S15	15S15
				12S17
				17S18
21	35S17	36S17	37S17	36S17
	35S18	34S18	35S18	37S18
22		25S28	27S28	36S29
		00S30	01S30	03S30
23		14S28	76S29	20S28
		71S29	16S30	64S28
		13S30		21S30
24		67S22	65S22	46S22
		34S28	33S28	46S28
25		15S23	12S23	01S26
		41S26	38S26	
		15S27	18S28	
		16S28		
26		24S26	24S26	106S27
		77S27	05S27	
27		14S23	50S25	10S22
		52S25	47S26	13S23
		13S27		17S24
				39S25
				13S28
28		69S24	12S22	50S24
		34S25	52S24	54S25
			37S25	11S28
			27S28	
29		21S22	100S23	103S23
		69S23		
		13S38		
30		24S22	60S22	55S22
		39S24	50S24	45S24
		16S26		

Note: FEDs (KJ) are given in S coordinates (Table 6-1).

TABLE 6-6
PREDICTED BAND INTENSITIES FOR URACIL
BY FORCE FIELDS FROM VARIOUS METHODS AND THE CRYSTAL
ATOMIC POLAR TENSORS

S	NTRM	WC	WCD	STO-3G
1	101.8	103.5	102.3	101.3
2	99.7	88.0	98.8	98.6
3	10.7	12.2	7.8	10.9
4	8.9	11.3	11.8	8.6
5	983.6	381.1	961.3	734.7
6	462.4	965.4	375.0	640.8
7	3.5	70.0	63.4	19.2
8	65.8	42.9	8.1	80.2
9	23.6	65.1	109.6	4.4
10	154.5	16.1	16.9	5.0
11	13.5	153.7	167.2	212.1
12	17.3	41.6	26.6	19.6
13	41.2	34.8	35.2	42.4
14	18.9	21.1	27.7	31.9
15	8.5	1.0	.7	7.2
16	.4	9.6	7.0	1.1
17	5.4	6.1	5.9	5.0
18	3.9	5.3	2.7	5.2
19	7.5	3.5	5.4	6.3
20	30.4	26.7	26.4	25.1
21	26.8	29.3	28.4	28.7
22	--	0	.1	1.6
23	--	27.7	77.1	94.3
24	--	84.1	0	23.5
25	--	3.2	24.0	43.1
26	--	370.8	326.0	301.1
27	--	40.3	130.3	24.4
28	--	116.8	73.7	140.9
29	--	11.0	19.5	14.1
30	--	1.3	4.5	12.4

Note: The intensities are given in km/mole. The crystal APTs and methods are explained in Section 6.1.

Table 6-7 is a summary of the statistical analysis for the predictions for these different methods. The CALC set examines errors in values calculated from each set compared with the same property for NTKM predictions of Tables 6-4 through 6-6, and C_{NTKM} values of Table 6-2. The EXPTL set examines differences between calculated properties and the experimental results. The experimental results are the frequencies and relative absorbances of the experimental IR spectrum of urocil (from studies[67] in a dilute Ar matrix at low temperatures) as analyzed by Scott-Lebron.[61] These experimental results are plotted schematically in Figures 6-2 and 6-3 under EXPTL label. In order to measure the statistical parameters of the EXPTL set of Table 6-7, the frequencies predicted by a given method (Table 6-4) were multiplied by 0.9, and the intensities (Table 6-6) were multiplied by 0.903 (the absorbance-intensity conversion constant. Figures 6-2 and 6-3 show the scaled frequencies and converted intensities (R.A.S) calculated by the various methods.

The CALC set of Table 6-7 indicates that results from the "WCD method" were closest to NTKN predictions. The EXPTL set of this table indicates that NTKN predictions were closest to experimental results, followed by results from the "WCD method." Hence it could be said that the closer a method was in reproducing the NTKM predictions, the better the prediction when compared to experimental results. From these rough trends one can make various decisions. The most important one is the selection of NTKM as the method

which imitates best the experimental results. Concerning scaling constants some interesting conclusions can be drawn. Nishimura et al.[30] calculated the C_{NTKM} values (Table 6-2) accurately from various molecules (fragments of uracil). On the other hand the C_{wd} values (Table 6-2) were calculated from HF SCF level studies with 4-31G and STO-3G basis sets using uracil at all times. Thus one might expect that C_{wd} values should be better than C_{NTKM} ones for the uracil molecule. As seen in previous chapters this would probably be true if the "F_w constants" of uracil had been evaluated at higher convergence (say 10^{-8} instead of $5 * 10^{-5}$), and with the optimized geometry (HF SCF with a 4-31G basis set) instead of the crystal geometry[48] of uracil. The case is that from Table 6-7 it can be concluded that C_{NTKM} were the best.

The predicted out-of-plane frequencies, FEDs, and intensities of uracil are reported in Tables 6-4 through 6-5 for the WC, WCD, and STO-3G cases. They are not given for NTKM since Nishimura et al.[30] did not report out-of-plane C_{NTKM} values. The out-of-plane predictions from these methods are not statistically analyzed in this study. The major reason for this is the fact that there were many controversies in the literature about the assignments of experimental out-of-plane modes of matrix isolated uracil.[67,75,76] Other reasons stem from the statistical observations on out-of-plane modes from previous chapters. In Chapter 5 it was seen that in some situations it is not advisable to scale out-of-plane force fields when

Figure 6-2. Comparison between the calculated IR in-plane fundamental modes ν1 through ν6 from various scaling methods and the corresponding fundamentals from experimental results. The experimental results, EXPT, are deduced from Reference 61. The methods of calculation are given in Chapter 6.

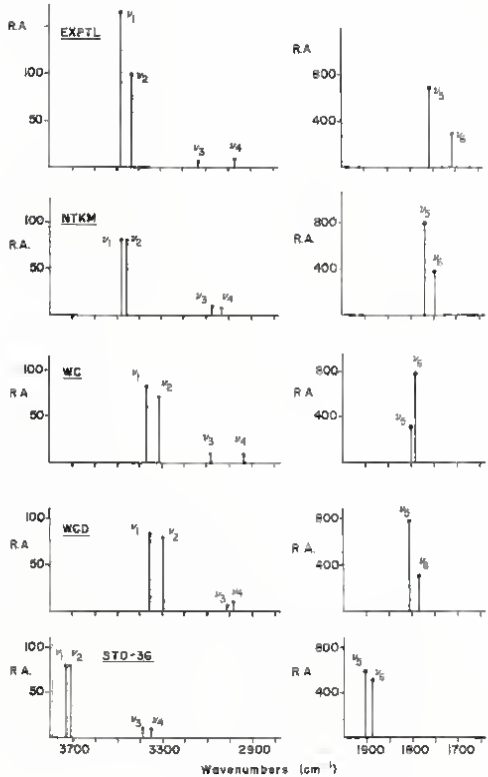
EXPTL
NTKM
WC
WCD
STO-3G
R.A
100
50
800
400
ν_1
ν_2
ν_3
ν_4
ν_5
ν_6
3700
3300
2900
1900
1800
1700
Wavenumbers (cm^{-1})

Figure 6-3. Comparison between the calculated IR in-plane fundamental modes ν7 through ν21 from various scaling methods and the corresponding fundamentals from experimental results. The experimental results, EXPT, are deduced from Reference 61. The methods of calculation are given in Chapter 6.

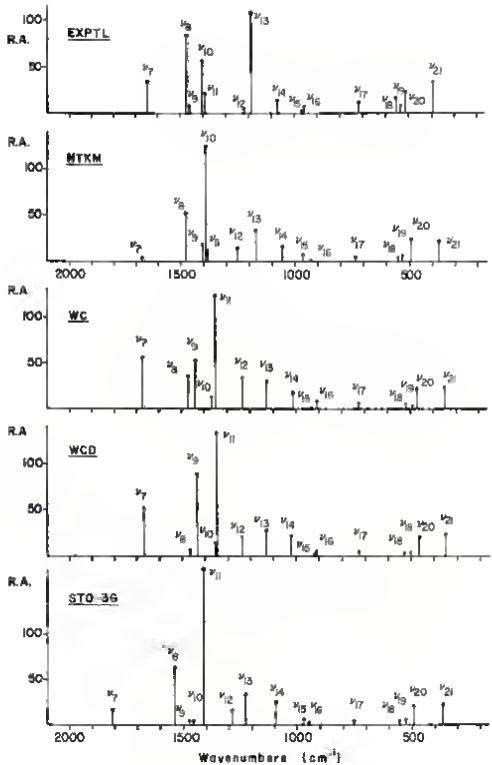
R.A.
EXPTL
MTKM
WC
WCD
STO-3G
2000
1500
1000
500
Wavenumbers (cm⁻¹)

TABLE 6-7
STATISTICAL ANALYSIS OF THE PERFORMANCE OF VARIOUS METHODS IN IMITATING THE IN-PLANE NTKM AND EXPERIMENTAL RESULTS

	CALC[a,b]				EXPTL[a,c]		
	WC	WCO	STO-3G	NTKM	WC	WCD	STO-3G
EPIP	45.6	45.4	103.7	22.4	46.9	49.4	97.3
ENIP	54.7	55.1	27.1	--	--	--	--
EIIP	75.9	31.4	40.7	27.8	66.2	32.7	38.6
MDIP	--	.0710	.0895	--	--	--	--
MIP	--	-.0439	.0743	--	--	--	--
FPIP	2	1	3	1	2	3	4
NPIP	2	3	1		-	-	-
IPIP	3	1	2	1	4	2	3
EFFIP	3	1	2	1	3	2	4

[a]The EF and EI terms are in cm^{-1} and km/mole respectively. The other terms are unitless. The terms are defined in Section 6.1.

[b]The methods are compared to NTKM results.

[c]The methods are compared to experimental spectra (Reference 61)

convergence is low. See for instance the LC case in Table 5-9. These situations deteriorated more when besides low convergence, the reference state was other than the optimized geometry (at same level of theory as the one used in the evaluation of force field). See for instance the EFOP values of Tables 5-20 and 5-21. Based on these observations the scaling constants evaluated from the "P_w constants" are not to be trusted (low convergence and crystal geometry[48] as reference state). To choose the best set of out-of-plane predictions from Tables 6-4 through 6-6 is hard, the safest choice being the STO-3G case.

6.2 IR Spectrum of 2-Pyrimidinone

The complete force field (in-plane and out-of-plane) for 2-pyrimidinone was evaluated at the HF SCF level with an STO-3G basis set using the FREQ subroutine of GAUSSIAN 82[32] (Section 2.1.1.3). The reference state was the optimized geometry at this same level of theory (Section 2.1.1.1). The optimized geometry is referred to as 3GG of 2-pyrimidinone and is given in Table 6-8 (defined in Figure 6-4). The force field is referred to as the STO-3G force field of this molecule and is given in Table 6-9 in S coordinates. These symmetrized internal coordinates are given in Table 6-10.

Ab initio calculations of diagonal force constants and atomic polar tensors of 2-pyrimidinone were carried out with GAUSSIAN 76[53] (at $5 * 10^{-5}$ convergence, 10^{-6} integral threshold) at two reference states. These reference states were the previously mentioned 3GG and another labelled as XL. The XL geometry was obtained from x-ray crystallographic

Figure 6-4. Structure, atom numbering and in-plane internal coordinates of 2-pyrimidinone used in this work. The out-of-plane internal coordinates are the out-of-plane bends and torsions given in Table 6-1.

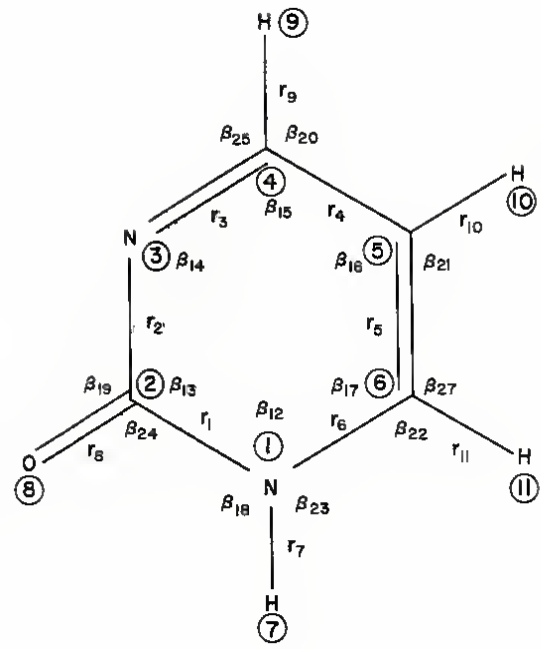
H
9
r9
β25
β20
4
β15
r3
r4
H
10
r10
N
3
β14
5
β16
β21
r2
r5
β19
2
β13
β17
6
β27
β12
r1
r6
β22
r11
H
11
β24
r8
O
8
1
N
β18
β23
r7
H
7

TABLE 5-8
THE STO-3G OPTIMIZED 3GG AND CRYSTAL STRUCTURE XL OF 2-PYRIMIDINONE

r_i	3GG[a,b]	XL	θ_i	3GG[a,c]	XL
1	1.436	1.384	12	123.1	122.9
2	1.462	1.367	13	116.2	118.3
3	1.294	1.320	14	117.2	118.1
4	1.463	1.403	15	126.5	124.7
5	1.331	1.355	16	117.3	116.9
6	1.393	1.353	17	119.7	119.1
7	1.020	1.014	18	117.0	118.7
8	1.219	1.244	19	123.0	121.9
9	1.092	1.080	20	117.3	121.6
10	1.077	1.080	21	122.4	119.2
11	1.087	1.080	22	115.9	116.4
			23	119.9	118.4
			24	120.8	119.8
			25	116.2	113.7
			26	120.3	123.9
			27	124.4	124.5

[a]Bond lengths, r, and angles, θ, are according to Figure 6-4.

[b]The 3GG was obtained by BFGS procedure (References 32 and 54) at HF SCF level with an STO-3G basis set.

[c]The crystal XL geometry was obtained from experimental results and considerations on NH and CH bonds (References 5 and 48).

TABLE 6-9
FORCE CONSTANTS FOR 2-PYRIMIDINONE
IN SYMMETRIZED INTERNAL COORDINATES
EVALUATED AT THE HF SCF LEVEL WITH AN STO-3G BASIS SET

	S1[a,b,c,d]	S2	S3	S4	S5	S6
S1	7.23498					
S2	.50644	6.11104				
S3	-.31723	.32873	13.12770			
S4	.17400	-.36551	-.91375	6.89451		
S5	-.41787	.37800	-.46001	.86423	12.37780	
S6	.61717	-.30085	.49190	-.64987	.82840	8.70424
S7	-.05488	-.00577	-.06699	.05703	-.11346	.00243
S8	1.14289	.92016	-.19571	-.05268	-.16209	-.01995
S9	-.04685	.02753	.17022	-.02275	-.01427	-.01627
S10	.02036	-.02748	-.01933	-.03594	.00256	-.11118
S11	-.06269	.01233	-.03274	.02463	-.06964	.02849
S12	.19806	.28030	.27571	.03793	-.01330	-.19624
S13	.21012	-.33178	-.09578	.08295	-.37953	.11388
S14	.05624	-.33727	-.53746	.27396	.04200	-.33429
S15	.02987	-.00023	-.04014	.06014	.00809	-.19572
S16	-.51603	.39842	-.05208	.07324	-.06918	.15330
S17	.00231	-.03796	-.35736	.15639	.00110	.02175
S18	-.03843	.03122	.01069	-.18603	.22477	-.01395
S19	-.04109	-.01373	-.00857	.00305	-.13813	.24049

---

continued

TABLE 6-9 continued

	S7	S8	S9	S10	S11	S12
S7	9.38087					
S8	-.05045	16.46912				
S9	.00021	.01410	7.36213			
S10	.00376	-.01503	- 00044	7.74211		
S11	-.00082	.01060	+.00136	.01693	7.54319	
S12	-.07967	.29278	.07641	-.09091	.08451	1.68422
S13	-.07387	.20326	-.08181	.03906	.01817	.03597
S14	.01904	-.33030	.02592	-.06739	.06567	.02032
S15	.01539	-.00864	-.00139	-.00176	.02175	.00708
S16	.01823	-.08925	-.00836	.00873	-.01470	-.02402
S17	-.00110	- 01523	-.01117	- 01507	00435	-.00926
S18	.00437	.00221	.01734	.01505	-.01599	.00429
S19	-.02600	.02264	-.00559	.01457	.00742	.02884

	S13	S14	S15	S16	S17	S18	S19
S13	1.55059						
S14	-.07313	1.63200					
S15	.00551	.13406	.66792				
S16	- 16366	-.02279	.05793	1.20486			
S17	.04017	.08272	-.00561	-.02565	.77415		
S18	-.09364	-.05930	-.01592	- 00757	01349	.64601	
S19	.10019	-.02133	.00840	-.02758	-.01691	.01104	.69706

---

continued

TABLE 6-9 continued

	S20	S21	S22	S23	S24	S25	S26	S27
S20	.31987							
S21	-.04458	.23725						
S22	.14067	.07411	.30884					
S23	.12366	.08200	.04146	.16518				
S24	-.04124	-.08248	.02910	-.03535	.75501			
S25	-.16548	.18477	.09678	-.02462	-.05083	.66475		
S26	.20286	-.00856	.25187	.04425	-.00668	-.02830	.57088	
S27	-.18187	-.05464	-.20894	-.04158	-.00035	-.02960	-.15434	.64726

[a]The reference geometry was the STO-3G optimized geometry of 2-pyrimidinone (3GG of Table 6-8).

[b]The symmetrized internal coordinates are defined in Table 6-10.

[c]The units are md/A for stretch-stretch, md for bend-stretch, and md-A for the rest.

[d]The force field is symmetrized where the interaction between in-plane and out-of-plane force constants is zero, and $F_{ij} = F_{ji}$

TABLE 6-10
SYMMETRIZED INTERNAL COORDINATES FOR 2-PYRIMIDINONE

In-plane[a,b]

R1 = $\Delta r1$	= rN1C2
S2 = $\Delta r2$	= rC2N3
S3 = $\Delta r3$	= rN3C4
S4 = $\Delta r4$	= rC4C5
R5 = $\Delta r5$	= rC5C6
S6 = $\Delta r6$	= rC6N1
R7 = $\Delta r7$	= rN1H
S8 = $\Delta r8$	= rC2O
S9 = $\Delta r9$	= rC4H
S10 = $\Delta r10$	= rC5H
S11 = $\Delta r11$	= rC6H
S12 = $(1/6)^{0.5}[\Delta\beta12-\Delta\beta13+\Delta\beta14-\Delta\beta15+\Delta\beta16-\Delta\beta17]$	= δIβ
S13 = $(1/12)^{0.5}[2\Delta\beta12-\Delta\beta13-\Delta\beta14+2\Delta\beta15-\Delta\beta16-\Delta\beta17]$	= δIIθ
S14 = $(1/2)[\Delta\beta13-\Delta\beta14+\Delta\beta16-\Delta\beta17]$	= δIIIθ
S15 = $(1/2)^{0.5}[\Delta\beta18-\Delta\beta23]$	= δN1H
S16 = $(1/2)^{0.5}[\Delta\beta19-\Delta\beta24]$	= δC2O
S17 = $(1/2)^{0.5}[\Delta\beta20-\Delta\beta25]$	= δC4H
S18 = $(1/2)^{0.5}[\Delta\beta21-\Delta\beta26]$	= δC5H
S19 = $(1/2)^{0.5}[\Delta\beta22-\Delta\beta27]$	= γC6H

---

continued

TABLE 6-10 continued

Out-of-plane[a,b]

$S20 = (1/6)^{0.5}\{\delta\tau1-\delta\tau2+\delta\tau3-\delta\tau4+\delta\tau5-\delta\tau6\}$	$= \tau I\theta$
$S21 = (1/2)\{\delta\tau1-\delta\tau3+\delta\tau4-\delta\tau6\}$	$= \tau II\theta$
$S22 = (1/12)^{0.5}\{-\delta\tau1+2\delta\tau2-\delta\tau3-\delta\tau4+2\delta\tau5-\delta\tau6\}$	$= \tau III\theta$
$S23 = \delta\gamma H7$	$= \gamma H7$
$S24 = \delta\gamma O8$	$= \gamma O8$
$S25 = \delta\gamma H9$	$= \gamma H9$
$S26 = \delta\gamma\theta10$	$= \gamma H10$
$S27 = \delta\gamma\theta11$	$= \gamma H11$

[a]The nomenclature and numbering according to Figure 6-4. The recommendetions of Puley et al. (Reference 11) are carried out.

[b]The atoms involved in torsions are: $\tau1$=6123, $\tau2$=1234, $\tau3$=2345, $\tau4$=3456, $\tau5$=4561, and $\tau6$=5612.

dete[5] (except for NH and CH bonds which were modified as decided by Chin et al.[46]). The XL geometry is given in Table 6-6 (according to Figure 6-4). The 3GG force constants and 3GG APTs were evaluated with 3GG as reference state. The XL force constants and XL APTs were evaluated with XL as reference state.

By the "WCD method" of Chapter 4 the 3GG diagonal force constants and the STO-3G force field of 2-pyrimidinone were used to obtain the scaling constants C_{3GG} (Table 6-11) and the 3GG "near 4-31G" force field. Similarly the XL diagonal force constants and the STO-3G force field of 2-pyrimidinone were used to obtain the C_{XL} values (Table 6-11) and the XL "near 4-31G" force field. The 3GG and XL APTs are given in Tables 6-12 and 6-13 respectively according to the orientations of Tables 6-14 and 6-15. The 3GG frequencies, PEDs, and intensities of Tables 6-16 through 6-18 were obtained from the 3GG "near 4-31G" force field and the 3GG APTs. The XL parameters in these tables were obtained from the XL "near 4-31G" force field and the XL APTs.

Tables 6-16 through 6-18 also give NTKM and STO-3G results. The NTKM frequencies and normal modes were obtained by using a "near 4-31G" force field evaluated by the "SC method" of Chapter 4. This "near 4-31G" force field was evaluated from the scaling constants of Nishimura et al.,[30] C_{NTKM} of Table 6-11, and the STO-3G force field of 2-pyrimidinone (Table 6-9). The NTKM intensities were obtained by using this "near 4-31G" force field and the XL

TABLE 6-11
THE 4-31G/STO-3G SCALING CONSTANTS FOR 2-PYRIMIDINONE FROM VARIOUS METHODS

S	C_{NTRM}	C_{3GG}	C_{XL}
1	.96	.6929	.9645
2	.96	.6586	1.1364
3	.82	.7441	.8618
4	.96	.7489	.9611
5	.82	.8079	.9090
6	.96	.7211	.9573
7	.87	.7610	.8470
8	.82	.7460	.8912
9	.82	.7530	.8511
10	.82	.7666	.8409
11	.82	.7615	.8520
12	1.00	.7223	.9645
13	1.00	.7056	1.0153
14	1.00	.7201	1.0169
15	.91	.7976	.9341
16	1.08	.6726	1.1025
17	.91	.7625	.8484
18	.91	.7797	.8920
19	.91	.7701	.8907
20	--	.7653	2.2801
21	--	1.2021	2.8551
22	--	1.0094	1.5416
23	--	1.3039	2.4527
24	--	1.1842	1.3739
25	--	.8972	1.5760
26	--	.8765	1.3933
27	--	1.0687	1.7078

Note: The "WCD method" was used. Further details are given in Section 6.2.

TABLE 6-12
ATOMIC POLAR TENSORS
FOR 2-PYRIMIDINONE WITH STO-3G OPTIMIZED GEOMETRY

N1[a,b,c]

-.69824	.31169	0
-.34814	-1.13528	0
0	0	-.67423

H7

.18407	-.05252	0
-.02722	.16604	0
0	0	.43644

C2

1.07448	.16218	0
-.00545	2.36390	0
0	0	.74141

O8

-.42785	-.09296	0
.14105	-1.78856	0
0	0	-.57563

N3

-.51425	.08922	0
.29425	-1.19894	0
0	0	-.46297

H9

-.08887	.09853	0
.12488	-.04369	0
0	0	.12450

C4

.69146	.30531	0
.08307	1.12361	0
0	0	.21770

H10

.05906	.01404	0
.01097	-.12175	0
0	0	.18790

C5

-.91995	.00353	0
-.14660	-.32845	0
0	0	-.39781

H11

-.06644	-.05187	0
-.06038	.03298	0
0	0	.16240

C6

.70653	-.78716	0
-.06643	.93014	0
0	0	.24027

---

[a] Units are in electrons (e).

[b] APTs are determined at HF SCF level with 4-31G basis set using STO-3G geometry (Table 6-10) as reference state.

[c] The atom numbering is given in Figure 6-4, the coordinate system of orientation is the principal cartesian coordinates of Table 6-14.

TABLE 6-13
ATOMIC POLAR TENSORS
FOR 2-PYRIMIDINONE WITH CRYSTAL XL GEOMETRY

N1[a,b,c]			H7		
-.63617	.52855	0	.20104	-.04865	0
-.34700	-1.25179	0	-.02622	.19340	0
0	0	-.59071	0	0	.42266

C2			O8		
.95752	.11535	0	-.52489	-.05402	0
-.16334	2.46533	0	.16387	-1.77264	0
0	0	.70792	0	0	-.61362

N3			H9		
.53441	-.15572	0	-.07956	.07413	0
.50816	-1.35541	0	.13282	-.00500	0
0	0	-.40258	0	0	.12841

C4			H10		
.89580	.46676	0	-.05862	.01567	0
.16184	1.23063	0	-.03560	-.11592	0
0	0	.23411	0	0	.18929

C5			H11		
-1.03715	-.00569	0	-.04756	-.05269	0
-.26662	-.32915	0	-.04638	.03501	0
0	0	-.41134	0	0	.15716

C6		
.74676	-.88371	0
-.09154	.90556	0
0	0	.25871

---

[a] Units are in electrons (e).

[b] APTs are determined at HF SCF level with 4-31G basis set using crystal geometry (Table 6-10) as reference state.

[c] The atom numbering is given in Figure 3-3; the coordinate system of orientation is the principal cartesian coordinates of Table 3-6.

TABLE 6-14
PRINCIPAL CARTESIAN COORDINATES, GROUND STATE ENERGIES, AND GROUND STATE DIPOLE MOMENTS OF 2-PYRIMIDINONE AT THE 3GG GEOMETRY

	X[a]	Y[a]	Z[a]
N1	1.174045	-.200061	0
C2	-.018249	-1.000213	0
N3	-1.286001	-.271430	0
C4	-1.224288	1.021498	0
C5	-.009041	1.835182	0
C6	1.156160	1.192479	0
H7	2.065174	-.696748	0
O8	.047512	-2.217638	0
H9	-2.179858	1.549207	0
H10	-.075177	2.910150	0
H11	2.127465	1.680693	0

ENERGY (AU)[b]

= -333.21688641 (10^{-9} CG, 10^{-10} IT, STO-3G BS)[c]

= -337.04140900 ($5 * 10^{-5}$ CG, 10^{-6} IT, 4-31G BS)[d]

DIPOLE (DEBYES)[b]

= 4.5402 (10^{-9} CG, 10^{-10} IT, STO-3G BS)[c]

= 7.1117 ($5 * 10^{-5}$ CG, 10^{-6} IT, 4-31G BS)[d]

[a]Principal cartesian coordinates are in A. The optimized STO-3G geometry (3GG) is used (Table 6-8) The atom numbering is shown in Figure 6-4

[b]The terms CG, IT, and BS stand for the convergence, integral threshold, and basis set respectively, that were used in the corresponding calculation

[c]The calculation was performed with GAUSSIAN 82 (Reference 32).

[d]The calculation was performed with GAUSSIAN 76 (Reference 53).

TABLE 6-15
PRINCIPAL CARTESIAN COORDINATES, GROUND STATE ENERGY, AND DIPOLE MOMENT OF 2-PYRIMIDINONE AT THE XL GEOMETRY

	x[a]	y[a]	z[a]
N1	1.137739	-.207724	0
C2	-.030594	-.949650	0
N3	-1.222909	-.261013	0
C4	-1.195651	1.036705	0
C5	-.025936	1.613415	0
C6	1.152426	1.144469	0
H7	2.025603	-.697512	0
O6	.026201	-2.192353	0
H9	-2.175391	1.493137	0
H10	-.018713	2.693391	0
H11	2.123610	1.616500	0

ENERGY (AU)[b]

= -337.04532766 (5 * 10^{-5} CG, 10^{-6} IT, 4-31G BS)

DIPOLE (DEBYES)[b]

= 7.6610 (5 * 10^{-5} CG, 10^{-6}, 4-31G BS)

[a]Principal cartesian coordinates are in A. The crystal XL1 geometry is shown in Table 6-6. The atom numbering is shown in Figure 6-4.

[b]The terms CG, IT, and BS stand for the convergence, integral threshold, and basis set used in the calculation. The calculation was performed with GAUSSIAN 76 (Reference 53).

APTs (Table 6-12). The STO-3G frequencies, PEDs, and intensities were obtained from the unscaled STO-3G force field of 2-pyrimidinone (Table 6-9) and the XL APTs (Table 6-12).

Table 6-19 summarizes the statistical analysis for the in-plane predictions of the various methods of Tables 6-16 through 6-18. The errors are measured with respect to NTKM predictions for 2-pyrimidinone. The MDIP and MIP values are measured with respect to C_{NTKM} values of Table 6-11. In this Table one can see that XL case imitated best the NTKM results, followed by STO-3G and 3GG cases. Although we do not have an experimental spectrum of isolated 2-pyrimidinone we believe from the uracil observations that NTKM is the closest to experimental results followed by XL. Thus we choose the NTKM predictions of Tables 6-16 through 6-18 as best for the in-plane fundamental modes of the experimental spectrum of isolated 2-pyrimidinone. As in the observations on uracil one is confronted with a choice of scaling constants (Table 6-11) from which C_{NTKM} values are chosen as best followed by in-plane C_{XL} constants.

Arguing from nonstatistical angles one can arrive at similar conclusions. The "near 4-31G" force fields of NTKM cases for uracil and 2-pyrimidinone cases were obtained by scaling the force field (at the same level of theory) of two closely related molecules by the same set of conversion constants (C_{NTKM}). The APTs for both molecules were evaluated at the same level of theory with similar crystal structures as reference states. Thus if the NTKM case for

TABLE 6-16
PREDICTED BAND FREQUENCIES FOR 2-PYRIMIDINONE
FROM FORCE FIELDS OF VARIOUS METHODS

ν	NTRM	3GG	XL	STO-3G
1	3843.6	3593.4	3792.7	4119.3
2	3417.4	3303.3	3464.1	3772.8
3	3368.9	3245.6	3431.3	3719.0
4	3325.8	3185.4	3387.8	3671.2
5	1938.7	1797.4	2006.9	2095.9
6	1866.9	1765.7	1915.6	2017.6
7	1730.0	1615.4	1761.7	1856.7
8	1636.7	1486.4	1645.4	1709.9
9	1546.9	1421.7	1550.3	1618.8
10	1506.7	1369.9	1511.0	1589.3
11	1345.8	1207.3	1355.8	1392.7
12	1281.8	1133.2	1282.2	1331.9
13	1201.6	1069.7	1211.3	1249.4
14	1105.7	975.7	1107.0	1138.9
15	1097.2	928.3	1083.7	1104.0
16	864.3	738.9	903.2	889.2
17	696.9	578.4	704.1	698.0
18	611.9	504.7	617.4	616.3
19	510.2	419.8	516.3	498.6
20	--	1183.7	1470.7	1159.9
21	--	1056.3	1378.9	1140.3
22	--	874.9	1186.3	903.3
23	--	804.2	1098.8	835.7
24	--	646.7	830.7	619.8
25	--	506.8	721.9	473.0
26	--	388.0	536.8	369.3
27	--	116.0	170.9	118.4

Note: The frequencies are in cm^{-1}. The methods are explained in Section 6.2.

TABLE 6-17
PREDICTED POTENTIAL ENERGY DISTRIBUTION FOR 2-PYRIMIDINOL
IR FUNDAMENTAL BANDS FROM FORCE FIELDS OF VARIOUS METHODS

S	NTKM	3GG	XL	STO-3G
1	100S7	100S7	100S7	100S7
2	92S10	94S10	79S10	92S10
			19S11	
3	92S11	94S11	19S10	92S11
			80S11	
4	99S9	99S9	99S9	99S9
5	66S8	81S8	71S8	79S8
6	23S3	18S3	20S3	29S3
	35S5	54S5	46S5	39S5
	10S19			
7	25S3	50S3	39S3	40S3
	13S4	11S4	12S4	27S5
	20S5	18S5	17S5	
8	12S3	25S6	14S3	31S6
	30S6	27S7	31S6	24S15
	16S15	18S18	25S15	16S18
	16S18	11S19	11S18	11S19
	11S19			
9	12S4	10S4	14S4	12S4
	29S15	36S15	28S15	30S15
	16S18	20S18	17S18	11S17
	18S19	22S19	22S19	15S18
				20S19
10	10S2	14S3	10S1	13S3
	21S3	70S17	20S2	58S17
	47S17		39S17	
11	31S1	10S5	11S1	23S1
	10S2	22S18	10S15	16S15
	15S15	42S19	29S17	20S19
	12S17			
12	10S2	30S1	22S18	18S1
	25S18	12S2	46S19	14S2
	40S19	12S6		30S18
		25S18		26S19
13	17S5	13S2	14S5	12S5
	30S6	38S6	33S6	39S6
	11S15	10S16	11S15	12S15
	28S18		32S18	18S18
14	60S4	10S1	66S4	70S4
		69S4		
15	82S12	90S12	88S12	90S12
16	28S1	28S1	31S1	28S1
	50S2	53S2	44S2	52S2

continued

TABLE 6-17 continued

S	NTKM	3GG	XL	STO-3G
17	54S13	56S13	54S13	57S13
	20S14	23S14	20S14	20S14
18	23S13	25S13	23S13	23S13
	62S14	63S14	62S14	64S14
19	71S16	77S16	10S13	75S16
			71S16	
20		23S26	15S26	38S26
		93S27	92S27	78S27
21		100S25	97S25	96S25
22		30S24	86S20	12S24
		53S26	18S24	58S26
				21S27
23		20S20	78S26	53S20
		55S24	12S27	46S24
		23S26		
24		28S20	74S23	24S20
		70S24	32S24	17S22
				35S23
				31S24
25		29S20	39S21	11S20
		42S21	46S24	28S21
		24S23		57S23
		10S24		
26		35S21	38S21	41S21
		56S22	41S22	40S22
			19S23	13S23
27		33S20	22S20	25S20
		35S21	28S21	41S21
		40S22	53S22	41S22

Note: The "KJ method" (Section 2.2.4) was used to calculate the FEDs in symmetrized internal coordinates (Table 6-1). Details of the methods are given in Section 6.2.

TABLE 6-18
PREDICTED BAND INTENSITIES FOR 2-PYRIMIDINONE
FROM VARIOUS FORCE FIELDS AND ATOMIC POLAR TENSORS

ν	NTKM	3GG	XL	STO-3G
1	79.8	67.3	79.8	79.0
2	9.1	11.1	10.5	9.2
3	11.9	14.8	11.5	11.8
4	41.5	49.7	40.8	41.5
5	994.1	756.2	961.7	881.1
6	112.9	209.8	144.3	172.1
7	236.6	204.3	265.5	282.5
8	26.9	11.7	27.5	22.4
9	48.5	17.6	38.4	46.7
10	37.4	23.7	18.0	24.8
11	18.8	20.5	28.8	17.9
12	41.3	40.6	30.6	38.2
13	23.8	86.1	27.5	54.2
14	20.1	4.6	21.2	22.7
15	13.1	9.0	8.9	10.7
16	.6	.2	1.9	2.2
17	.3	.4	.5	.7
18	3.4	.6	2.9	1.9
19	2.4	2.0	2.4	3.0
20	--	.8	.8	1.6
21	--	.8	.8	2.5
22	--	152.7	32.7	114.2
23	--	11.0	81.3	21.1
24	--	84.1	153.7	42.3
25	--	77.2	12.8	129.6
26	--	49.4	72.0	44.5
27	--	.8	0	.3

Note: The intensities are in km/mole. The methods are defined in Section 6.2.

uracil gave succeasful correlations with in-plane experimental findings so should the NTKM case of 2-pyrimidinone.

Thus one can be confident that the in-plane NTKM predictions for 2-pyrimidinone are quite close to the experimental results. As far as the out-of-plane predictions are concerned we do not have a satisfactory answer. Based on observations of the out-of-plane modes of uracil, we conclude that it is safer to use the STO-3G out-of-plane predictions of Tables 6-16 through 6-18 as the best set of results. The out-of-plane predictions for 3GG and XL cases are reported in order to provide researchers with more tools at their disposal but not much more can be said about them.

We conclude this chapter by presenting Figure 6-5 which compares the unscaled predicted spectra of the two tautomers of 2-oxopyrimidine. In this figure the spectrum of 2-pyrimidinol is obtained from the unscaled results of Table 3-7. This corresponds to our best predicted spectrum for this tautomer at the "full 4-31G" study of Chapter 3. The spectrum of 2-pyrimidinone in this figure depends on two sets of predictions. The in-plane predictions are from the NTKM results and the out-of-plane from the STO-3G results (Tables 6-16 and 6-18). This is our predicted best spectrum for 2-pyrimidinone. The quality of the latter should be inferior to the 2-pyrimidinol spectrum.

TABLE 6-19
STATISTICAL ANALYSIS
OF THE ABILITY OF THE VARIOUS METHODS
IN IMITATING THE NTKM RESULTS FOR 2-PYRIMIDINONE

	3GG	XL	STO-3G
EFIP	134.6	25.2	116.6
ENIP	29.3	16.3	14.6
EIIP	28.4	8.3	14.8
MDIP	.1715	.0372	.0953
MIP	-.1715	.0204	.0868
FPIP	3	1	2
NPIP	3	2	1
IPIP	3	1	2
EFFIP	3	1	2

Note: The EF and EI terms are in cm^{-1} and km/mole respectively. The other parameters are unitless. The methods are given in Section 6.2.

Figure 6-5 Simultaneous display of best calculations of the present work for the IR spectra of the tautomers of 2-oxopyrimidine. The results for 2-pyrimidinol are the unscaled calculations of the full 4-31G study (Table 3-7). The results for 2-pyrimidinone correspond to in-plane NTKM and out-of-plane STO-3G methods (Tables 6-16 and 6-18).

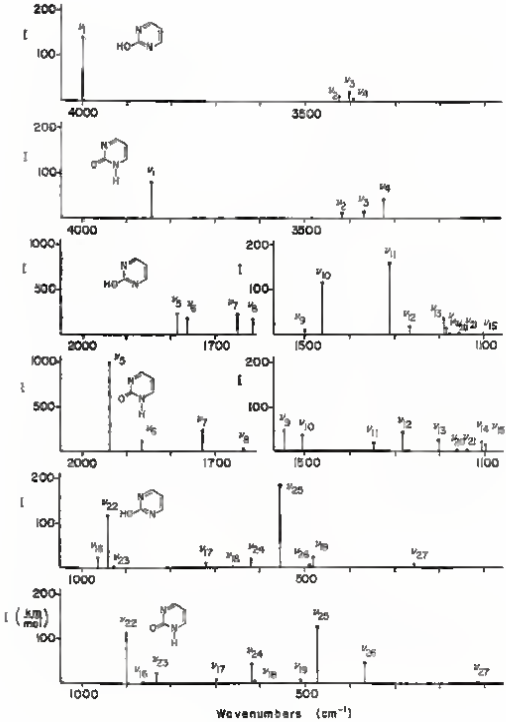
200
100
4000
3500
2000
1700
1500
1100
1000
500
ν1
ν2
ν3
ν4
ν5
ν6
ν7
ν8
ν9
ν10
ν11
ν12
ν13
ν14
ν15
ν16
ν17
ν18
ν19
ν22
ν23
ν24
ν25
ν26
ν27
Wavenumbers (cm⁻¹)

CHAPTER 7
SUMMARY AND COMMENTS

The calculations of the IR spectra of 2-oxopyrimidine tautomers are quite useful for studies of molecules of similar structure. For instance they may be helpful in analysing experimental matrix IR spectra of nucleic acid bases which exhibit various tautomeric forms, and of the halogenated 2-oxopyrimidines.[6] These results can be further implemented in more ambitious aims trying to interpret the spectra of nucleotides.

The calculated spectra are helpful in order to understand better the experimental results. This is particularly true for large molecules with low symmetry or short lived species such as radicals and ions. The methods and results of Chapters 4 and 5 can be of utility in further attempts to improve the quality of calculated spectra by scaling to fit other calculations or experimental results. The mathematical and statistical level of these analyses clearly needs to be developed more. The various tables in these chapters include results which can be further analyzed in the future when more sophisticated approaches are conceived.

The assignment of spectra by referring to calculated frequencies only is demonstrated to be insufficient. This

approach is analogous to a mathematician trying to find the values of n^2 variables from n simultaneous equations. The predicted normal modes and the predicted band intensities are expected to be helpful in these correlations. Person and Kubulat are developing a method analogous to the FED case whereby the intensities are described in terms of internal coordinates.[77] Correlations of spectra based on predicted frequencies and intensities (ideally simultaneous instead of independently), in conjunction with their corresponding interpretations, would provide the mathematician of the analogy with more relationships that would help him to solve his simultaneous equations with less assumptions.

Correlations of spectra from calculations based on the usage of simple basis sets such as 4-31G and STO-3G, is recommended as a reasonable system for the development of more sophisticated mathematical and statistical methods of analysis. This is partly based on the idea that the wavefunction of the molecule is better understood from these basis sets than from experimental facts.

Various observations are made with regards to convergence, integral threshold, and reference state. It is found that a desirable level of precision must be observed in ab initio calculations. The choice of geometry to be used at different times in the calculations is a difficult problem. This "geometry parameter" enters in the calculations at various points. Reference states for evaluation of force constants, APTs, frequencies, and intensities of IR spectra. Our observations indicate that a

force field calculated at a given level of theory should use for a reference state the geometry optimized at the same level of theory. Scaling methods, including other methods besides the presented ones, deserve further study.

Due to the high cost and further complications involved in ab initio calculations of IR spectra, particularly of large molecules, various researchers are compiling data from various research centers as well as synchronizing the nature of these calculations. Along these lines we have calculated 4-31G/STO-3G conversion constants for the in-plane modes of pyridine, using our results calculated with an STO-3G basis set together with the calculations of Wiberg et al.[31] who used a 4-31G basis set. These conversion constants were surprisingly similar to the C_s constants (Table 4-3) for 2-pyrimidinol implying some sense of universality in these calculations. Similar work including experimental results can be seen in the work of Pongor et al.[78] who combined data on the out-of-plane modes of pyridine,[31,79,80] or in the conclusions of Harsanyi et al.[76] who combined data[30,45,48] on the in-plane and out-of-plane modes of uracil. More thorough reviews can be seen on previously indicated references.[17,19,34] It is in this spirit of cooperation that most of the work of Chapters 4 and 5 was carried out.

In the present work the usage of ab initio calculations at the HF SCF level with basis sets such as STO-3G and 4-31G shows to be helpful in the interpretation of IR spectra (particularly in the case of large molecules

with low symmetry). The level of correlation between the presented experimental and theoretical results is good. The objective of reliable predictions of the spectra of the tautomers of 2-oxopyrimidine, and of the interpretation and correlation with experimental matrix observations, is achieved at a reasonable level of confidence. The more generalised basis of investigating the quality of ab initio calculations of IR spectra do lead to enlightening but certainly not conclusive facts. It is emphasized that these calculations need to be studied at greater depth in the future.

REFERENCES

1. M. J. Nowak, K. Szczepaniak, A. Barski, and D. Shugar, J. Mol. Struct. 62, 47 (1980).

2. R. Czerminski, K. Kuczera, H. Rostkowska, M. J. Nowak, and K. Szczepaniak, J. Mol. Struct. 140, 235 (1986).

3. P. Beak, F. S. Fry, J. Lee, and F. Steelle, J. Am. Chem. Soc. 98, 171 (1976).

4. D. Shugar and K. Szczepaniak, Int. J. Quantum Chem. 20, 573 (1981).

5. S. Furberg and J. Solbakk, Acta Chem. Scand. 24, 3230 (1970).

6. M. J. Nowak, H. Rostkowska, and K. Szczepaniak, to be published.

7. J. C. Slater, Phys. Rev. 36, 57 (1930).

8. J. A. Pople in "Modern Theoretical Chemistry," H. F. Schaeffer III, Ed. (Plenum Press, New York, 1977). Vol. 4.

9. W. J. Hehre, R. F. Stewart, and J. A. Pople, J. Chem. Phys. 51, 2657 (1969).

10. J. S. Binkley, J. A. Pople, and W. J. Hehre, J. Am. Chem. Soc. 102, 939 (1980).

11. P. Pulay, G. Fogarasi, F. Pang, and J. E. Boggs, J. Am. Chem. Soc. 101, 2550 (1979).

12. R. Ditchfield, W. J. Hehre, and J. A. Pople, J. Chem. Phys. 54, 724 (1971).

13. W. J. Pietro, M. M. Francl, W. J. Hehre, D. J. DeFrees, J. A. Pople, and J. S. Binkley, J. Am. Chem. Soc. 104, 5039 (1982).

14. P. C. Hariharan and J. A. Pople, Mol. Phys. 27, 209 (1974).

15. W. J. Hehre, R. Ditchfield, and J. A. Pople, J. Chem. Phys. 56, 2257 (1972).

16. P. C. Hariharan and J. A. Pople, Theor. Chim. Acta 28, 213 (1973).

17. W. J. Hehre, L. Radom, P. R. Schleyer, and J. A. Pople, "Ab Initio Molecular Orbital Theory" (John Wiley and Sons, New York, 1986).

18. Henry F. Schaeffer III, "The Electronic Structure of Atoms and Molecules" (Addison-Wesley Publishing Co., Reading, Massachusetts, 1972).

19. G. Fogarasi and P. Pulay, in "Vibrational Spectra and Structure," J. R. Durig, Ed. (Elsevier, Amsterdam, 1985), Vol. 14.

20. P. Pulay, in "Modern Theoretical Chemistry," H. F. Schaeffer III, Ed. (Plenum Press, New York, 1977), Vol. 4.

21. R. H. Schwendeman, J. Chem. Phys. 44, 2115 (1966).

22. D. Steele, Mol. Phys. 38, 145 (1979).

23. H. B. Schlegel, S. Wolfe, and F. J. Bernardi, J. Chem. Phys. 63, 3632 (1975).

24. D. Staale, J. Mol. Struct. 79, 13 (1982).

25. D. Bougeard, S. Bruggenthies, and B. Schrader, J. Mol. Struct. 80, 155 (1980).

26. P. Pulay, J. G. Lee, and J. E. Boggs, Chem. Phys. 79, 3382 (1983).

27. C. E. Blom and C. Altona, Mol. Phys. 31, 1377 (1976).

28. W. Meyer and P. Rosmus, J. Chem. Phys. 63, 2356 (1975).

29. J. A. Pople, H. B. Schlegel, R. Krishnan, D. J. DeFrees, S. Binkley, M. J. Frisch, R. A. Whiteside, R. F. Hout, and W. J. Hehre, Int. J. Quantum Chem.: Quantum Chemistry Symposium 15, 269 (1981).

30. Y. Nishimura, M. Tsuboi, S. Kato, and K. Morokuma, J. Am. Chem. Soc. 103, 1354 (1981).

31. M. B. Wiberg, V. A. Walters, K. N. Wong, and S. D. Colson, J. Phys. Chem. 88, 6087 (1984).

32. J. S. Binkley, M. J. Frisch, D. J. DeFrees, K. Raghavachari, R. A. Whiteside, H. B. Schlegel, E. M. Fluder, and J. A. Pople, Department of Chemistry, Carnegie-Mellon University, Pittsburgh, PA.

33. J. A. Pople, Acct. Chem. Res. 3, 217 (1970).

34. B. A. Hess Jr. and L. J. Schaad, Chem. Rev. 86, 709 (1986).

35. P. Pulay and W. Meyer, J. Mol. Spectrosc. 40, 59 (1971).

36. W. Meyer and P. Pulay, J. Chem. Phys. 56, 2109 (1972).

37. P. Pulay and W. Meyer, Mol. Phys. 27, 473 (1974).

38. W. Bleicher and P. Botschwina, Mol. Phys. 30, 1029 (1975).

39. P. Botschwina, W. Meyer, and A. M. Semkow, Chem. Phys. 15, 25 (1976).

40. G. Fogarasi, P. Pulay, K. Molt, and W. Sawodny, Mol. Phys. 33, 1585 (1977)

41. K. O. Christe, E. C. Curtis, W. Sawodny, H. Hartner, and G. Fogarasi, Spectrochim. Acta 37A, 549 (1981)

42. C. Pouchan, D. Liotard, A. Dargelos, and M. Chaillet, J. Chim. Phys. 73, 1046 (1976)

43. J. B. Schachtschneider and R. G. Snyder, Spectrochim. Acta 19, 117 (1963)

44. P. Gans, "Vibrating Molecules" (Chapman & Hall Ltd., London, 1971)

45. P. Pulay, G. Fogarasi, G. Pongor, J. E. Boggs, and A. J. Varghs, J. Am. Chem. Soc. 105, 7037 (1983).

46. P. Pulay, G. Fogarasi, and J. E. Boggs, J. Chem. Phys. 74, 3999 (1981).

47. K. W. Hipps and R. D. Poshusta, J. Phys. Chem. 86, 4112 (1982).

48. S. Chin, I. Scott, K. Szczepaniak, and W. B. Person, J. Am. Chem. Soc. 106, 3415 (1984).

49. K. Szczepaniak, M. Szczesniak, M. Nowak, I. Scott, S. Chin, and W. B. Person, Int. J. Quantum Chemistry: Quantum Biology Symposium 10, 547 (1984).

50. Y. Sugawara, Y. Hamada, A. Y. Hirakawa, M. Tsuboi, S. Kato, and K. Morokuma, Chem. Phys. 50, 105 (1980).

51. W. B. Person, in "Vibrational Intensities in Infrared and Raman Spectroscopy," W. B. Person and G. Zerbi, Eds. (Elsevier Scientific Publishing Co., Amsterdam, 1982), Chap. 4.

52. R. Krishnan and J. A. Pople, Int. J. Quantum Chem. 20, 1067 (1981).

53. W. J. Hehre, M. D. Newton, J. S. Brinkley, R. A. Whiteside, P. C. Hariharan, M. Seeger, and J. A. Pople, "GAUSSIAN 76-An ab initio Molecular Orbital Program", Program No. 391, Quantum Chemstry Program Exchange, Indiana University, Bloomington, IN, 1976. IBM translation by C. M. Cook, Department of Chemistry, Princeton University, Princeton, NJ.

54. J. D. Head and M. C. Zerner, Chem. Phys. Lett. 122(3), 264 (1985).

55. R. Czerminski, B. Lesyng, and A. Pohorille, Int. J. Quantum Chem. 16, 1141 (1979).

56. S. Chin, Ph.D. Dissertation, University of Florida, 1984.

57. S. Califano, "Vibrational States" (John Wiley and Sons, New York, 1976).

58. F. A. Cotton, "Chemical Applications of Group Theory" (Wiley, New York, 1971).

59. E. B. Wilson, Jr., J. C. Decius, and P. C. Cross, "Molecular Vibrations" (McGraw-Hill, New York, 1955).

60. T. Miyazawa, J. Chem. Phys. 29, 246 (1958).

61. I. Scott-Lebron, Ph.D. Dissertation, University of Florida, 1986.

62. W. B. Person and J. H. Newton, J. Chem. Phys. 61, 1040 (1974).

63. J. Overend in "Infrared Spectroscopy and Molecular Structure," M. Davies, Ed. (Elsevier, Amsterdam, 1963), Chap. 10.

64. J. H. Newton, M. A. Levine, and W. B. Person, J. Chem. Phys. 67, 3282 (1977).

65. Y. Morino and K. Kuchitsu, J. Chem. Phys. 20, 1809 (1952).

66. G. Keresztury and G. Jalsovsky, J. Mol. Struct. 10, 304 (1971).

67. M. Szczaaniak, M. J. Nowak, H. Roatkowaka, K. Szczapaniak, W. B. Peraon, and D. Shugar, J. Am. Chem. Soc. 105, 5969 (1983).

68. W. B. Parson, J. S. Kwiatkowaki, and R. J. Bartlett, to ha published.

69. L. J. Ballamy, "Tha Infra-red Spactra of Complex Moleculaa" (Chapman and Hall Ltd., London, 1975).

70. S. Furberg, J. Grogaard, and B. Smedsrud, Acta Chem. Scand. B33, 715 (1979).

71. A. Langaeth and P. E. Stoicheff, Can. J. Phya. 34, 350 (1956).

72. C. E. Blom and A. Muller, J. Mol Spectroac. 70, 449 (1978).

73. A. Kvick, Acta Crystallogr. B32, 220 (1978).

74. J. Rogera, Ph.D. Diaertation. Univeraity of Florida, 1980.

75. L. Harsanyi and P. Csaszar, Acta Chim. Hung. 113, 257 (1983).

76. L. Haraanyi, P. Caaszar, A. Caaszar, and J. E. Boggs, Int. J. Quantum Chem. 23, 799 (1986).

77. W. B. Person and K. KuBulat, to ba published.

78. G. Pondor, G. Fogarasi, J. Bogga, and P. Pulay, J. Mol. Spectroac. 115, (1986).

79. M. A. Kovner, Y. S. Koroatelev, and V. I. Berezin, Opt. Spectroac. 10, 457 (1961).

80. Y. Kakiuti, M. Akiyama, N. Saito, and H. Saito, J. Mol. Spactroac. 61, 164 (1976).

BIOGRAPHICAL SKETCH

Pedro Jose Zavala Darg was born in Lima, Peru, on the 26th day of October, 1955. In December 1972 he finished his high school education in Markham College, San Antonio, Lima (Peru). In May 1977 he received a B.S. in biology and chemistry magna cum laude from Seton Hall University, South Orange, New Jersey (USA). In December 1981 he received a Master of Science in Pharmacy (M.S.P.) from the University of Florida, Gainesville, Florida (USA). His advisor for this degree was Dr. Stephen G. Schulman, Professor of Pharmaceutics. In April 1988 he received a Ph.D. in chemistry from the same university. His advisor for this degree was Dr. Willis B. Person, Professor of Chemistry.

I certify that I have read this study and that in my opinion it conforms to acceptable standards of scholarly presentation and is fully adequate, in scope and quality, as a dissertation for the degree of Doctor of Philosophy.

Willis B. Person

Willis B. Person, Chairman
Professor of Chemistry

I certify that I have read this study and that in my opinion it conforms to acceptable standards of scholarly presentation and is fully adequate, in scope and quality, as a dissertation for the degree of Doctor of Philosophy.

Samuel O. Colgate

Samuel O. Colgate
Associate Professor of Chemistry

I certify that I have read this study and that in my opinion it conforms to acceptable standards of scholarly presentation and is fully adequate, in scope and quality, as a dissertation for the degree of Doctor of Philosophy.

William M. Jones
Professor of Chemistry

I certify that I have read this study and that in my opinion it conforms to acceptable standards of scholarly presentation and is fully adequate, in scope and quality, as a dissertation for the degree of Doctor of Philosophy.

James Wineforder

James Wineforder
Graduate Research Professor
of Chemistry

I certify that I have read this study and that in my opinion it conforms to acceptable standards of scholarly presentation and is fully adequate, in scope and quality, as a dissertation for the degree of Doctor of Philosophy.

Stephen G. Schulman
Professor of Pharmaceutics

This dissertation was submitted to the Graduate Faculty of the Department of Chemistry in the College of Liberal Arts and Sciences to the Graduate School, and was accepted as partial fulfillment of the requirements for the degree of Doctor of Philosophy

April 1988

Dean, Graduate School